W-Pos241

DIFFERENCE INFRARED SPECTROSCOPY OF THE H+,K+-ATPASE. ((V. Raussens, J.M. Ruysschaert and E. Goormaghtigh)) Department of Physical Chemistry of Macromolecules at Interfaces, Free University of Brussels CP206/2, 1050 Brussels, Belgium.

The gastric H+,K+-ATPase is an α, β heterodimer which belongs to the P-type ATPase family. These ATPases are thought to share a common mechanism and a common structure. However, little is known about their structure and reactions which couple ATP hydrolysis to cation transport. We recently used infrared spectroscopy in combination with a proteolytic approach to gain information on the structure of the membrane embedded part of the H+,K+-ATPase. In the present work we prepared oriented membrane multilayers on a germanium internal reflection element by drying tubulovesicle membranes. Linear infrared dichroism indicates a preferential transmembrane organisation of the helices. UV circular dichroism obtained on multilayers deposited on quartz plates confirms this preferential orientation of the helices. In order to investigate the changes occurring in the ATPase molecule upon ligand binding (K+, Mg++, ATP, vanadate and Mg-vanadate), we designed an experimental method to overlay the membrane multilayer system with a flowing buffer. Switching between two buffers containing two different ligands allowed us to record ATR infrared spectra of structural and chemical intermediates relevant of the catalytic cycle of the enzyme. With a noise level in these measurements less than 10^{-4} absorbance units, changes at the level of 1 or 2 amino acid residues should be observed. Our measurements indicate that changes are of very small amplitude with however some reproducible features emerging from the noise level in difference spectra. The origin of these features remains to be assigned. At this stage of the study, we demonstrate that the amplitude changes occurring in the ATPase molecule bound to the ligands tested so far are extremely small, ruling out any major structural change.

W-Pos242

FAST TRANSIENT CURRENTS IN THE Na,K-ATPASE INDUCED BY ATP CONCENTRATION JUMP EXPERIMENTS FROM DMB-CAGED ATP. ((V.S. Sokolov, H.-J. Apell, J.E.T. Corrie* and D.R. Trentham*)) Dept. of Biology, Univ. Konstanz, D-78434 Konstanz, Germany and *Natl. Inst. for Med. Res., London NW7 1AA, U.K.

Electrogenic ion transport by Na,K-ATPase was investigated in a model system of protein-containing membrane fragments adsorbed to planar lipid bilayers. Sodium transport was triggered by ATP-concentration jump experiments in which ATP was released from an inactive precursor by an intense UV-light flash. Previous kinetic studies using the P^3-1-(2-nitrophenylethyl) ester of ATP (NPE-caged ATP) have been limited by the rate of photolytic release of ATP (~ 100 s^{-1} at pH 7 and 20°C). This is important for determination of the reaction sequence: $Na_3E_1 + ATP \rightarrow Na_3E_1 \cdot ATP \rightarrow (Na_3)E_1$-P + ADP (where $(Na_3)E_1$-P is the sodium-occluded form of the phosphorylated enzyme), which may have rates in this time domain. Therefore an alternative caged compound, DMB-caged ATP, the P^3-[1-(3,5-dimethoxyphenyl)-2-phenyl-2-oxo]ethyl ester of ATP (Thirlwell et al., Biophys J. 67, 2436-2447, 1994) was used which photolyses at $> 10^5$ s^{-1}. Under otherwise identical conditions ATP released from the DMB compound showed a significantly faster kinetics of the current transient compared to NPE experiments. In the presence of DMB-caged ATP the Na,K-ATPase showed kinetics independent of buffer pH range 6 to 8 and a current rise time independent of the concentration of the released ATP, in contrast to experiments with NPE-caged ATP. The rate constant of enzyme phosphorylation, subsequent to ATP binding (3.5×10^6 M^{-1}s^{-1}), was found to be 2000 s^{-1} at pH 7.2 and 20°C in buffer containing 150 mM NaCl.

W-Pos243

TREATMENT OF RABBITS WITH CAPTOPRIL ENHANCES THE NA+:K+ SELECTIVITY RATIO OF THE SARCOLEMMAL NA+-K+ PUMP. ((K.A.Buhagiar, D.F. Gray, P.S. Hansen, A.S. Mihailidou, H.H. Rasmussen.)) Cardiology Department, Royal North Shore Hospital, St Leonards, NSW, AUSTRALIA 2065 (Spon. by H. Rasmussen)

Treatment of rabbits with angiotensin converting enzyme inhibitors increases the apparent affinity of the Na+-K+ pump for intracellular Na+ (Na+$_i$) in cardiac myocytes. This increase could be due to an increase in the intrinsic affinity of binding sites for Na+ or an increase in the Na+$_i$:K+$_i$ selectivity ratio. Myocytes from control rabbits and rabbits treated with captopril (Capt) for 8 days were voltage clamped at -40 mV with ~ 1 MΩ patch pipettes containing 10 mM Na+ and a concentration of K+ ([K]$_{pip}$) of 0, 35, 70 or 140 mM (osmolality maintained constant with TMA.Cl). Pump current (I_p) was identified by the shift in holding current induced by 100 μM ouabain. Mean I_p ($\pm$SE) was significantly (P < 0.05) larger in myocytes from Capt treated rabbits than in myocytes from controls when [K]$_{pip}$ was 35, 70 or 140 mM (see figure). This difference was eliminated when myocytes from capt treated rabbits were exposed to 10 nM angiotensin II (AII) in vitro. A similar effect of exposure to 160 nM PMA was observed. Taken together these results suggest that background levels of AII regulate the Na+$_i$:K+$_i$ selectivity ratio of the pump. The mechanism for this may involve protein kinase C.
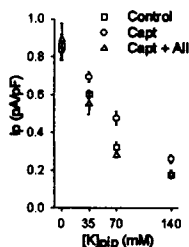
INTERCELLULAR COMMUNICATION

W-Pos244

THREE-DIMENSIONAL STRUCTURE OF A C-TERMINAL TRUNCATED CARDIAC GAP JUNCTION CHANNEL AT 7.5Å IN PLANE RESOLUTION
((V.M. Unger, N.M. Kumar, N.B. Gilula and M. Yeager))
The Scripps Research Institute, La Jolla, CA 92037 (Spon. by M. Yeager)

Gap junction membrane channels directly connect the cytoplasms of adjacent cells and thereby play an important role in tissue homeostasis. We recently utilized electron cryo-microscopy and image analysis to examine frozen-hydrated two-dimensional (2D) crystals of a recombinant, truncated α_1-connexin (α_1Cx263T). The projection map at 7Å resolution revealed a ring of transmembrane α-helices that lines the aqueous pore and a second ring of α-helices in close contact with the membrane lipids. The distribution of densities allowed us to propose a model in which the two apposing connexons that form the channel are staggered by $\sim 30°$. Furthermore, apparent non-crystallographic twofold axes predicted that the two apposing connexons adopt identical conformations. We have now recorded images of tilted, frozen-hydrated 2D crystals, and our current 3D map has been computed at an in plane resolution of ~ 7.5Å and a vertical resolution of ~ 35Å. As predicted by our model, the two apposing connexons that form the channel are staggered with respect to each other. The two connexons are related by non-crystallographic two-fold axes and the central channel is unobstructed, implying that both connexons adopt identical open conformations. Extensive surface interactions between connexin subunits within each hexamer presumably account for the stability of the connexin oligomer. Within the membrane interior each connexin subunit displays four rods of density, which are consistent with an α-helical conformation for the four transmembrane domains. Furthermore, arcs of density in the extracellular domain are suggestive of β-sheet structures. The stacking of putative extracellular β-sheets between apposed connexons may account for the stability of the dodecameric channel. The structural details revealed by our analysis will be essential for delineating the functional properties of this important class of channel proteins.

W-Pos245

ELECTRON CRYO-CRYSTALLOGRAPHY REVEALS THAT OLEAMIDE, A SLEEP INDUCING COMPOUND, CAUSES STRUCTURAL CHANGES OF A GAP JUNCTION CHANNEL ((V.M. Unger, D.W. Entrikin, X. Guan, B. Cravatt, N.M. Kumar, R.A. Lerner, N.B. Gilula and M. Yeager))
The Scripps Research Institute, La Jolla, CA 92037 (Spon. by A. Cheng)

Gap junction membrane channels mediate the electrical and metabolic coupling between cells. Detailed structural information is essential to delineate the molecular basis for channel gating. We recently utilized electron cryo-microscopy and image analysis to examine frozen-hydrated two-dimensional (2D) crystals of a recombinant, truncated α_1-connexin (α_1Cx263T). The projection map at 7Å resolution revealed a ring of transmembrane α-helices that lines the aqueous pore and a second ring of α-helices in close contact with the membrane lipids. However, it was not possible to discern whether the channel was in the open or closed conformation. Functional studies of BHK cells that express α_1Cx263T demonstrated that oleamide, a sleep inducing compound, blocks in vivo dye transfer. As previously demonstrated for other connexins, this behavior is an indication that oleamide causes closure of α_1Cx263T. These results encouraged us to examine whether oleamide affects the structure of the channel. 2D crystals of α_1Cx263T grown in the presence of oleamide displayed reflections to ~ 11Å resolution by optical diffraction and in many cases to better than 7Å resolution after correction for lattice distortions. The oleamide treated crystals exhibit p6 symmetry with unit cell dimensions of a=b=76.8±1.2Å and γ=120.3±0.5°. A projection density map at 7Å resolution derived from 9 images displayed differences compared with our previous map of the untreated channel. Based on the density distribution in the projected structure of the closed α_1Cx263T, channel closure does not appear to involve an overall change in the tilt of the connexin subunits.

W-Pos246

DYE COUPLING IN THE CORNEAL EPITHELIUM: THE EFFECTS OF BUFFERING COMPONENTS AND HEPTANOL. ((K.K. Williams*, H. Bhagat • and M.A. Watsky*)) *Dept. of Physiology and Biophysics, College of Medicine, University of Tennessee, Memphis, TN 38163. •Alcon Laboratories R&D, Ft. Worth Texas.

This study compares dye coupling between corneal epithelial cells *via* gap junctions when exposed to (1) solutions containing different buffering components or (2) heptanol. Epithelial gap junctions have been shown to be functional in a recent study from our lab. Microelectrode dye injection techniques were used to inject 5,6-carboxyfluorescein into epithelial cells of isolated rabbit corneas bathed in solutions buffered with either bicarbonate, HEPES, or phosphate. Injections were started in the first layer and proceeded stepwise into underlying epithelial layers until spread was observed. Results were determined based on initial spread layer and apparent dye travel distance. In addition, we used this procedure to determine the dose response of corneal epithelial gap junctions to heptanol (a classic gap junction inhibitor), and whether or not this response was time dependent. On average, corneas bathed in HEPES buffered Ringer's showed initial spread in the third layer from the top. Corneas bathed in either bicarbonate or phosphate Ringer's showed, on average, initial spread in the second layer. The corneas bathed in phosphate buffered Ringer's, however, appeared to be severely compromised, which may indicate loss of one or more epithelial layers. Following at least 30 minutes exposure to heptanol at 2.5 mM, cells became completely uncoupled in all five layers of the epithelium. At 1.0 mM complete uncoupling occurred in 5 of 7 trials, and at 0.5 mM, heptanol promoted partial uncoupling of the epithelial cells, causing initial spread to occur in the fourth layer in 4 of 7 trials. With less than 30 minutes exposure to heptanol, little or no uncoupling occurred at any of the three concentrations. In all instances where spread occurred, there was no significant differences in the apparent dye travel distance. In conclusion, the buffering component of a Ringer's solution can affect the initial dye coupling spread layer in the corneal epithelium. In addition, heptanol appears to uncouple gap junctions of the corneal epithelium in both a dose dependent and time dependent manner.
Supported by NIH Grant EY10178 and Alcon Laboratories, Ft. Worth, TX.

W-Pos247

GAP JUNCTION FORMATION FROM HEMICHANNELS. ((D. L. Beahm, M. Kreman, G. A. Zampighi and J. E. Hall)) University of California, Irvine; Irvine, CA 92697-4560.

The Xenopus paired-oocyte system has been used to follow the rate of gap junction formation between oocytes expressing connexin RNA. This rate is dramatically increased when pairing of oocytes is delayed relative to the time of RNA injection, indicating that a pool of junctional precursors have accumulated in the membranes of the individual oocytes. (Dahl, G., Levine, E., Rabadan-Diehl, C., and Werner. 1991. *Eur.J.Biochem.* 197:141-144,.). Recently, biophysical evidence has been presented by Bukauskas and Weingart (1994. *Biophys.J.* 67:613-625), and Trexler et al (1996. *PNAS* 93:5836-5841) suggesting that hemichannel opening may be a prerequisite to junctional formation. We are exploiting the ability of cx46 and cx50 to form functional hemichannels that open in low Ca^{++} conditions to control the state of the junctional precursors prior to and during gap junction formation. We have combined freeze-fracture electron microscopy and electrophysiological measurements to determine the rate of junctional conductance increase as a function of hemichannel conductance and of the number and nature of hemichannel particles found in the oolemma. These studies place constraints on the nature of the precursors that form functional gap junctions.
This work was supported by NIH grants EY5661 to JEH and EY04110 to GAZ.

W-Pos248

WHY DO PANCREATIC β-CELLS IN THE ISLET OF LANGERHANS EXHIBIT COMPLEX OSCILLATIONS? HYPOTHESIS ON GLUCAGON OSCILLATION ((Teresa Ree Chay)) University of Pittsburgh, Pittsburgh, Pennsylvania 15260 USA

In β-cells embedded in the islet of Langerhans, about 30% of $[Ca^{2+}]_i$ exhibits a slow oscillation with a frequency ranging from 0.05 min^{-1} to 0.5 min^{-1}. Superimposed on this slow oscillation is a faster oscillation with a frequency of about 3 min^{-1} (Valdeolmillos et al., 1989). In conjunction with this slow $[Ca^{2+}]_i$ oscillation, a slow underlying wave with frequency 0.3–0.5 min^{-1} has also been observed in electrical bursting in 30% of intact ß-cells (Henquin et al., 1982; Cook, 1983). To explain this type of complex oscillation, we have included in Chay's mathematical model [1] two types of intra-islet cells, both of which respond when glucose is added in the medium (Hellman et al., 1995). These are the α-cells which secret glucagon and the δ-cells which secrete somatostatin. In this model, glucagon when it is bound to a receptor (that activates the adenylate-cyclase signalling pathway) raises c-AMP in β-cells. The c-AMP thus raised by glucagon releases luminal Ca^{2+} from the intracellular calcium store. Somatostatin, on the other hand, inhibits secretion of glucagon when the latter hormone concentration becomes undesirably high. The feedback between these two hormones results in a slow oscillation in glucagon, which in turn gives rise to a slow oscillation in c-AMP in β-cells. The oscillatory c-AMP releases luminal Ca^{2+} in an oscillatory manner from the calcium store. Thus, the very slow underlying wave (with a periodicity which lasts for several minutes) sometimes seen in electrical bursting and the $[Ca^{2+}]_i$ oscillation in β-cells can be attributed to the oscillation in glucagon in the islet of Langerhan.

[1] CHAY TR, Proc. International Symposium on Nonlinear Theory and Its Application (NOLTA'95), pp 1049-1052 (1995); Neural Computation 8, 951-978 (1996); WCNN'96, pp 675-679 (1996); IEICE Fed. Trans. E79-A: 1565-1600 (1996); Biol. Cybern. 75, (1996); Proc. World Congress in Nonlinear Analysis (WCNA'96) Athens, Greece, July, 1996.

W-Pos249

GATING OF THE rCX43 GAP JUNCTION CHANNEL DEPENDS ON THE WATER ACTIVITY INSIDE THE LUMEN OF THE CHANNEL ((K. Banach, S.V. Ramanan, E. Peterson and P.R. Brink)) Dept. of Physiology and Biophysics, SUNY at Stony Brook, Stony Brook, NY 11794-8661.

The aim of our present investigation was to examine the permeability properties of the rat connexin43 (rCx43) gap junction channel. A mouse neuroblastoma cell line solely transfected with rCx43 served as a preparation. The junctional current between pairs of these cells was registered by means of the dual voltage clamp technique. In a salt concentration of 110mM KCl , the junctional current through the rCx43 exhibited voltage dependent inactivation. Half maximal inactivation arose at +-75mV. Intracellular solutions of 110mM and 270mM KCl revealed single channel conductances of 100pS and 122pS respectively, indicating, that a saturation of I_j occured. For the examination of lower salt concentrations of 55mM and 30mM KCl, sucrose was added to the intracellular solution at concentrations of 110mM and 160mM respectively, to maintain the osmolarity. The decrease in salt concentration shifted the voltage dependent inactivation of I_j to higher transjunctional voltages. This effect was reversed, when sucrose was replaced by 25% dextran (10000), a substance whose size makes it unlikely to permeate the channel. The effect on the gating may be due to the changing water activity and its influence via osmolarity (J. Zimmerberg and V.A. Parsegian, Nature, 323:36(1986)) on channel gating. From our results we also conclude, that the KCl equilibrium permeability of rCx43 is already at a maximum at low concentrations.
(Supported by the BASF-Postdoctoral Fellowship, Germany, and NIH 3310B)

W-Pos250

SATURATION AND GATING OF CONNEXIN 37. ((S. V. Ramanan, K. Banach, K. Varadaraj, K. Cronin, K. Schirrmacher and P. R. Brink)) Dept of Physiology and Biophysics, SUNY at Stony Brook, NY 11794-8661.

The conductance-concentration curve in KCl was determined for connexin37 in the range 30-360 mM by the DWCP method. The channel conductance tends to saturate at the higher KCl concentrations used. At lower concentrations, the conductance remains high. This can be interpreted in terms of a surface charge effect. Preliminary modelling indicates a charge of 3 e at a distance of 0.5 nm from the channel mouth.V0 as determined from macroscopic records is influenced by the magnesium concentration. Lowering the [Mg] in both cells of a coupled pair from 3 mM to 100 nM changes V0 from ~25 mV to ~45 mV. This effect is also seen as asymmetric gating in records where one cell had 10 mM [Mg] and the other cell had 100 nM [Mg]. Such records also place an upper limit on the Mg permeability though connexin 37.
This work was supported by NIH grant 3310B.

W-Pos251

IS CONNEXIN COOPERATIVITY NECESSARY FOR CHEMICAL GATING OF GAP JUNCTION CHANNELS? ((X.G. Wang, and C.Peracchia)) Department of Pharmacology and Physiology, University of Rochester, School of Medicine, Rochester, NY.

Gap junction channels can be heterotypic (made of two connexons each expressing a different connexin) or homotypic (made of two connexons expressing the same connexin). In addition, connexons can be heteromeric (composed of different connexins) (Brink et al., 1996) or homomeric (made of the same connexin). Thus, the channels can be homomeric-homotypic, homomeric-heterotypic, monoheteromeric (one connexon heteromeric and the other homomeric), biheteromeric (both connexons heteromeric), etc. To learn about the gating behavior of heteromeric connexons, we have tested the effect of 3 min exposures to 100% CO_2 on junctional conductance (G_j) in oocyte pairs expressing either wild-type Cx32 (*32-32*), or a Cx32 mutant, 5R/N (*RN-RN*), as well as in oocyte pairs of which one (*mixed*) expressed a 50/50 mixture of Cx32 wild-type and 5R/N and the other either wild-type Cx32 (*32*) or 5R/N (*RN*), creating *mixed-32* and *mixed-R/N* pairs. In the 5R/N mutant, 5 R res. at the base of the C-ter chain were replaced with N res., resulting in great increase in CO_2 sensitivity. With CO_2 G_j dropped by 15±5% and 93±3% in *32-32* and *RN/RN* pairs, respectively, whereas in *mixed-32* G_j decreased minimally and in *mixed-R/N* it dropped by only 62±8%. This is close to the theoretical difference in gating efficiency one would expect between oocyte pairs (*32-32* and *R/N-R/N*) in which the hemichannels of both oocytes are gating competent and pairs (*mixed-32* and *mixed-R/N*) in which the hemichannels of only one of the two oocytes (*32* or *R/N*, homomeric hemichannels) are gating competent. This indicates that in heteromeric hemichannels gating is impaired and suggests that connexin cooperativity within a hemichannel may be needed for normal gating. Supported by NIH GM20113.

W-Pos252
RELATIONSHIP BETWEEN WHOLE ISLET ELECTRIC ACTIVITY (EIG) AND MEMBRANE POTENTIAL OF INDIVIDUAL CELLS

(R. Khawaled and Y. Palti) Department of Physiology and Biophysics. Rappaport Faculty of Medicine, Technion - Israel Institute of Technology, and Carmel BioSensors, Haifa 31096, Israel.

The electric activity of a whole islet of Langerhans, the Electro-Islet-Gram or EIG (Palti & al. Diabetes, 45:595-601, 1996), was measured simultaneously with the membrane potential of an individual cell within the islet. The membrane potential was measured using the perforated patch technique. On the basis of these measurements the islet cells could be divided into two groups: 1. Cells that do not fire action potentials. The membrane potential of these cells showed slow depolarizations, 20-30 mV in amplitude, in place with the EIG, i.e at about 1 Hz. 2. The majority of the spike firing, or excitable cells, showed firing modulated by the EIG which induce rhythmic membrane depolarization. Some of them fire bursts of spikes in synchrony with the EIG. The rate firing of the others was modulated by the EIG. When the membrane of the excitable cells was hyperpolarized by a current clamp, the firing rate was reduced and the membrane spikes per burst decreased. Other cells, the firing rate of which had no relationship to the EIG, were infrequently encountered.

It is assumed that the membrane potential of practically all resting cells in the islet is modulated, in the form of slow depolarization waves, by the activity of the active cells. Excitable cells, such as β cells, fire spikes in response to the depolarization thus induced. In other cells, one can only monitor passive membrane potential changes.

INTRACELLULAR COMMUNICATION

W-Pos253
IN VITRO CELLULAR PROTECTIVE EFFECTS OF PERFLUBRON (LIQUIVENT®).

((V.V. Obraztsov, E.S. Kornbrust, G.G. Neslund and S.F. Flaim)) Alliance Pharmaceutical Corp., San Diego, CA 92121.

Perflubron is a biologically stable perfluorochemical (PFC) with high gas solubility, intermediate vapor pressure, low lipid and extremely low aqueous solubilities. Perflubron (LiquiVent®) partial liquid ventilation (perflubron PLV) is under development to improve oxygen transport and pulmonary function during acute respiratory distress. Compared to conventional gas ventilation, perflubron PLV has also been found to reduce the local inflammatory response to lung injury. The purpose of this in vitro study was to characterize the effects of perflubron and other neat PFCs with varying vapor pressures and lipid solubilities on cellular responses to injury challenge. Human neutrophils or swine alveolar macrophages were preincubated with PFCs (8% v/v) for 30-60 min at 37°C and then challenged with phorbol myristate acetate (PMA). Superoxide anion release from the leukocytes during activation was determined by measuring the rate of reduction of ferric cytochrome c to its ferrous form. Saline-washed human red blood cells (RBC) were incubated with PFCs (10% v/v) for up to 6 hr at 37°C, added at various timepoints to a hypotonic saline solution challenge, and then measured for hemoglobin release. Swine platelets were incubated with PFCs (5% v/v) for 45 min at 37°C, challenged with agonists (thrombin, collagen, ADP), and then platelet activation was assessed using a whole blood lumi-aggregometer. The leukocyte superoxide anion release response to PMA challenge, the RBC hemolytic response to hypotonic saline challenge, and the platelet activation response to agonist challenge were all attenuated in cells exposed in vitro to PFCs. The degree of attenuation appears to be directly correlated with the lipid solubility and vapor pressure of the PFCs. The effect of perflubron was slight compared to other PFCs having higher lipid solubilities and higher vapor pressures. These results suggest that the positive anti-inflammatory effects of perflubron PLV in the injured lung may be associated with a local cellular protection against injury resulting from a beneficial effect of perflubron at the level of the cell membrane.

W-Pos254
INTEGRATED FRAMEWORK FOR MODELING AND SIMULATION OF CELL PHYSIOLOGY WITH REAL IMAGE DATA: APPLICATIONS IN CALCIUM DYNAMICS AND ELECTROPHYSIOLOGY.

((J.C. Schaff, C.C. Fink[1], J.H. Carson[2], L.M. Loew[1])) Center for Biomedical Imaging Technology, Department of Physiology[1] and Biochemistry[2], University of Connecticut Health Center, Farmington, CT 06030. (Sponsored by M.D. Wei)

A method (The Virtual Cell) is described for modeling and simulation of cell physiology that allows direct comparison of simulation with experimental results. The spatial organization of cellular structure is captured by incorporating geometry derived from volume data sets (often confocal microscopy images). This geometry is segmented into regions that are associated with specific cellular components (e.g. cytosol, ER, mitochondria). This segmented geometry is uniformly sampled into discrete simulation elements where each element is assigned a single component type. The physiology of a component includes electro-diffusion and a collection of models representing discrete mechanisms for chemical reactions and membrane phenomena. These additional models include specific chemical reactions, pumps, and channels and can be selected from a database of predefined models. User defined models can also be automatically generated to extend the database. An optimization tool guides the user in creating a balanced simulation from a collection of models (e.g. achieving initial homeostasis before any stimulus is added). The simulated chemical dynamics are represented as fluxes of molecular species across element boundaries and chemical reaction rates within the elements. These fluxes can be functions of diffusion, ion drift, electric potential, channels, pumps, or any other relationship involving the spatial distribution of molecular species. Membranes are represented by element boundaries separating dissimilar component types. The concentrations of molecular species and the electric potential within each simulation element constitutes the state variables of the system. Direct correlation of simulation results with experimental time series volume datasets is possible because they are spatially coincident. The Virtual Cell builds a structure for encapsulating knowledge about intracellular mechanisms in a framework that allows one to simulate complex physiology. An application of this simulation method to calcium waves in neuroblastoma cells is presented, see Fink et al. Many other applications of the current implementation are possible. (Supported by NIH Grant GM35063 and The Critical Technologies Program of Connecticut.)

W-Pos255
NANOLITER VOLUME SAMPLING AND SEPARATION OF CYTOPLASM FROM XENOPUS OOCYTES.

((V. Luzzi, C. L. Lee, N. L. Allbritton)) Dept. of Physiology and Biophysics, Univ. of California, Irvine, CA 92697-4560

Measurement of spatial gradients of metabolite concentrations in single cells is important to understand intracellular signal transduction. Most metabolites cannot currently be measured in single cells. We have developed a technique to sample nanoliter-sized volumes from small regions of intact, living Xenopus oocytes. The end of a fused silica capillary was etched with hydrofluoric acid to a 50-20 μm outer diameter. To control the depth of penetration and to prevent deformation of the plasma membrane of the oocyte, the tip of the capillary was rapidly driven into the oocyte with a piezoelectric motor element. The volume of cytoplasm sampled could be increased by placing the capillary deeper into the oocyte or by applying a vacuum to the capillary during aspiration. The aspirated volumes were reproducible, and ranged from less than 1 nl to greater than 30 nl. An injection depth of 300 μm combined with application of a vacuum for 250 ms removed 14 nl from an oocyte. Electrophoresis through the capillary and separation of cytoplasmic components was initiated immediately following withdrawal of the tip from the oocyte. Analysis of cytosol (~0.2 nl) from an oocyte previously injected with fluorescein yielded a single fluorescent peak with a migration time similar to that of fluorescein alone. With this technique nanoliter-sized volumes can be rapidly removed from oocytes, and analyzed for the presence of endogenously generated metabolites or previously introduced compounds.

W-Pos256
QUANTITATIVE MEASUREMENT OF FREE Ca²⁺ CONCENTRATION IN RAT HEART MITOCHONDRIA INJECTED INTO XENOPUS LAEVIS OOCYTES.

((Shey-Shing Sheu and Virendra K. Sharma)) School of Medicine and Dentistry, University of Rochester, Rochester, NY 14642.

The free mitochondrial Ca^{2+} concentration ($[Ca^{2+}]_m$) in rat heart mitochondria was quantitated by loading isolated mitochondria with fura-2 and injecting them into Xenopus laevis oocytes. This novel technique allows the quantitative measurement of rat heart $[Ca^{2+}]_m$ into a physiological environment without contamination of fura-2 fluorescence from cytosol or other intracellular organelles. The resting $[Ca^{2+}]_m$ and $[Ca^{2+}]_c$ were 110±10 nM (n=20) and 80±9 nM (n 20) respectively. Thapsigargin, an inhibitor of the sarcoplasmic reticulum Ca^{2+} ATPase, produced a nonoscillatory sustained increase in cytosolic Ca^{2+} concentrations ($[Ca^{2+}]_c$). The increase in $[Ca^{2+}]_c$ by 2 μM thapsigargin evoked a sustained increase in $[Ca^{2+}]_m$. The rising phase of this increase lagged behind the increase in $[Ca^{2+}]_c$ by about 30 seconds. However, the declining phase of the $[Ca^{2+}]_m$ lasted several minutes more than the declining phase of the $[Ca^{2+}]_c$. The thapsigargin-induced increase in $[Ca^{2+}]_m$ was inhibited by the proton ionophore carbonyl cyanide m-chlorophenyl-hydrazone (CCCP), and by ruthenium red, a mitochondrial Ca^{2+} uniporter inhibitor. Inhibition of thapsigargin-induced increase in $[Ca^{2+}]_m$ by ruthenium red shows that the transmission of $[Ca^{2+}]_c$ signal to the mitochondrial matrix is dependent upon the operation of a mitochondrial ruthenium red-sensitive Ca^{2+} uniporter. Neither CCCP nor ruthenium red inhibited the thapsigargin-induced increase in $[Ca^{2+}]_c$. The implications of these findings will be discussed. Supported by NIH grant HL 3333 and CTR grant 4299R1.

W-Pos257

MULTIPLE CELLULAR SPECIALIZATIONS DEFINE WAVE PROPAGATION SITES WITH ELEVATED Ca^{2+} RELEASE KINETICS IN OLIGODENDROCYTES.
((P.B. Simpson and J.T. Russell)) LCMN, NICHD, NIH, Bethesda, MD 20892.

Methacholine (MCh, 0.1 mM) activates propagating Ca^{2+} wavefronts in cultured cortical oligodendrocytes. Ca^{2+} waves were measured at high spatiotemporal resolution (0.8 μm-wide slices along cell processes, 1 image every 66 ms), followed by immunocytochemistry or direct staining of organelles while the cells remained on the microscope. Several regions with elevated kinetics of Ca^{2+} release (high amplitude Ca^{2+} response and rapid rise time) were typically found along processes. Using the dyes JC-1 and $DiOC_6(3)$, mitochondria were always observed at these amplification sites, alone or in convoluted groups, and were not found elsewhere in processes. Immunocytochemistry using antibodies against type 2 inositol trisphosphate receptors and calreticulin revealed that both of these ER proteins are distributed in bead-like patches at these specialized Ca^{2+} release sites. In addition, staining with BODIPY FL-thapsigargin showed that thapsigargin binding sites (SERCA pumps) are highly concentrated in these domains. Inhibition of mitochondrial activity using FCCP or antimycin markedly altered MCh-evoked Ca^{2+} signals. Also, using rhod 2 as the reporter, we measured Ca^{2+} uptake into mitochondria during the cytosolic Ca^{2+} wave. From these results we conclude that Ca^{2+} wave propagation in oligodendrocytes is supported by amplification sites with enhanced Ca^{2+} release rates. Further, these sites are identified by accumulations of the ER proteins calreticulin, type 2 inositol trisphosphate receptors and SERCA pumps, and by the presence of mitochondria, which may modulate the Ca^{2+} release process.

W-Pos258

THE INOSITOL (1,4,5) TRISPHOSPHATE RECEPTOR; REGULATORY EFFECTS OF ATP. ((Thrower, E., Lea, E.J.A. and Dawson, A.P.)) School of Biological Sciences, University of East Anglia, Norwich NR4 7TJ., UK.

The role of ATP as an allosteric activator of the Inositol (1,4,5) trisphosphate-sensitive calcium channel (or IP_3 receptor, IP_3R) is, to date, fairly well documented. Concentrations of up to 10μM ATP have been found to potentiate dramatically IP_3-induced calcium flux in vesicles containing purified IP_3R (Ferris et al, 1990. Proc. Natl. Acad. Sci. USA 87: 2147-2151). Single channel experiments have substantiated this information, generally illustrating that, IP_3-activated channels, in the presence of submillimolar concentrations of ATP have an increased probability of opening (Ehrlich & Watras, 1988. Nature 336: 583-586; Bezprozvanny et al, Nature 751-754), increased lifetimes (Bezprozvanny et al, 1993. Neuron 10: 1175-1184), and in some cases an altered conductance (Maeda et al, 1993. J. Biol. Chem. 266: 1109-1116).
Using purified IP_3R incorporated into planar lipid bilayers, we have seen both short (ranging from 5-20ms) and long (up to, and in excess of 100ms) openings. In our current study we set out to determine whether the allosteric effects of ATP modified either the long, short, or both populations of open times. We incorporated purified IP_3R into planar lipid bilayers prepared by Schindler's technique (Schindler, H., 1980. FEBS LETTS. 122: 77-79). In the presence of 4μM IP_3 and 200nM free Ca^{2+} (in the cis compartment) and a holding potential of -50mV or -100mV, using 500mM K^+ as current carrier, single channel activity was observed. Subsequently, a range of ATP concentrations (50μM, 100μM and 200mM) were added to the cis chamber. Data suggests that in the presence of ATP the population of short lifetimes decreases but the longer openings remain and increase in duration at higher ATP concentrations.

W-Pos259

Ca^{2+} COUPLING BETWEEN ER AND MITOCHONDRIA DURING Ca^{2+} OSCILLATIONS ((Hajnóczky G, Robb-Gaspers LD & Thomas AP)) Thomas Jefferson University, Philadelphia, PA 19107 (Spon. by J.B. Hoek)

Cytosolic Ca^{2+} ($[Ca^{2+}]_c$) spikes evoked by mobilization of Ca^{2+} from the endoplasmic reticulum (ER) are efficiently transmitted to the mitochondria. Mitochondrial Ca^{2+} ($[Ca^{2+}]_m$) spikes lead to activation of Ca^{2+}-sensitive mitochondrial dehydrogenases and so represent an important mechanism to control cellular energy metabolism. To study the mechanisms of Ca^{2+} coupling between ER and mitochondria, we have developed fluorescence imaging techniques to monitor luminal $[Ca^{2+}]$ in the organelles of interest in individual permeabilized cells.
The Ca^{2+} mobilization induced by inositol 1,4,5-trisphosphate (IP3) was manifested in a rapid decrease of luminal $[Ca^{2+}]$ in ER ($[Ca^{2+}]_{ER}$) and a concurrent increase of $[Ca^{2+}]_m$. Heparin prevented the IP3-induced decrease of $[Ca^{2+}]_{ER}$ and increase of $[Ca^{2+}]_m$, whereas ruthenium red only prevented the increase of $[Ca^{2+}]_m$. These data demonstrate that redistribution of Ca^{2+} from ER to mitochondria is established by extraluminal Ca^{2+} transfer from IP3-receptors to ruthenium red-sensitive mitochondrial Ca^{2+} uptake sites.
Ca^{2+} mobilization in response to suboptimal IP3 levels was manifest as oscillations of $[Ca^{2+}]_{ER}$ and these were accompanied by inverse oscillations of $[Ca^{2+}]_m$. Mitochondrial uncoupler did not abolish $[Ca^{2+}]_c$ oscillations in intact cells challenged with IP3-linked hormones and did not prevent $[Ca^{2+}]_{ER}$ oscillations in permeabilized cells stimulated with IP3. Thus, mitochondrial Ca^{2+} uptake was not essential for calcium oscillations. Nevertheless, decreases of $[Ca^{2+}]_{ER}$ evoked by suboptimal IP3 were potentiated in the presence of mitochondrial uncoupler or ruthenium red. Buffering of extraluminal $[Ca^{2+}]$ prevented this potentiation. These data suggest, that Ca^{2+} uptake by the mitochondria can modulate feed back control exerted by released Ca^{2+} on IP3 receptors.

W-Pos260

MITOCHONDRIA, FREE RADICALS & INTRACELLULAR CALCIUM IN CELL INJURY STUDIED IN SINGLE MAMMALIAN CELLS.
((Michael R.Duchen, Eric Boitier, Jake Jacobson, Anne Leyssens & Stefan Peuchen, Dept. of Physiology, UCL, Gower St., London WC1E 6BT))

Many clinical states are associated with cell damage by free radicals. As mitochondria represent a major site of free radical generation, we have developed a model which allows controlled generation of reactive oxygen species (ROS)within the mitochondria of single cells in short term culture. Generation of ROS provoked brief transient depolarisations of mitochondria localised to discrete parts of the cell or even to individual mitochondria revealed using fluorescence imaging of the mitochondrial potentiometric probe, TMREE in all cell types so far studied: cardiomyocytes, astrocytes, hippocampal and cerebellar neurons. These transient events were much reduced by blockade of ER/SR Ca^{2+} release by thapsigargin and by ryanodine in cardiomyocytes, and were also much reduced by blockade of the mitochondrial Ca^{2+} uniporter by microinjection of cobaltammine analogues of ruthenium red. Thus, ROS generation appears to promote localised release of Ca^{2+} from ER/SR. The resulting microdomains of raised $[Ca^{2+}]_i$ lead to Ca^{2+} uptake by nearby mitochondria, confirmed by imaging intramitochondrial Ca^{2+} with rhod-2. Eventually, the mitochondria were completely uncoupled. This was associated with rigor in cardiomyocytes, signalling ATP depletion. The progression was slowed by free radical scavengers, and by cyclosporin A and trifluoperazine, strongly suggesting a coordinated action of free radicals, Ca^{2+} release from SR/ER stores and opening of the mitochondrial permeability transition leading to mitochondrial uncoupling, ATP depletion and irreversible cell injury.

W-Pos261

$[Ca^{2+}]_i$ OSCILLATIONS AND $[Ca^{2+}]_i$ WAVES IN RAT MEGAKARYOCYTES ((Svetlana Tertyshnikova & Alan Fein)), Dept. of Physiology, University of Connecticut Health Center, Farmington, CT 06030-3505

ATP activated $[Ca^{2+}]_i$ oscillations were measured in single rat megakaryocytes using fluorescence ratio microscopy. With increasing ATP concentration the duration of the $[Ca^{2+}]_i$ oscillations increased, however, there was considerable variation from cell to cell in the absolute value of the peak $[Ca^{2+}]_i$ and the frequency and duration of the oscillations. This variation depended, in part, on the level of Fura-2 loading suggesting that megakaryocytes are sensitive to buffering of $[Ca^{2+}]_i$ by Fura-2. Agents, that increase the level of intracellular cGMP (sodium nitroprusside and 8-pCPT-cGMP) or cAMP (prostacyclin, IBMX, forskolin and 8-bromo-cAMP) reversibly inhibited $[Ca^{2+}]_i$ oscillations.
Using video rate fluorescence ratio imaging we found that the agonist-induced $[Ca^{2+}]_i$ oscillations were the result of a well-defined $[Ca^{2+}]_i$ wave, which spread across the cell with an average speed of about 35 μm/s, during the rising phase of each oscillatory spike. After reaching a peak, $[Ca^{2+}]_i$ decreased uniformly across the whole cell during the falling phase of the spike. Analysis of the temperature dependence of $[Ca^{2+}]_i$ waves showed that the rate of $[Ca^{2+}]_i$ decay exhibited a strong temperature dependence ($Q_{10} \approx 4$), whereas, the rate of rise exhibited a weak temperature dependence ($Q_{10} \approx 1.3$), suggesting, that the rate limiting process for $[Ca^{2+}]_i$ wave propagation in rat megakaryocytes is the rate of $[Ca^{2+}]_i$ diffusion.

W-Pos262

ATP INDUCES $[Ca^{2+}]$ OSCILLATIONS AND RELEASE IN/FROM MUCIN SECRETORY GRANULES IN RESPIRATORY GOBLET CELLS. ((W.C. Chin, T. Nguyen, P. Verdugo)) Center for Bioengineering, University of Washington, Seattle, WA 98195

Calcium stored in mucin secretory granules has been thought to have a primary role as a shielding cation in the condensation of the mucin network. Although mucin granules could also function as a storage compartment for Ca^{2+} release in signal transduction, direct evidence on the dynamics of Ca^{2+} in mucin secretory granules is still missing. The work described here was designed to study the dynamics of Ca^{2+} inside secretory granules ($[Ca^{2+}]_{SG}$) and of cytosolic-calcium $[Ca^{2+}]_c$ in intact respiratory goblet cells in primary tissue cultures. Quinacrine was used as a marked for secretory granules and the fluorescent Ca-probes Rhod2-AM, and Ca-orange-5N AM, combined with digital optical sectioning techniques (JCB 116:745,1992) were applied to monitor the $[Ca^{2+}]$ in the two cellular compartments. Following purinergic stimulation (100 μM ATP) Ca-orange-5N AM reports an increase of $[Ca^{2+}]_{SG}$ followed by a train of damped oscillations at a frequency of about 0.1 Hz. Quantitative assessment of $[Ca^{2+}]$ was not possible has exposure of granules to Ca-ionophores results in mucin granule lysis. The fast $[Ca^{2+}]_{SG}$ peak is followed by an increase in the $[Ca^{2+}]_c$ as reported by Rhod2-AM, lasting 30-60 sec, and the degranulation and exocytic release of mucin from the goblet cells. These results are the first indication that Ca^{2+} stored in mucin secretory granules can undergo fluctuations and can be released to the cytosol inducing corresponding oscillations of $[Ca^{2+}]_c$ which precede the exocytic release of mucins. (Supported by grants from Melon Foundation, and the University of Washington Royalty Research Fund)

W-Pos263

MECHANISMS OF CA²⁺ WAVE PROPAGATION IN DIFFERENTIATED NEUROBLASTOMA CELLS BY FAST DIGITAL IMAGING MICROSCOPY AND IMAGE-BASED SIMULATIONS. ((C.C Flsk, J.C. Schaff¹, L.M. Loew)) Department of Physiology and Center for Biomedical Imaging Technology¹. University of Connecticut Health Center, Farmington, CT 06030.

Calcium waves are a much studied and important physiological phenomenon in many cell types, but how calcium waves propagate with a particular geometry and oscillatory behavior in a given cell type is still poorly understood. Differentiated N1E-115 neuroblastoma (NB) cells show calcium waves when stimulated with bradykinin (BK). BK causes IP₃ production at the plasma membrane and subsequent IP₃-triggered calcium release from endoplasmic reticulum (er). Calcium waves were imaged at speeds up to 15 images/second by single wavelength fura-2 imaging via a CCD camera. 0.5 μM BK consistently stimulated a calcium wave within 7 seconds of application, which always originated in the middle of one of the processes, spreading to the growth cone and soma (where the calcium increase was seen to be the greatest). Recovery would occur first in the processes, followed by a slower recovery in the soma. The wave was very fast, typically traversing the length of the cell in less than 5 seconds. It is not certain whether the wave initiates in the process because of physiological differences compared to other parts of the cell, or if it is the geometry alone that is dictating this propagation pattern. To model these calcium waves, we used Virtual Cell, a simulation program developed in the laboratory (see J.C. Schaff *et al* at this meeting). An advantage of this simulation method over others is that the cell can be modeled with the same geometry and element characteristics as seen experimentally. N1E-115 NBs are a well characterized cell line which make them particularly accessible for modeling. In particular, N1E-115 NBs lack ryanodine receptors, so calcium release from the er is known to be entirely mediated through the IP₃ receptors. For this simulation, the geometry of the cell was taken directly from a confocal microscope image, with the er processed so that the relative proportions of er concentration was maintained throughout the cell. For simplification, the minimum number of elements thought to be involved with the calcium wave were modeled (the major elements being er, nucleus, cytosol, and extracellular solution; composed of SERCA pumps, IP₃ and BK receptors, IP₃, BK, and calcium). The simulation shows calcium waves initiating and progressing with the same geometry as seen physiologically, suggesting that the process is the initiation site simply because of its high surface-to-volume ratio (which allows IP₃ to rapidly build up). The power of the simulation is that we are able to visualize elements that can't be measured biologically, such as IP3 concentration and in vivo receptor and pump activity. Experiments have been done initiating a calcium wave in the soma by local application of BK. This was also simulated with results closely following those seen physiologically. These studies show that the geometry of the cell is sufficient to explain the initiation site and propagation behavior of calcium waves in the N1E-115 NBs. It is not necessary to invoke uneven distributions of receptors or er to understand these phenomena. It is hoped that continuing this line of research, combining biological experimentation with computer modeling, will give us greater insight into the cellular behavior than what we could accomplish using either method alone.

W-Pos264

SIMULTANEOUS 3D IMAGING OF CA²⁺ SPARKS AND IONIC CURRENTS IN SINGLE SMOOTH MUSCLE CELLS.
((M.T. Kirber†*, E. F. Etter*, J.J. Singer*, J.V. Walsh, Jr.*, F.S. Fay*))†Rhode Island Hospital and Brown University School of Medicine, Providence, RI and *University of Massachusetts Medical School, Worcester, MA 01655. (Spon. by J. Dobson)

Spontaneous transient outward currents (STOCs) are observed in a wide variety of cell types, including smooth muscle cells. Considerable indirect evidence has accumulated to suggest that a single, transient, and apparently spontaneous local release of Ca²⁺ from intracellular stores (a Spark) generates a STOC by turning on a cluster of Ca²⁺-activated K⁺ channels. We have obtained high speed images of Sparks using the fluorescent indicator Fluo-3 in cat esophageal smooth muscle cells. Using a piezoelectric device that rapidly focuses through the cell, five successive two-dimensional images of planes of the entire cell were captured every twenty-six milliseconds, spanning the thickness of the cell. Utilizing these images, three dimensional reconstructions of Sparks were generated. Simultaneously, in the same cell, we recorded STOCs with tight-seal, whole-cell patch recording. Thus, the relationship between Sparks and STOCs could be studied at high temporal and spatial resolution. We found 1.) Sparks vary substantially in intensity and duration, some remaining quite localized and others spreading out over a small region of the cell; 2.) Sparks that are clearly associated with STOCs appear to arise beneath the plasma membrane and not deep in the cell's interior; 3.) There appear to be regions of the cell where Sparks occur repeatedly ("hot spots"), suggesting that there may be specialized structures involved in Spark generation. [Supported by NIH HL47530 and DK 47223, NSF BIR, and a R.I. Hospital development grant.]
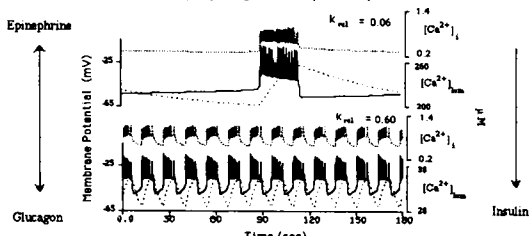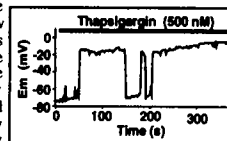
W-Pos265

CALRETICULIN EXHIBITS SERCA 2 ISOFORM SPECIFICITY IN THE MODULATION OF CA2+ WAVES IN *XENOPUS* OOCYTES ((L.M. John, J.D. Lechleiter and P. Camacho)) Department of Neuroscience, University of Virginia, Charlottesville, VA 22908.

Endoplasmic reticulum Ca2+ ATPases (SERCA s) clear cytosolic Ca2+ and refill internal stores after Ca2+ mobilization by IP3R activation. In *Xenopus* oocytes, we demonstrated that SERCA1 (skeletal muscle) overexpression increased Ca2+ wave frequency (*Science*. 260: 226). The alternatively spliced products of the SERCA 2 gene differ in functional properties: SERCA2a (cardiac muscle) has a higher Kd for Ca2+ (~400 nM) than SERCA2b (non-muscle, Kd ~ 200 nM), and in addition, SERCA 2b has a lower transport capacity (Lytton, et al.1992. *J.Biol.Chem*. 267: 14483). In agreement, we also find isoform specificity in the patterns of Ca2+ waves generated when SERCA2 a and 2b are overexpressed in *Xenopus* oocytes. SERCA2b has a sharper leading wavefront (lower Ca2+ activation threshold) but wider wavewidths (lower transport capacity) than SERCA 2a.. Protein levels and correct targeting to the ER was demonstrated by western blot analysis and by confocal immunofluorescence. Tagging SERCAs with GFP (S65T) was also used to demonstrate equivalent levels of expression. Overexpression of the luminal Ca2+ binding protein Calreticulin (CRT) in *Xenopus* oocytes results in a sustained elevation of intracellular Ca2+ with a concomitant inhibition of repetitive Ca2+ waves following IP3R activation (*Cell*. 82: 765). This sustained elevation was also observed when CRT was co-expressed with SERCA 2b. These results were consistent with a modulation of Ca2+ release involving either the IP3R (to prolong release) and/or with SERCA2b (to inhibit store refilling). Here we report that co-expression of CRT with SERCA 2a does not inhibit IP3-mediated repetitive Ca2+ waves. SERCA2b has an additional transmembrane domain with a glycosylation consensus sequence on the C-terminus facing the ER lumen. Since CRT is a chaperone with lectin activity, we are currently testing whether this potential glycosyation site is involved in the differential modulation of SERCA 2 inhibition by CRT. These data suggest that the chaperones CRT and Calnexin, which normally function in protein folding and maturation, may dynamically modulate ER resident glycoproteins. Supported by grant NIH RO1 #GM48451.

W-Pos266

INTERACTIONS BETWEEN THE ANOMALOUS RECTIFIER AND CAPACITATIVE Ca²⁺ ENTRY CURRENTS GENERATE OSCILLATIONS IN MEMBRANE POTENTIAL AND [Ca²⁺]ᵢ IN RBL-1 CELLS. ((M.J. Mason, K.M. Bambha, J. Limberis and G.G. Schofield)) Dept. of Physiol., Tulane Univ. New Orleans, LA 70112

Single cell fura-2 measurements of $[Ca^{2+}]_i$ in RBL-1 cells have revealed rapid oscillatory changes in $[Ca^{2+}]_i$ following depletion of Ca^{2+} stores induced by thapsigargin. Given the sensitivity of capacitative Ca^{2+} entry to membrane potential, these oscillatory changes in $[Ca^{2+}]_i$ may be a direct result of rapid transitions in membrane potential between a hyperpolarized and a depolarized state. We have employed single cell, whole cell current clamp measurements to address this hypothesis. Addition of thapsigargin was accompanied by a slow, modest depolarization followed by a rapid transitional change in potential to a depolarized value. This depolarization was frequently followed by oscillations between a hyperpolarized and a depolarized state (see Figure). No marked changes in membrane potential were detected in control experiments. Voltage clamp experiments demonstrated that the depolarizing responses to thapsigargin were associated with the generation of new, stable zero current potentials more positive than the resting membrane potential before thapsigargin. Such changes in the IV relationship can be accounted for by the interaction between the inward capacitative Ca^{2+} entry current and the low conductance outward region of the anomalous rectifier. We propose that interactions between the capacitative Ca^{2+} entry current, the low conductance region of the anomalous rectifier current, inhibitory influences of depolarization on the Ca^{2+} current and inhibition of the anomalous rectifier current by elevations in $[Ca^{2+}]_i$ interact to induce oscillatory changes in membrane potential. These oscillations would be expected to have marked effects upon $[Ca^{2+}]_i$ and upon Ca^{2+} dependent secretion of inflammatory mediators.

W-Pos267

WHY DO PANCREATIC β-CELLS BURST? A HYPOTHESIS ON FREQUENCY ENCODING BY AN INTRACELLULAR CALCIUM STORE ((T.R. Chay* and Y.S. Lee**)) *Department of Biological Sciences, University of Pittsburgh, Pittsburgh, PA 15260 USA and **Hangyang University, Ansan, Korea.

Through mathematical modelling, we demonstrate how the intracellular calcium store in pancreatic β-cells participates in encoding the frequency of bursting. A central assumption of the model [1] is that a Hodgkin-Huxley type mechanism is inappropriate for describing bursting of β-cells. In the current model, the slow cyclic variation of luminal Ca^{2+} in the calcium store, $[Ca^{2+}]_{lum}$, drives electrical bursting and $[Ca^{2+}]_i$ oscillation. A non-selective cationic channel (which is activated by depletion of the calcium store) plays the role of initiating electrical bursting and maintaining the bursting. The model successfully simulates the effect of glucagon and epinephrine on the frequency and plateau fraction of β-cell bursting. The model predicts that the intracellular calcium store is an *internal clock* that regulates the insulin secretion by adjusting the burst periodicity.

[1] CHAY T. R., NOLTA'95. 1049-1052. 1995. *Neural Compu.* 8, 951-978. 1996 *Biol. Cybern.* 75. 1996.

W-Pos268

DEPLETION-STIMULATED CALCIUM INFLUX IN OVINE TRACHEAL EPITHELIAL CELLS. ((T. Poole-Harris and R. J. Bookman)), Department of Molecular and Cellular Pharmacology, University of Miami, School of Medicine, Miami, Fl. 33136

Cytoplasmic calcium $([Ca^{2+}]_i)$ is believed to play a critical role in the regulation of ciliary motility. Despite its importance, the mechanisms responsible for regulating Ca^{2+} influx in tracheal epithelial cells are not well defined. The purpose of this research is to define the contribution of extracellular Ca^{2+} $([Ca^{2+}]_o)$ to the replenishment of depleted Ca^{2+} stores and to determine its role in shaping the Ca^{2+} signals that control ciliary beat frequency. In the present study, cultured ovine tracheal epithelial cells were loaded with fura 2-AM and $[Ca^{2+}]_i$ was measured by ratio-imaging video microscopy. The importance of $[Ca^{2+}]_o$ to fill depleted Ca^{2+} stores was evaluated by exposing the cell to multiple 10 μM acetylcholine (ACh) applications in the presence and absence of extracellular Ca^{2+} or $NiCl_2$. ACh released stored Ca^{2+} repeatedly in the presence of $[Ca^{2+}]_o$, however, in the absence of external Ca^{2+} there was a progressive elimination of the $[Ca^{2+}]_i$ transient. The Ca^{2+} transient returned when $[Ca^{2+}]_o$ was reintroduced. Results utilizing the Ca^{2+} channel blocker, $NiCl_2$, were similar. To test whether the elimination of the Ca^{2+} signal was a result of store depletion or receptor desensitization, we used a similar protocol in which thapsigargin (Tg) was added after the Ca^{2+} signal was eliminated by ACh. As expected, Tg did not elicit a Ca^{2+} transient, consistent with store depletion. Furthermore, Tg induced a sustained elevation of $[Ca^{2+}]_i$ above baseline which was attenuated by $NiCl_2$ and the removal of $[Ca^{2+}]_o$. Results from this study suggest that Ca^{2+} influx across the plasma membrane is a significant contributor to the regulation of ciliary beat frequency. (Supported by NIH Research Training Grant 5T32HL07188-20 and NHLBI-20989).

W-Pos269

IP$_3$-ACTIVATED Ca^{2+}-SELECTIVE CHANNELS FROM PLASMA MEMBRANE OF HUMAN CARCINOMA A431 CELLS. ((Kirill I.Kiselyov, Anton G.Mamin, Svetlana B.Semyonova and Galina N.Mozhayeva)) Institute of Cytology, Russian Academy of Sciences, St.Petersburg, Russia

A commonly accepted point of view postulates that IP$_3$-dependent Ca^{2+} influx is triggered by an unknown signal from emptied intracellular Ca^{2+} stores. On the other hand, the data exist picturing the influx as a result of direct activation of plasma membrane Ca^{2+} channels by IP$_3$. In the present study we used conventional patch clamp technique to demonstrate the existence of low-conductance IP$_3$-sensitive Ca^{2+} channels in the plasma membrane of A431 carcinoma cells. Application of 0.2-15 μM IP$_3$ to excised patches of plasma membrane of A431 cells activated Ca^{2+}-selective channels. The channels were found to exhibit 2 conductance substates with minimal conductance of 1.1 pS for both Ca^{2+} and Ba^{2+}; extrapolated reversal potentials were found to exceed +75 mV indicating high selectivity of the channels for the divalent cations over potassium. Washout of IP$_3$ or addition of heparin was followed by the disappearance of activity that could be restored by subsequent application of IP$_3$. This argues against the proposition that channel activation is due to depletion of Ca^{2+} stores attached to the patch. Open probability (NP$_o$) of channels activated by 5 μM IP$_3$ averaged 0.57±0.19 (n=14). Mean open time for the first sublevel averaged 6.35±0.65 ms (n=5). The channels exhibit rather high potential dependence, with open probability decreased at membrane potentials close to -30 mV; half maximal value was achieved at -73 mV (n=15). IP$_3$ binds to one site on the receptor with apparent binding constant of about 0.18 μM. The dependence of channel activity on intracellular free Ca^{2+} concentration is bell-shaped but differs markedly from that reported for endoplasmic IP$_3$ receptor. Channel activity induced by IP$_3$ could be enhanced substantially by the addition of 100 μM GTPγS. Application of ATP (0.1 or 1 mM) was not found to affect the channel activity. Activity of the channels with identical characteristics can be induced in cell-attached mode by introducing UTP or bradykinin into the pipette or bath solution. The data obtained show that plasma membrane of A431 cells contains IP$_3$ receptor coupled with Ca^{2+}-selective channels; they are found to have properties different from that of endoplasmic reticulum.

W-Pos270

CELLS DEFICIENT IN THE TYPE 1 INOSITOL 1,4,5-TRISPHOSPHATE RECEPTOR ARE RESISTANT TO APOPTOSIS
((T. Jayaraman and A.R. Marks)) Mount Sinai School of Medicine, N.Y., N.Y. 10029

Elevation of cytoplasmic calcium (Ca) concentration has been proposed as a regulatory signal in apoptosis. The inositol 1,4,5 trisphosphate receptor (IP3R) is an intracellular Ca release channel located on the endoplasmic reticulum of most cell types. Human T cells (Jurkat) were made deficient in the type 1 IP3R by stable transfection with antisense cDNA. These cells lacked IP3-induced Ca release. Strikingly, IP3R1-deficient T cells were resistant to multiple inducers of apoptosis. Monoclonal antibody to CD3 (αCD3), glucocorticoids, irradiation, and Fas ligand all induced apoptosis in ~40% of parental Jurkat at 48 hrs (determined by assaying for DNA fragmentation) but not in IP3R1 deficient cells (n=≥3 in each case, p<0.01), suggesting that these pathways involve a Ca-dependent step. Indeed, cells loaded with fluorescent Ca-sensitive dyes (fluo-3, fura-2 or Indo-1) exhibited elevations in cytosolic Ca after stimulation with αCD3, Fas ligand, and dexamethasone. Mitogen withdrawal did trigger apoptosis in both parental and IP3R1-deficient cells, possibly due to persistent hyperphosphorylation of retinoblastoma protein despite growth factor deprivation. Induction of apoptosis by mitogen withdrawal indicated that transfection with IP3R1 antisense had not induced a non-specific defect in apoptotic signaling. Thus, IP3R1 appears to play an important role in Ca-dependent apoptotic signaling in Jurkat T cells.

W-Pos271

THE ANTI-APOPTOTIC PROTEIN BCL-2 INHIBITS DEPLETION OF THE INTRACELLULAR CALCIUM POOL
((E. Kobrinsky, A. Antipenko, P. Rosenberg, M. Kirchberger and A.R. Marks)) Mount Sinai School of Medicine, N.Y., N.Y. 10029.

The anti-apoptotic protein bcl-2 protects cells against apoptosis via an unknown mechanism. To investigate whether bcl-2 acts by regulating intracellular Ca pools we expressed human recombinant bcl-2 in Xenopus oocytes and examined Ca signaling. Endogenous Ca-activated chloride (Cl) current was used to monitor IP3-induced Ca release activated by three methods: 1) IP3 (1 μM) injection; 2) application of lysophosphatidic acid (LPA, 2 μM); and 3) co-expression of M1 muscarinic receptor with bcl-2 followed by application of acetylcholine (1 μM). In all three cases, Bcl-2 had no effect on IP3-induced Ca release. In contrast, bcl-2 significantly inhibited thapsigargin (Tg)-induced depletion of intracellular Ca pools. Incubation with Tg (1 μM) and EGTA (1 mM) activated a Ca entry pathway resulting in a rise in cytosolic Ca after extracellular application of 2 mM Ca: Ca-activated Cl current amplitude was 242±35 nA (n=31) in control oocytes compared to 46±16 (n=16) in bcl-2 expressing oocytes (p<0.001). This difference was not due to a direct effect on Ca entry as the Ca-activated Cl current induced by application of extracellular Ca (2 mM) was not significantly different in control vs. bcl-2 expressing oocytes following ER Ca-depletion with LPA or acetylcholine. Tg (100 nM) inhibited ~100% of Ca uptake in control oocyte vesicles but only 47±8% in bcl-2 expressing cells (n=4, p<0.01). Similarly, Tg (100 nM) blocked 97±3% of Ca-ATPase activity in control oocytes and only 31±15% in bcl-2 expressing oocytes. Thus, bcl-2 inhibited endoplasmic reticular Ca depletion by reducing the sensitivity of Ca-ATPase to Tg, and had no effect on IP3-induced Ca release or depletion-induced Ca entry. We propose that the anti-apoptotic effects of bcl-2 may be due to direct action on the Ca-ATPase.

W-Pos272

THE MECHANISM BY WHICH Ca EFFLUX AND INFLUX ARE MATCHED TO MAINTAIN STEADY-STATE Ca IN CARDIAC CELLS. ((S.Y. Wang, L. Dong & G.A. Langer)) Cardiovascular Research Labs, UCLA School of Medicine, Los Angeles, CA 90024-1760.

The study examines the feed-back mechanism by which Ca efflux via Na/Ca exchange adjusts to match Ca influx via Ca channels - the condition which must obtain if cellular steady-state Ca level is to be maintained in cardiac cells. It is proposed that variation in Ca channel influx produces changes in sarcoplasmic reticulum (SR) content which, in turn, sets the level of Na/Ca exchange-mediated efflux. We use cultured rat neonate cardiomyocytes and measure Ca channel influx with whole cell voltage clamp, Ca efflux via Na/Ca exchange by high resolution ^{45}Ca washout technique and SR Ca content by combination of the latter with "instantaneous" sarcolemmal membrane isolation. Ca channel influx is varied by Bay K 8644 or nifedipine. Ca influx via Ca channels was increased by 37.8% with Bay K and decreased by 68% with nifedipine. The Ca compartment of the SR, contributing to Na/Ca exchange-mediated Ca efflux was increased by 36.7% with Bay K and reduced by 66.8% with nifedipine. The results from this study agree with a recently developed model of the sarcolemmal cleft space which predicts that these changes in SR release into the cleft will determine the amount of Ca which exits the cell with each beat via Na/Ca exchange so as to maintain Ca at steady state.
(Supported by NIH, Laubish and Castera Funds)

W-Pos273

INTRACELLULAR CALCIUM STORES REGULATE AGONIST-INDUCED CALCIUM INFLUX IN SMOOTH MUSCLE CELLS FROM RABBIT AORTA.
((M. Gericke, R.M.Weisbrod, R.A.Cohen, V.M. Bolotina))
Vascular Biology Unit, Boston Medical Center, Boston, USA

Angiotensin II (AII) is known to contract smooth muscle cells (SMC) by increasing intracellular calcium (Ca^{2+}) concentration due to both release of Ca^{2+} from IP$_3$-sensitive stores and Ca^{2+} influx. However, the mechanisms regulating AII-induced Ca^{2+} influx in SMC are not clear. Here we present evidence for functional connection between AII- induced Ca^{2+} influx and the state of filling of IP$_3$-sensitive intracellular Ca^{2+} stores in smooth muscle cells of rabbit aorta. Using Fura-2 imaging we show that inhibition of IP$_3$- sensitive Ca^{2+} channels by caffeine (10-20 mM) in SMC pretreated with ryanodine (10-20 μM) causes a significant reduction in both AII- induced intracellular Ca^{2+} release and Ca^{2+} influx. In Ca^{2+} -free solution, AII caused a transient rise in F$_{340}$/F$_{380}$ ratio from basal level of 0.76 ± 0.03 to 1.58 ± 0.07 in control cells and from 0.70 ± 0.04 to 0.98 ± 0.17 in the presence of caffeine. Readdition of extracellular Ca^{2+} caused Ca^{2+} influx and a maximum rise in fluorescence ratio to 1.18 ± 0.05 in control cells with no significant change in cells treated with caffeine (0.69 ± 0.02 versus basal 0.70 ± 0.04). Washing out caffeine quickly restored both AII-induced Ca^{2+} release and influx to control levels. Thapsigargin caused Ca^{2+} influx in rabbit aortic SMC similar to that induced by AII, both being blocked by nickel and by SKF 96365. Thus, inhibition of Ca^{2+} release from IP$_3$ -sensitive Ca^{2+} stores prevented AII-induced Ca^{2+} influx, while irreversible depletion of the same stores by blocking Ca^{2+}- ATPase with thapsigargin caused Ca^{2+} influx similar to that triggered by AII.

W-Pos274

PRIMING MECHANISM OF CALCIUM IONOPHORES IN ACTIVATION OF NEUTROPHIL RESPIRATORY BURST ((V.G.Safronova, A.A.Alovskaya, A.G.Gabdulha-kova, E.N.Dedkova, V.P.Zinchenko, N.K.Chemeris)) Institute of Cell Biophysics, Russian Academy of Sciences, Pushchino, Russia

It is considered for many types of animal cells that increasing of intracellular cytoplasmic Ca^{2+} concentration ([Ca^{2+}]$_{in}$) by calcium ionophores and simultaneous activation of PKC by phorbol esters result in more complete cell reaction. The aim of this work was to compare effectiveness of calcium ionophores ionomycin, A23187 and 4-Br-A23187 to intensify respiratory burst of neutrophils activated by PMA. Neutrophils were obtained from peritoneal cavity of mice after zymosan injection. Generation of reactive oxygen species (ROS) by neutrophils was monitored by luminol-dependent chemiluminescence technique. PMA, 1 μM, was added to the cells 2 min after ionophores. [Ca^{2+}]$_{in}$ level was measured using fluorescent Ca^{2+} probe, fura-2. In standard medium (1 mM Ca^{2+}) the ROS production induced by PMA was dramatically enhanced (to 3 fold) if neutrophils were pretreated with 0.001- 0.5 μM of ionomycin or 0.05-2 μM of A23187. However, 4-Br-A23187 does not show such effect. In the presence of 2 mM EGTA (no added Ca^{2+}) synergistic effects were low for 0.2-10 μM A23187 and 1-5 μM ionomycin. 4-Br-A23187 pretreatment (1-10 μM) blocked the PMA effect on respiratory burst to 50% in both media. Comparative studies of the ability of calcium ionophores to increase the [Ca^{2+}]$_{in}$ have shown that dependence of [Ca^{2+}]$_{in}$ from ionomycin and A23187 concentration demonstrates complex character and cannot be explained by ionophore properties only. Low concentrations of ionophores initiate Ca^{2+} mobilization from endoplasmic reticulum and activate Ca^{2+} entry through Ca^{2+} channels. Ionomycin and A23187 were more effective to mobilize Ca^{2+} than 4-Br-A23187. Priming effect of calcium ionophores in neutrophil respiratory burst depends heavily on properties of ionophore using and extracellular Ca^{2+} concentration. It is possible that activation of native Ca^{2+}-transport systems causes to prime the cells by ionophores.
The work was supported by the RFFI N96-04-49515 & R. Fox Foundation grants.

W-Pos275

PHOSPHATASE MODULATION OF I_{CRAC} IN JURKAT T LYMPHOCYTES.

((A. Lepple-Wienhues[1,2], G.R. Ehring[1], H.H. Kerschbaum[1], T. Laun[2], F. Lang[2] and M.D. Cahalan[1])) [1]Physiology & Biophysics, UC Irvine, CA 92697; [2]Physiology, Univ. Tuebingen, Germany 72076

We studied the effects of phosphatase inhibition on divalent and monovalent currents through Ca^{2+} release-activated Ca^{2+} (I_{CRAC}) channels in Jurkat T lymphocytes. Whole-cell currents were activated following depletion of Ca^{2+}-stores by cell dialysis with pipette solutions buffered to 10 nM $[Ca^{2+}]_i$ with 12 mM BAPTA or 12 mM EGTA. In the presence of 20 mM extracellular Ca^{2+} (Ca^{2+}_o), a calcium current, I_{Ca}, activated with a time constant (τ_a) of 145 s and then slowly declined ($\tau_d \sim 2000$ s). After activation of I_{Ca}, reduction of Ca^{2+}_o to 10 μM permitted Na$^+$ current (I_{Na}) through I_{CRAC} channels; I_{Na} declined with a biexponential time course ($\tau = 4$ and 22 s). I_{CRAC} channels could then be reactivated by the readdition of Ca^{2+}_o. Inclusion of sodium orthovanadate (NaVO$_4$, 1mM) in the pipette solution reduced I_{CRAC}. When application of NaVO$_4$ was delayed by backfilling the pipette, I_{Ca} and I_{Na} were initially normal, but vanished after diffusion of NaVO$_4$ into the cytoplasm. Lower concentrations of NaVO$_4$ (10-300 μM) accelerated both the rate of activation and subsequent decline of I_{CRAC} ($\tau_a = 14$ s, $\tau_d = 70$ s), as did 10 μM IP$_3$ ($\tau_a = 19$ s, $\tau_d = 373$ s), perhaps implying more rapid stores depletion coupled to a subsequent inactivation process. Neither IP$_3$ nor NaVO$_4$ affected the rate of deactivation of I_{Na}. However, upon readdition of 20 mM Ca^{2+}_o, reactivation of Ca^{2+} current was reduced with internal NaVO$_4$ or with 50 nM calyculin A, but not with IP$_3$. We conclude that Ca^{2+}-dependent potentiation of I_{CRAC} can be modulated by a phosphatase. Supported by NIH grant NS14609 and DFG Le792/2

W-Pos276

INTERLEUKIN-2 ACTIVATED LYMPHOCYTES INCREASE MICROVASCULAR ENDOTHELIAL PERMEABILITY BY A CALCIUM AND ACTIN DEPENDENT MECHANISM.

((W.D. Ehringer[1], F.N. Miller[1,3], K.A. Wintergerst[3], A. Cox[3], S.M. Ladson[1], A. Haq and M.J. Edwards[1,2])). Center Appl. Microcirc. Res.[1], Depts of Surg.[2] and Phys.[3], Univ. of Louisville, School of Med., Louisville, KY 40292.

Elevated levels of interleukin-2 (IL-2) or tumor necrosis factor-α (TNF-α) can alter endothelial permeability to serum proteins. However, the toxicity of these cytokines on the endothelium is poorly understood. To determine the mechanism of endothelial permeability induced by IL-2, TNF-α or IL-2 activated lymphocytes, human microvascular endothelial cells (HMVEC) from lung were grown in a two chamber system separated by a microporous membrane. The endothelium was labeled with FURA-2 to monitor intracellular calcium mobilization. In addition, 1 mg/ml of a FITC-human serum albumin was added to the upper chamber. The confluent endothelium were then exposed to either IL-2 alone, TNF-α, or IL-2 activated lymphocytes. Changes in the FURA-2 340/380 ratio was monitored concurrent to flux of the FITC-albumin across the HMVEC monolayer. Lymphocytes activated with IL-2 (10,000 U/ml) for 24 hrs significantly increased HMVEC intracellular calcium (155±22.8 nM) compared to control lymphocytes (110±12.8 nM). Neither IL-2, nor TNF-α, had any effect on HMVEC intracellular calcium compared to control (70±5 nM). Increases in intracellular calcium were correlated to HMVEC permeability to FITC-albumin. Permeability coefficients were derived from the data every 1 minute for the 2 hr experiment. The 24 hr IL-2 activated lymphocytes significantly increased the HMVEC permeability coefficient to FITC-albumin at 50 minutes (8.01 x 10^{-6} cm/sec) compared to control (2.0 x 10^{-6} cm/sec). Untreated lymphocytes (6.2 x 10^{-6} cm/sec), TNF (1.90 x 10^{-6} cm/sec), and IL-2 (1.99 x 10^{-6} cm/sec) also were significantly different from control treated HMVEC monolayers. We determined that the kinetics of the increase in endothelial permeability correlated with the extravasation of IL-2 activated lymphocytes across the endothelial monolayer, as well as matrix metalloprotease expression. F-actin photomicrographs of HMVEC stained with BODIPY-phalloidin indicated that the 24 hr IL-2 activated lymphocytes qualitatively increased HMVEC actin stress fibers, leading to contraction and gaps in the monolayer. TNF-α, and to a lesser extent IL-2 alone, increased stress fiber production in the HMVEC monolayer, however few gaps in the endothelium were observed. These data demonstrate that IL-2 and TNF-α alone do not significantly alter endothelial barrier function via a calcium-actin dependent mechanism. Furthermore, any IL-2-induced alterations in endothelial barrier function that utilize this pathway are likely mediated through IL-2 activated lymphocytes.

W-Pos277

SPATIAL HETEROGENEITY OF ATP-INDUCED Ca SIGNALS IN SINGLE CULTURED VASCULAR ENDOTHELIAL CELLS

((Ursula Hüser, Jaclyn R. Holda and Lothar A. Blatter)) Dept. of Physiology, Loyola University Medical Center, Maywood, IL 60153 (spon. by M. Sedova)

The vasoactive compound ATP elicits intracellular Ca ($[Ca]_i$) transients in endothelial cells. We have studied the properties of ATP-induced $[Ca]_i$ transients in a endothelial cell line derived from bovine pulmonary artery using the Ca-sensitive dye fluo-3 AM in combination with laser scanning confocal microscopy. The cultured cells typically showed long fine processes extending from the cell body which contained the nucleus. $[Ca]_i$ started to increase shortly after stimulation in one or several cell processes. $[Ca]_i$ transients recorded from the processes displayed a rapid upstroke followed by a monophasic decline to resting levels, which was maintained throughout the stimulation period. Ca release starting in the processes subsequently propagated into the cell body. In the continous presence of agonist, repetitive $[Ca]_i$ spikes could be detected only in the soma but

Fig.: Onset of the ATP-induced Ca release transient in cell processes (a, b), cell soma (c), and nucleus (d).

not in the cell processes. Furthermore, during the onset of the agonist-induced Ca release the $[Ca]_i$ transient was in many cases preceeded by a discrete small $[Ca]_i$ increase ('Ca foot', see fig.). In some cells agonist stimulation evoked very small, highly localized, non-propagating release events originating from 1 - 3 μm wide regions. These local $[Ca]_i$ release events, probably reflecting elementary Ca release events in endothelial cells, were frequently observed preceeding large amplitude release transients. Therefore, the Ca feet at the onset of release transients might be caused by successive recruitment of release units with non-linear kinetics.
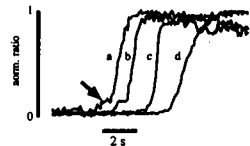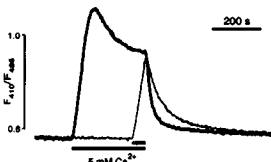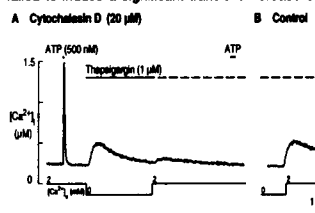
W-Pos278

DISRUPTION OF THE CYTOSKELETAL ACTIN MICROFILAMENT NETWORK INHIBITS CAPACITATIVE CALCIUM ENTRY IN SINGLE VASCULAR ENDOTHELIAL CELLS.

((Jaclyn R. Holda and Lothar A. Blatter)) Department of Physiology, Loyola University Chicago, Maywood, IL 60153

Depletion of intracellular Ca^{2+} stores activates store-operated ('capacitative') Ca^{2+} influx in endothelial cells. The involvement of actin microfilaments in capacitative Ca^{2+} entry was investigated using single, vascular endothelial cells derived from bovine pulmonary arteries (CPAE cells). Changes of cytoplasmic Ca^{2+} concentration ($[Ca^{2+}]_i$) were measured with fluorescence microscopy using the Ca^{2+}-sensitive dye indo-1/AM. To activate capacitative Ca^{2+} entry, the intracellular Ca^{2+} stores were depleted using thapsigargin in the absence of extracellular Ca^{2+}. Capacitative Ca^{2+} entry was monitored as a large transient increase of $[Ca^{2+}]_i$, subsequent to the readdition of Ca^{2+} to the extracellular solution (B). Cells treated with cytochalasin D (cytoD), an inhibitor of actin microfilament formation, displayed a normal ATP-induced $[Ca^{2+}]_i$-transient (A), indicating that the IP$_3$-dependent release of Ca^{2+} was unaffected by cytoD. Subsequently the stores were depleted with thapsigargin in the absence of extracellular Ca^{2+}. In cells treated with cytoD, readmission of extracellular Ca^{2+} failed to induce a significant transient increase of $[Ca^{2+}]_i$ (A) when compared to control (B),

demonstrating the inhibition of capacitative Ca^{2+} entry. Staining of endothelial cells with FITC-conjugated phalloidin to visualize F-actin revealed an organized microfilament network in the control cells and its absence in the cytoD treated cells. These results suggest that actin microfilaments are an integral part of the capacitative Ca^{2+} entry mechanism in vascular endothelial cells. The requirement of an intact microfilament network would support a conformational coupling model for store-operated Ca^{2+} influx.

W-Pos279

CAPACITATIVE Ca^{2+}-ENTRY ENHANCES PLASMALEMMAL Ca^{2+}-ATPase ACTIVITY IN VASCULAR ENDOTHELIAL CELLS

((Andrey Klishin, Marina Sedova and Lothar A. Blatter)) Department of Physiology, Loyola University Chicago, Maywood, IL 60153

Depletion of intracellular calcium stores activates calcium entry across the plasma membrane (capacitative Ca^{2+} entry) in many cell types. Using the Ca^{2+}-sensitive dye indo-1/AM we investigated the ability of the plasmalemmal Ca^{2+}-ATPase to prevent overloading of the cell by Ca^{2+} during prolonged activation of capacitative Ca^{2+}-entry in an endothelial cell line derived from bovine pulmonary artery (CPAE cells). Intracellular calcium stores of single CPAE cells were depleted by thapsigargin (0.5 μM) or cyclopiazonic acid (1 μM) in Ca^{2+}-free solution (1 mM EGTA). Readdition of extracellular Ca^{2+} (5 mM) led to a biphasic change of $[Ca^{2+}]_i$ with a rapid elevation followed by a gradual decrease to a sustained higher plateau level (see figure, bold line). This decrease was not affected by changes in membrane potential, PKC activity or inhibition of plasmalemmal Na$^+$/Ca^{2+} exchange. Subsequent removal of extracellular Ca^{2+} caused a rapid decrease of $[Ca^{2+}]_i$ to its initial value. We used the rate of $[Ca^{2+}]_i$ restoration after activation of capacitative Ca^{2+} entry as a measure of plasmalemmal Ca^{2+}-ATPase efficacy. We found that the latter varied with the duration of Ca^{2+} readdition after depletion of intracellular Ca^{2+} stores. As shown in the figure the capacitative Ca^{2+} entry transient decreased more rapidly to control level

after prolonged exposure to extracellular Ca^{2+} (bold line) than after only a short exposure (thin line) although $[Ca^{2+}]_i$ had reached the same amplitude. Inhibition of calmodulin kinase II partially attenuated this acceleration. We propose that Ca^{2+}/calmodulin-dependent activation of the plasmalemmal Ca^{2+}-ATPase protects from Ca^{2+} overload during sustained capacitative Ca^{2+} entry. The delay in this activation (see fig.) is related to the time required for the formation of Ca^{2+}/calmodulin/Ca^{2+}-ATPase complex.

W-Pos280

THE PROTEIN KINASE INHIBITOR K252A BLOCKS INACTIVATION OF CALCIUM INFLUX DURING STORE REFILLING IN CHO CELLS.

((M. Condrescu and J. P. Reeves)) Physiology Department, UMDNJ-NJ Medical School, Newark, NJ 07103

In many cells, release of Ca from InsP$_3$-sensitive stores accelerates influx of extracellular Ca or Mn through specialized channels, which become inactive when the stores refill with Ca. In the presence of hexokinase (0.3 mg/ml) and glucose (10 mM), addition of ATP (0.3 mM), a purinergic agonist, elicited a brief increase in $[Ca]_i$ in fura-2-loaded CHO cells; the ATP was then rapidly consumed by the hexokinase and the InsP$_3$-sensitive stores refilled with Ca. Under these conditions, the protein kinase inhibitor K252a (1 μM) increased the rate of Ca or Mn influx following addition of ATP, without affecting refilling of the InsP$_3$-sensitive stores. K252a also accelerated Ca or Mn influx in the absence of ATP, but the effect was smaller than with ATP. K252a and the SERCA inhibitor thapsigargin (Tg) stimulated Mn influx equally and non-additively: Tg-induced Mn influx was not further accelerated by K252a. Ca or Mn influx induced by either K252a or Tg was blocked by calyculin A (100 nM), an inhibitor of protein phosphatases 1 and 2A (PP1/2A), and by the mitochondrial uncoupler Cl-CCP (2 μM). We suggest that SDCI is initiated through activation of PP1/2A and that blocking rephosphorylation of the protein targets of PP1/2A maintains store-operated channels in an open state, despite refilling of the Ca stores.

W-Pos281

ELEVATED INTRACELLULAR Ca^{2+} IS REQUIRED FOR CYCLIC ADP-RIBOSE INDUCED Ca^{2+} RELEASE IN SEA URCHIN EGGS. ((Xiaoqing Guo and Peter L. Becker)) Dept. of Physiol., Emory Univ. Sch. of Med., Atlanta, GA.

Cyclic ADP ribose (cADPr) has been demonstrated to mobilize Ca^{2+} from a ryanodine-sensitive store in sea urchin eggs and a variety of mammalian cell types. Both cADPR and its metabolic enzymes appear to be ubiquitously distributed, supporting the hypothesis that cADPr is a general endogenous messenger of Ca^{2+} signaling. However, the mechanism by which cADPR releases Ca^{2+} is unknown. We have examined the kinetics of Ca^{2+} transients in intact sea urchin eggs induced by step increases in intracellular cADPr in contrast to those induced by IP$_3$. Eggs were microinjected with the calcium dye fluo-3 and either caged-cADPr or caged-IP$_3$, and subjected to a single UV-flash lamp burst. While peak changes in fluo-3 fluorescence induced by cADPr or IP$_3$ were similar in magnitude, these two messengers produced distinct temporal patterns of Ca^{2+} release. The onset of the rise in [Ca^{2+}] by IP$_3$ was immediate and fast, and with a hyperbolic profile. In contrast, as we previously reported (*Circ Res* 79:147, 1996), the initial phase of the Ca^{2+} transient elicited by cADPr was slow and displayed a sigmoidal shape, with an effective delay of several hundred msecs. To further investigate the underlying basis for the slow kinetics of cADPr-induced Ca^{2+} release, we manipulated the [Ca^{2+}] by co-loading eggs with either caged calcium (NP-EGTA) or excess Ca^{2+} buffer. The delay before maximal release was eliminated when a jump in [Ca^{2+}] was coincident with the photoliberation of cADPr, whereas increases in the intracellular Ca^{2+} buffering capacity profoundly prolonged the delay (to 13.0 ± 2.1 secs; n=4). These results demonstrate that an elevated intracellular [Ca^{2+}] is required for Ca^{2+} mobilization by cADPr.
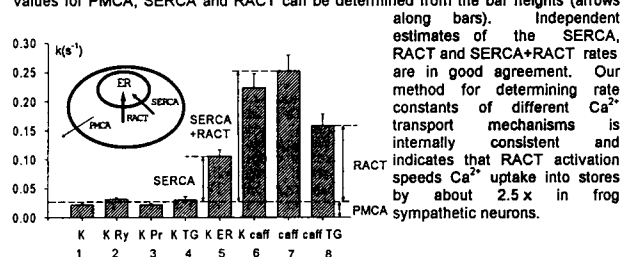
W-Pos282

POSITIVE INOTROPY MEDIATED BY THE DIACYLGLYCEROL/PROTEIN KINASE C SIGNALING PATHWAY IN RAT VENTRICULAR MYOCYTES. ((Y.Q. Pi, X.P. Huang, R. Sreekumar and J.W. Walker)) Department of Physiology, University of Wisconsin, Madison, WI 53706.

Regulation of myocardial contraction by diacylglycerol (DAG) and protein kinase C (PKC) was evaluated in living adult rat ventricular myocytes. The DAG analogue dioctanoylglycerol (diC$_8$) was photoreleased from a caged compound incorporated into the myocyte membrane while monitoring electrically paced twitch amplitude (0.5 Hz, 1 mM Ca^{2+} Ringers pH 7.4, 22°C; Huang et al., Biophys. J. 70:2448, 1996). This approach permitted us to avoid exposure of myocytes to extracellular DAG and yet to control the concentration and duration of DAG released into the cells. Conditions were defined whereby photorelease of diC$_8$ produced up to a 406±42% (mean±sem, n=26) enhancement of twitch amplitude. The response was dose-dependent, stereospecific for the S-enantiomer of diC$_8$ (Sreekumar et al., Bioorg. Med. Chem. Let. in press), and blocked by the PKC inhibitor chelerythrine chloride. Moreover, cis-unsaturated fatty acids were found to enhance the response to photoreleased diC$_8$ in a synergistic manner suggesting a physiological role for parallel activation of phospholipase C (which produces DAG) and phospholipase A$_2$ (which produces cis-unsaturated fatty acids) by cell surface receptors. The data provide evidence for a major role for DAG/PKC signaling pathway in short term regulation of cardiac myocyte contractility. This pathway may, in part, mediate the response of myocytes to an array of positive inotropic agents including endothelin, α-adrenergic agonists and angiotensin II. [Supported by NIH]

W-Pos283

RYANODINE-INDUCED ENHANCEMENT OF Ca^{2+} SEQUESTRATION BY INTRACELLULAR STORES IN SYMPATHETIC NEURONS. ((M.A. Albrecht and D.D. Friel)) Dept. of Neurosciences, Case Western Reserve University, Cleveland, OH 44106

Sympathetic neurons respond to membrane depolarization with a rise in the cytosolic free Ca^{2+} concentration ([Ca^{2+}]$_i$) that depends on both Ca^{2+} entry across the plasma membrane and Ca^{2+} uptake and release from internal stores. It has been proposed that the caffeine-sensitive store (CSS), in particular, acts as a source of Ca^{2+}-induced Ca^{2+} release (CICR) that speeds [Ca^{2+}]$_i$ elevations induced by membrane depolarization. In support of this idea, inhibitors of CICR (e.g. ryanodine, 1 µM) slow depolarization-induced elevations in [Ca^{2+}]$_i$. One possible explanation is that ryanodine depletes the CSS and reduces the chemical driving force favoring net Ca^{2+} release. To examine this idea further, the reversible SERCA pump inhibitor 2,5-di(tert-butyl-)-1,4-hydroquinone (BHQ) was used to assess the Ca^{2+} content of the CSS and its sensitivity to ryanodine. BHQ elicited a transient rise in [Ca^{2+}]$_i$ that was virtually unchanged by ryanodine, indicating that ryanodine does not simply prevent Ca^{2+} accumulation by the CSS. That ryanodine enhances net Ca^{2+} accumulation was suggested by the observation that following treatment with the irreversible SERCA pump inhibitor thapsigargin (TG, 500 nM), the rise in [Ca^{2+}]$_i$ induced by weak depolarization in ryanodine-treated cells was accelerated (22/23 cells). Ryanodine-induced enhancement of Ca^{2+} accumulation by the CSS may therefore contribute to the slowing of [Ca^{2+}]$_i$ responses elicited by membrane depolarization.

W-Pos284

RATE CONSTANTS OF Ca^{2+} TRANSPORT IN NEURONS OF FROG SYMPATHETIC GANGLIA ((Z. Cseresnyés, A.I. Bustamante, M.G. Klein, M.F. Schneider)) Dept. Biochem. and Molec. Biol., Univ. of Maryland School of Med., Baltimore, MD 21201

The slow component of decay of [Ca^{2+}]$_i$ after elevation by 50-[K$^+$]$_o$ and the entire decline of [Ca^{2+}]$_i$ after Ca^{2+} release by caffeine were fit by a single exponential to obtain rate constant values (bar graph). Bar 1: 50-[K$^+$]$_o$ (K); 2: 50-[K$^+$]$_o$ with 20 µM ryanodine (K Ry); 3: 50-[K$^+$]$_o$ with 10 mM procaine (K Pr); 4: 50-[K$^+$]$_o$ with 200-500 nM thapsigargin (K TG); 5: 50-[K$^+$]$_o$ in the presence of pre-depleted ER (K ER); 6: caffeine applied during [Ca^{2+}]$_i$ decay after 50-[K$^+$]$_o$ (K caff); 7: control caffeine (caff); 8: caffeine in the presence of 200-500 nM thapsigargin (caff TG). A cell model (insert) shows the transport systems that act in parallel to lower [Ca^{2+}]$_i$: the plasma membrane ATPase (PMCA), the SERCA pump and a release-activated Ca^{2+} transport (RACT) mechanism proposed to account for the rapid decay of [Ca^{2+}]$_i$ after caffeine (Biophys.J. 70: A181, 1996). Rate constant values for PMCA, SERCA and RACT can be determined from the bar heights (arrows

along bars). Independent estimates of the SERCA, RACT and SERCA+RACT rates are in good agreement. Our method for determining rate constants of different Ca^{2+} transport mechanisms is internally consistent and RACT indicates that RACT activation speeds Ca^{2+} uptake into stores by about 2.5x in frog sympathetic neurons.

W-Pos285

CALRETININ IS PRESENT IN A SUBSET OF HAIR CELLS OF THE FROG SACCULUS. ((B. Edmonds and W.M. Roberts)) Institute of Neuroscience, University of Oregon, Eugene, OR 97403.

Hair cells of the frog (*Rana pipiens*) sacculus are thought to contain a high concentration (mM range) of an unidentified, diffusable Ca^{2+} buffer. Modeling studies indicate that when Ca^{2+} influx occurs through a cluster of voltage-activated Ca^{2+} channels in the hair cell membrane, the cell's native Ca^{2+} buffer restricts the region over which the free Ca^{2+} concentration is elevated (space constant = 30nm) and hastens the decay of the Ca^{2+} transient by about 100-fold after Ca^{2+} channels close. The native buffer is therefore important for rapid, short-range Ca^{2+} signaling in hair cells. To investigate the identity of the hair cells' native buffer we have used antibodies made against a range of Ca^{2+}-binding proteins including the 28kD calbindin (CB) and a related 29kD protein, calretinin (CR). In thin sections, polyclonal antibodies against CB and CR both label a subset of hair cells with a distinct long, thin morphology; short, fat hair cells are not labeled. To test further for the presence of CB in hair cells we used a monoclonal antibody generated against CB in chicken. Hair cells were not labeled; however, labeling of Purkinje cells in frog cerebellum confirmed that the antibody recognizes calbindin in frog. Moreover, in Western blots of sacculus and cerebellum both of the polyclonal antibodies label only a 29kD band in hair cells and a 28kD band in cerebellum. The long, thin hair cells therefore appear to contain only the calretinin-like protein; the labeling observed with polyclonal α-CB on hair cells is apparently due to cross-reactivity to CR.

Antibodies were a generous gift of Dr. Marco Celio.

W-Pos286

ELECTRON TOMOGRAPHY OF MITOCHONDRIA: MEMBRANE CONTACTS

((G. Perkins*†, C. Renken*, M. Martone†, V. Edelman†, T. Deerinck†, S. Young, M. Ellisman† and T. Frey*)) *Dept. of Biology, San Diego State University; †Neurosciences Dept. and NCMIR, UCSD.

Our mitochondrial reconstructions were calculated from tilt series of semi-thick sections of tissue over an angular range from -60° to +60° and have a resolution of 7-10 nm. The inner and outer membranes were clearly delineated with the inner membrane topographically divided into two components whose surfaces are contiguous. The inner boundary membrane is the component which lies close to the outer membrane, and the cristae are invaginations of the inner membrane forming predominantly tubular and lamellar structures which span the interior volume. In agreement with published reports, we found that the outer membrane and the inner boundary membrane lie parallel to one another over most of the mitochondrial surface with a mean width of 20-25 nm across both membranes. The invaginations connecting cristae to the inner boundary membrane were relatively small (approximately 30 nm diameter) for both tubular and lamellar cristae, and lamellar cristae frequently had multiple small openings to different regions of the inner boundary membrane. We identified contact sites--believed to be in the import pathway for precursor proteins targeted to the matrix--as regions of our reconstruction where the inner and the outer membrane could not be separately resolved, and these had a mean width of 13-15 nm measured across both membranes. Discrete contact sites are small (11 - 17 nm mean diameter parallel to the membranes) and occupy a small fraction of the surface area. The density of contact sites varied from 100-400/µ². We did not find an association between contact sites and the sites of inner membrane invagination that was statistically different from a random placement suggesting that contact sites do not play a role in stabilizing these invaginations which form cristae.

W-Pos287

EFFECT OF CHELATORS ON Ca²⁺ CLEARANCE BY RAT BRAIN MICROSOMES. ((X.-J. Meng and R. F. Abercrombie)). Department of Physiology, Emory University School of Medicine, Atlanta, GA 30322.

The aim of this study was to evaluate a method for measuring calcium accumulation kinetics by, and to determine the effects of mobile calcium chelators on, rat brain microsomal Ca pumps. Microsomes were isolated by differential centrifugation in media lacking calcium chelators, then resuspended in a physiological intracellular solution at 30 °C, pH 7.0 - 7.4, in a 10 µl volume chamber. Free calcium was measured with Ca-sensitive mini-electrodes after injections of Ca, with and without Ca chelators and with and without MgATP. When ~ 10 µM free calcium, [Ca²⁺], and ATP were injected, the free calcium first rose then fell to below 1 µM. When ATP was removed or injections were made into a microsome-free inert medium, the fall in [Ca²⁺] was greatly attenuated. The net total calcium uptake rate (in units of µmol s⁻¹ g protein⁻¹) was approximated from the change in free calcium, $\Delta[Ca^{2+}]/\Delta time$, the calculated extra-vesicular buffer ratio, $\Delta boundCa/\Delta[Ca^{2+}]$, and the protein concentration. Without chelators, Ca uptake at 1 µM [Ca²⁺], was ~1 nmol g⁻¹ s⁻¹ and varied roughly with the square of [Ca²⁺]. The calcium chelators, 20 µM EGTA, 10 µM parvalbumin, 40 µM BAPTA, and 40 µM Dibromo-BAPTA, significantly increased net total Ca uptake at low but not high [Ca²⁺]. In summary, clearance of Ca by rat brain microsomes is ATP-dependent and facilitated by native and exogenous calcium chelators. (NIH-NS19194)

W-Pos288

ENHANCEMENT OF CALCIUM TRANSPORT IN RAT BRAIN MICROSOMES BY IMMOBILIZED NITR-5. ((Nabil F. Al-Baldawi and R. F. Abercrombie)). Emory University School of Medicine, Department of Physiology, Atlanta, GA 30322.

Mobile Ca chelators have been shown to enhance Ca transport into sarcoplasmic reticulum (Berman, J. Biol. Chem. 257, 1953-1957) and brain microsomal vesicles. A BAPTA-like Ca chelator, Nitr-5, was attached to agarose polymer beads via 1,4-butanediol-diglycidyl ether (a long spacer arm) or 1,2:3,4-diepoxybutane (a short spacer arm), to test the ability of immobilized chelators to enhance Ca transport. Specific calcium binding to the immobilized chelators was measured: $K_{1/2}$ = 14 - 43 µM, and B_{max} = 26 - 32 nmol/g for the long and short spacer-arm resins, respectively. Columns of the immobilized chelators were equilibrated with a solution containing physiological salts, 1 µM [Ca²⁺], and tracer ⁴⁵Ca (equilibration buffer). Microsomes from rat brain were placed in the equilibration buffer (in the presence or absence of MgATP) and were poured over the columns, collected on ice, trapped on filters, washed with non-radioactive solution, and the ⁴⁵Ca measured by liquid scintillation. At 24-37°C, the ATP-dependent ⁴⁵Ca accumulation was significantly greater in those microsomes that had been exposed to the immobilized chelator than in microsomes placed in this equilibrium buffer but without chelator exposure. Under similar conditions, the long spacer-arm matrix contributed more ATP-dependent Ca uptake than did the short arm matrix. Thus, chelator immobilization did not entirely block its enhancement of ATP-dependent Ca uptake. (NIH-NS19194)

W-Pos289

BIOGENESIS OF POLYTOPIC MEMBRANE PROTEINS IN THE ENDOPLASMIC RETICULUM. ((S.M. Simon, M. Baez, A. Borel, M. Friedlander)) Rockefeller University, 1230 York Ave, N.Y., N.Y. 10021; Scripps Res Inst, 10666 North Torrey Pines Road; La Jolla, CA 90024

The initial steps in the biogenesis of membrane proteins parallel that of secretory proteins. The translocation of membrane proteins, however, must be interrupted prior to completely traversing the membrane. This is followed by their folding and integrating into the lipid bilayer. Our experiments indicate that translocation can be broken into two partial reactions: First, the sequential movement of transmembrane segments (TMS) across the membrane (perpendicular to the membrane surface) and second the integration of the transmembrane segments into the lipid bilayer (movement parallel to the membrane surface). Our results indicate that as each latent TMS in a polytopic membrane protein emerges from the ribosome, it sequentially translocates across the membrane. However, while these translocated TMSs are still attached to their biosynthetic ribosomes they can be extracted from the membrane with urea. This suggests that nascent TMSs do not integrate into the bilayer as they achieve a transmembrane topography. The integration is delayed until after the protein is synthesized and released from the ribosome. Prior to insertion into the bilayer, these TMSs appear to be stabilized by salt-sensitive electrostatic bonds within an aqueous accessible compartment. We have started to examine the effects of mutations responsible for retinitis pigmentosa that affect the biogenesis of opsin.

W-Pos290

Role of subcellular pH in multidrug resistant human breast cancer cell lines ((N. Altan, S. M. Simon, M. Schindler)) Rockefeller Univ, NY NY 10021 Mich State Univ, E Lansing, MI 48862.

Multidrug resistance is a significant clinical problem in the chemotherapeutic treatment of breast cancer. It is associate with a number of phenotypic changes in cellular function. We have observed that one such change is the loss of acidification within the intracellular compartments of the exocytotic pathway in the MCF-7 human drug-sensitive breast tumor cells. In marked contrast, the MCF-7adr drug resistant cells demonstrate normal lumenal/cytoplasmic pH gradients. We hypothesize that drug resistance is the consequence of protonation of the chemotherapeutic drugs in acidic secretory compartments resulting in their sequestration and subsequent secretion from the cell. To test our hypothesis we have studied the subcellular distribution of pH and chemotherapeutics in two different breast cancer cell lines, MCF-7/ MCF-7ADR and MDA-231/MDA-A1, using confocal fluorescence microscopy and immunoelectron microscopy. Our results show that the drug-resistant cell lines have acidified cytoplasmic vesicular compartments that also contain chemotherapeutics. Drug sensitive cells, in contrast, have lost their intracellular pH gradients and have lost their ability to sequester drugs from the cyto-nucleoplasm within acidic vesicular compartments. Furthermore agents that reverse multidrug resistance block the acidification and thus accumulation of chemotherapeutics in both MCF-7/ADR and MDA-A1 breast cancer cell lines.

W-Pos291

ACIDIFICATION AND IONIC FLUXES OF THE ENDOCYTIC PATHWAY OF DICTYOSTELIUM DISCOIDEUM. Juan M. Rodriguez-Paris, Roderick Cowthorn, Jeff Weeks, J. Abra Watkins and Jonathan Glass. Center for Excellence in Cancer Research, Treatment and Education, Department of Medicine, Henmatology/Oncology Section, LSUMC, Shreveport, LA 71130.

While it is well established that vesicular acidification plays a critical role in the traffic of receptors and ligands, little is known about the bioenergetics or regulation of this process in the endocytic pathway. Using highly purified fractions of the Dictyostelium discoideum endocytic pathway prepared by high gradient magnetic separation, we have analyzed the mechanism of ATP-dependent acidification and ion membrane permeability properties. Our results indicate that ATP-dependent acidification is electrogenic, with proton transport accompanied by the generation of a negative membrane potential due to cation efflux being greater than anion influx. The proton gradient was dissipated by ion fluxes. No vesicle acidification nor deacidification was observed in absence of ions. Replacement of permeable anions with less permeable anions (e.g. replacing Cl⁻ with gluconate) decreased acidification, however, cations K⁺ and Na⁺ were equally effective. ATP-dependent acidification was not coupled to any specific anion or cation, although, DIDS completely inhibited acidification suggesting a strong coupling with Cl⁻ fluxes. The lysosomal membrane was found to be extremely permeable to protons. Thus, the internal acidification of the endocytic pathway is likely to reflect a dynamic equilibrium of protons regulated by the intrinsic ion permeabilities of the membrane, in addition to the activity of the ATP-driven proton pump as well as cation/anion channels and antiports.

Fraction	Pulse x Chase (min)	Kacid (s⁻¹)	Kleak (s⁻¹)	ΔpH
Pinosomes	3 x 0	0.00636	0.0002	~1.4
Lysosomes	15 x 15	0.04320	0.0074	~2.0
Postlysosomes	15 x 60	0.00376	0.0005	~1.1
Contractile Vacuoles		0.09753	0.0001	~2.0
Phagosomes		0.00940	0.0018	~1.6

Acidification was found to be specific for ATP. GTP did not support acidification as well as did not have any effect on ATP-acidification. cAMP, ADP and AMP had no effect on acidification. These results highlight differences in flux regulation during endocytic processing that suggest the importance of lipid composition and channel regulation.

W-Pos292

NUCLEO-CYTOPLASMIC TRANSPORT OF THE TUMOR SUPPRESSOR P53 AS ANALYZED BY QUANTITATIVE LASER SCAN MICROSCOPY. ((G. Middeler, K. Zerf, S. Jenovai, A. Thülig, M. Tschödrich-Rotter, U. Kubitscheck and R. Peters)) Institut für Med. Physik und Biophysik, Westfälische Wilhelms-Universität Münster, D-48149 Münster, Germany

Human p53 was expressed in E. coli, purified and fluorescently labelled. The intracellular transport of p53 was analyzed by quantitative laser scan microscopy. Injected into the cytoplasm or nuclei of 3T3 cells p53 was imported into or exported from nuclei within minutes. Import was inhibited by coinjection of wheat germ agglutinine (WGA). In contrast, the peptide-protein conjugate NLS-HSA carrying the nuclear localization sequence of the SV40 T antigen was only imported but not exported. 3T3 polykaryons were injected with p53 and photobleached in such a manner that only a single nucleus per polykaryon remained non-bleached. p53 was found to migrate rapidly (halftime ~10 min) from non-bleached into bleached nuclei, while NLS-HSA did not. In digitonin permeabilized cells p53 was imported into nuclei. When removed from the medium after nuclear accumulation p53 was exported from the nuclei. Nuclear import and export of IAF-p53 both were rapid (halftimes of a few minutes, 22°C) and strongly inhibited by WGA or incubation on ice. NLS-HSA was only imported but not exported. We conclude that the nucleocytoplasmic transport of p53, in contrast to that of NLS-HSA, is bi-directional and that transport in both directions is carrier mediated and energy dependent. These results suggest that p53 contains nuclear export in addition to import signals and thus open new views on the potential regulation of p53 cellular functions. Supported by the Deutsche Forschungsgemeinschaft (Pe 138/14).

W-Pos293

EVIDENCE FOR REGULATION OF RAT PANCREATIC ZYMOGEN GRANULE K^{+} TRANSPORT AND MEMBRANE FUSION BY RAB3B. ((K. Gasser, S. Oh, H. McDonald, and C. Johnson)) Dept. Biol. Sciences, Northern Illinois Univ. DeKalb, IL, 60115 (Sponsored by G. Kresheck)

Pancreatic secretory granules contain transport pathways for K^{+} and Cl^{-} that may contribute to exocytotic membrane fusion or net fluid secretion. It is likely that the activation of these pathways are coordinated to coincide with vesicle docking and subsequent exocytosis with the plasma membrane. The results of immunoblotting showed that the membranes of purified rat pancreatic granules contain proteins that correspond to the K_{ATP} channel and rab3B g-protein. Since the initiation of net solute transport and swelling by the granule appears to be rate-limited by K^{+} permeability, the possibility of K^{+} channel regulation by the rab3B was investigated. This mechanism would provide the needed coupling to coordinate net transport with vesicle docking with the plasma membrane. ATP reduces the granule K+ permeability in a dose dependent manner, with 3 mM causing a reduction of approximately 79%. Using isolated secretory granules , the results show that mastoparan, or a synthetic peptide of the rab effector domain, restores up to 67% of the granule K^{+} transport capacity in the presence of 3mM ATP. These peptides also promoted (116%) the rate of in vitro fusion between granules and apical membrane (R18 dequenching or solubilization of the granule matrix) when incubated in 150 mM KCl (pH 7.0, 37°C) solutions but not when 300 mM sucrose replaced KCl in solution. The data therefore suggest that GTP hydrolysis by a g-protein, possibly the granule rab3B, promotes K^{+} transport and membrane fusion in vitro. (Supported by NIH GM 50952)

W-Pos294

CHARACTERISTICS OF A MEMBRANE RESERVOIR STUDIED BY MEMBRANE TETHERS EXTRACTED BY A LASER TWEEZER TRAP ((D. Raucher and M. P. Sheetz)) Department of Cell Biology, Duke University, Durham, NC 27710

Tether formation and elongation result from membrane moving into the tether. To better understand where tether membrane is drawn from, it is necessary to characterize dependence of the tether force on tether length. In the chick embryo fibroblasts and 3T3 fibroblasts the maximum tether lengths that can be pulled are in the range of 3-15 microns. The force vs. tether length curve consists of three parts. After the initial tether formation there was a small increase in force with increasing length. Then there was a plateau where tether elongation does not affect tether force, suggesting that membrane is drawn from currently unknown membrane reservoir. Finally, there is an abrupt exponential rise in force that brings the tether out of the trap, indicating depletion of the membrane reservoir. When the same bead was used to form multiple tethers, there was linear increase in tether lengths with the number of pulls. Increase in tether length resulted in elongation of the plateau in the force vs. length profile, suggesting that application of force on membrane through membrane tethers increased the area of the cell membrane. Increasing the area of cell membrane by formation of multiple tethers on one side of the cell resulted in longer tethers on the other side of the cell. We suggest that plasma membrane reservoir is continuous through the cell. We have examined effects of alterations of the cytoskeleton organization on the amount of that membrane reservoir. When cells are treated with cytochalasin B or D tether length increased dramatically. Similarly, treatment of the cells with colchicine and nocodazole resulted in more than two fold increase in tether length. These results indicate that membrane-cytoskeleton interaction is important factor in regulation of the amount of membrane reservoir. We have also examined membrane dynamics, using a new tracking system. We have applied a high force to a tether and measured the rate of elongation of the tether as a function of tether force. From these studies we find that the rate of increase of plasma membrane area is proportional to the tension applied through the tether.

MEMBRANE FUSION

W-Pos295

THE TARGET MEMBRANE INFLUENCES THE pH-DEPENDENCE AND KINETICS OF VIRAL FUSION. ((I. PLONSKY[1], E. LEIKINA[1], A.G.P. Oomens[2], G.W. BLISSARD[2], J. ZIMMERBERG[1], L. CHERNOMORDIK[1])) [1]NICHD, NIH, Bethesda, MD 20892; [2]Boyce Thompson Institute, Cornell Univ., Ithaca NY 14853.

To investigate the effects of the target membrane on virus-induced cell-cell fusion, we expressed OpMNPV baculovirus envelope glycoprotein GP64 in stably transfected Sf9 cells (Op-1D cell line). Fusion of Op-1D cells with wild type Sf9 cells and with human erythrocytes has been studied by fluorescence microscopy (fusion extent was assayed as a fluorescent lipid redistribution from labeled to unlabelled cells), and by time-resolved admittance measurements. For the Op-1D/erythrocyte combination, the pH dependence of the extent of fusion was shifted to less acidic by ~ 0.4 pH units, compared to Op-1D/Sf9. In spite of this striking difference in pH dependence, we found identical distributions of initial fusion pore conductance in both pairs, with mean conductances of 1.3 nS for both. For both target membranes, the initial fusion pore never flickered. However, waiting times from pH delivery to fusion pore appearance did change significantly: 0.16-4.65 s with a median of 0.440 s for Op-1D/erythrocyte fusion and 0.27-5.34 s, median of 0.883 s for Op-1D/Sf9 fusion. Our results indicate that the target membrane does not determine initial pore conductance but affects pH-dependence and fusion pore kinetics.

W-Pos296

Low temperature-arrested stage of influenza hemagglutinin mediated cell-cell fusion is subsequent to the lipid-sensitive fusion stage but prior to lipid mixing and fusion pore formation ((Eugenia A. Leikina[1], Vadim Frolov[1,2], Joshua Zimmerberg [1]& Leonid V. Chernomordik[1])) [1] LTPB, NICHD, NIH, Bethesda, MD 20892; [2] Frumkin Institute of Electrochemistry, RAS, Moscow, Leninsky pr-t 31, 117071, Russia

We have recently identified and isolated a pH-independent stage of hemagglutinin (HA)-mediated fusion, which is subsequent to conformational changes in HA upon its activation but precedes lipid mixing and fusion pore formation, and dramatically depends on membrane lipids. We have found now that if fusion of HA-expressing cells to erythrocytes was triggered by low pH medium at temperatures below 6° C, the reaction stopped at a stage downstream of this lipid-dependent stage but upstream of lipid mixing (including hemifusion) and fusion pore formation. Fusion proceeded to full completion upon warming of cells. In contrast to the lysophosphatidylcholine-arrested fusion stage, the low temperature-arrested stage can be transformed into complete fusion by application of osmotic shock. Low pH conformation of HA was required to achieve and to stabilize the low-temperature-arrested state, and to complete fusion upon warming. We hypothesize that at low temperature, fusion is arrested at a stage following lipid-dependent formation of a stalk intermediate, surrounded and supported by a fence of low pH conformations of HA assembled around the fusion site. Because of this fence, lipid mixing between membranes is severely hindered in this fusion intermediate until its expansion into an extended hemifusion diaphragm or until a fusion pore opening.

W-Pos297

PALMITOYLATION OF THE CYTOPLASMIC DOMAIN OF INFLUENZA VIRUS HEMAGGLUTININ (HA) INCREASES FUSION PORE FLICKERING.

((G.B. Melikyan,[1] H. Jin,[2] R.A. Lamb,[2] and F.S. Cohen.[1])) [1]Rush Medical College, Physiology, Chicago, IL. [2] Northwestern U., HHMI, Evanston, IL.

The fusion protein HA consists of three domains: ecto, transmembrane (TM), and cytoplasmic tail (CT). There are two cysteines in the ten residue CT of A/Udorn/72 HA and a third which resides within the TM domain near its interface with the CT. These three cysteines are conserved amongst different strains of influenza and are palmitoylated. To test the role of the CT in formation and evolution of fusion pores, we have both deleted the CT and mutated the three cysteines (to M, A, and Y) to prevent palmitoylation. HA was expressed on surfaces of CV-1 cells by infecting with recombinant SV40-HA. Cell surface densities of WT, CT-, and MAY HA were comparable, as determined by FACS analysis. The role of the CT in fusion was evaluated by monitoring fusion pores connecting HA-expressing cells to planar bilayers. For WT HA, fusion pore flickering preceded irreversible pore opening in 82% of experiments with an average of 5 flickers per planar bilayer. When CT- HA was expressed, flickering occurred in only 17% of the cases with 0.3 flickers per experiment. For MAY HA, flickering occurred in 13% of experiments with 0.25 flickers per bilayer, similar to the values for CT- HA. Once pores irreversibly opened, pore properties were the same for WT, CT-, and MAY HA. We conclude that acylation of the CT is essential for pore flickering, but that the CT does not affect growth of enlarged pores. Supported by NIH GM 27367, GM 54787, and AI20201.

W-Pos298

PROBING A HEMIFUSION-LIKE STAGE BETWEEN CELLS EXPRESSING INFLUENZA HEMAGGLUTININ (HA) AND RED BLOOD CELLS (RBCs).

((G.B. Melikyan, S.A. Brener, B.N. Deriy, and F.S. Cohen)) Dept. Physiol., Rush Medical College, Chicago, IL 60612. (Spon. By S. Popov).

Influenza virus HA induces membrane fusion at low pH. When fusion between RBCs and HA-expressing cells was triggered by lowering pH to 5.0 at 37 °C, both membrane (R18) and aqueous (carboxyfluorescein and rhodamine-tagged dextran, MW 40,000) dyes redistributed. However, when fusion was triggered at room temperature, membrane dye readily spread from RBCs to HA-expressing cells whereas the small aqueous dye was still confined to the majority of RBCs 5 - 8 min after the trigger. We refer to this hemifusion-like phenotype as "stunted fusion." Stunted fusion was converted into full fusion (spread of aqueous dye) by adding a low concentration (≈ 50 μM) of chlorpromazine (CPZ). CPZ also induced the conversion of true and stable hemifusion between RBCs and GPI-HA expressing cells to full fusion, but at significantly higher concentrations (≈ 500 μM). Increasing the concentration of CPZ resulted in large pores for stunted fusion whereas for stable hemifusion only small pores formed, as judged by the movement of small and large aqueous dyes. Thus, stunted fusion with wild type HA is different from the stable hemifusion caused by GPI-HA. Whole cell patch clamp experiments are in progress to determine whether small, unenlarged, fusion pores have formed in stunted fusion or whether an unstable hemifusion intermediate has occurred. Supported by NIH GM27367 and GM54787.

W-Pos299

STRUCTURAL STUDIES ON MEMBRANE-EMBEDDED INFLUENZA HEMAGGLUTININ AND ITS FRAGMENTS

((C. Gray, W. Rinehart, and L.K. Tamm)) Dept. of Mol. Physiol. and Biol. Physics, Univ. of Virginia Health Sciences Center, P.O. Box 10011, Charlottesville, VA 22906-0011

The mechanism of influenza virus hemagglutinin (HA)-mediated membrane fusion has been inferred in part from studies examining pH-induced structural changes in soluble HA derivatives lacking the viral membrane anchor and, sometimes, the fusion peptide (the C- and N-terminal residues of the HA2 subunit, respectively). To reconcile the mechanism of HA-mediated membrane fusion with functional studies performed on membrane-embedded HA in terms of structural changes, we have undertaken attentuated total reflection Fourier transform infrared (ATR-FTIR) spectroscopic analyses of membrane-embedded HA (strain X31) and its fragments reconstituted into supported lipid bilayers. The fragments correspond to proteolytic products with the majority of the HA1 subunit and, in some cases, the fusion peptide removed (THA2 and THA2^{F-}, respectively). In combination with R18 fluorescence dequenching to monitor the functional implications of HA1 subunit removal, we have assessed the influence of pH and target membrane presentation on the secondary structures, orientations, and dynamics of these molecules. We find that X31 HA and its triple coiled helical stem are more tilted towards the plane of the membrane under fusion than under resting conditions, and that several changes in the H/D exchange kinetics occur that can be interpreted as subtle changes in the dynamics of several elements of secondary structure as a result of acidification and target membrane presentation.

W-Pos300

MEMBRANE DESTABILIZATION BY CYTOPLASMIC α-HELIX OF MoMuLV ENVELOPE PROTEIN.

T. A. Mirzabekov[1], Y. Y. Rozenberg[2], Y.-L. Zhang[3], H. Aguilar[2], W. Hubbell[3], and W. F. Anderson[2]. [1]Dept. of Physiology, and [3]Jules Stein Eye Inst., UCLA School of Medicine, 760 Westwood Plaza, Los Angeles, CA, 90095, and [2]Gene Therapy Laboratories, Norris Comprehensive Cancer Center, USC School of Medicine, Los Angeles, CA 90033.

Moloney Murine Leukemia Virus (MoMuLV) envelope protein (env) catalyze the fusion of viral envelope with the host cell membrane. We found that the synthetic peptide 598-616 corresponding to the cytoplasmic region of the evn has strong membrane destabilizing activity. This peptide adopted amphiphilic α-helical structure in the presence of liposomal membranes, but not in aqueous environment. α-Helix half way embedded into the membrane parallel to the membrane surface. Electrophisiological studies demonstrated that 598-616 peptide has strong membrane destabilizing activity similar to the activity of such lytic peptides as magainin and melittin. At 5 μM concentration 598-616 peptide induced approx. 60% release of K$^+$-from large unilamellar liposomes formed from PC/PS/PE=3/1/1. Lytic activity of the env peptide was higher on the membranes containing negatively charged lipids. At 1-3 μM concentrations the peptide increased planar bilayer membrane conductance in non-ion selective manner, with a following membrane disrupture.

Substitution of the proximal domain of the MoMuLV env by a amphiphilic α-helix of melittin produced fusion-competent virions indicating that the cytoplasmic region is determined by its secondary structure.

W-Pos301

LIPOPHOSPHOGLYCAN OF *LEISHMANIA DONOVANI* INHIBITS LIPID VESICLES FUSION INDUCED BY THE N-TERMINAL EXTREMITY OF VIRAL FUSOGENIC HIV AND SIV PROTEINS.

((MARTIN I, TURCO S.[1], EPAND R. M.[2], RUYSSCHAERT J-M.)) Laboratoire de Chimie-Physique des Macromolécules aux Interfaces CP206/2, Université Libre de Bruxelles. 1050 Brussels, Belgium. [1]Department of Biochemistry, University of Kentucky, College of Medecine, Lexington, Kentucky 40536, USA. [2]Department of Biochemistry, McMaster University, Health Sciences Centre, 1200 Main Street West, Hamilton, Ontario, Canada L8N3Z5.

Lipophosphoglycan (LPG), the major glycoconjugate of *Leishmania* parasites, was recently shown to be a potent inhibitor of viral membrane fusion. To understand the mechanism by which this natural membrane amphiphilic compound inhibits viral fusion, the effect of LPG on the vesicle lipid mixing-induced by HIV/SIV fusion peptide was studied. LPG was an effective inhibitor of lipid mixing at very low concentrations in the fusion buffer whereas depolymerized LPG was ineffective. Fourier transform infrared spectroscopy revealed that LPG modifies the structure and the orientation of HIV/SIV fusion peptides although the viral peptides still interact with the lipid membrane. Taken together, these results provide additional evidence that LPG influences membrane structure through its inherent property as a bilayer stabilizer.

W-Pos302

ACTIVATION OF APPARENT LIPOSOME FUSION BY ENZYMATIC CLEAVAGE OF A NOVEL PEPTIDE-LIPID

((Charles C. Pak, Andrew S. Janoff, Shaukat Ali, Paul Meers)) The Liposome Company, 1 Research Way, Princeton, NJ 08540-6619 (Spon. C. C. Pak)

Development of liposomes that can be specifically triggered to fuse with cell plasma membranes at sites of therapeutic intervention is an important goal for gene and drug delivery. Dioleoyl phosphatidylethanolamine (DOPE) is known to promote liposome-liposome and liposome-cell fusion. We hypothesized that covalent linkage of DOPE to a peptide sequence recognized by an enzyme would render the lipid non-fusogenic until enzyme mediated removal of the peptide reactivates the fusogenicity. To test this hypothesis DOPE was conjugated to an elastase substrate, N-acetyl-ala-ala-, via an amide linkage. Elastase is an abundant enzyme released by activated neutrophils in acute infections and in chronic inflammatory conditions, such as rhematoid arthritis. The resulting peptide-lipid (N-Ac-AA-DOPE) differed from DOPE in its ability to form stable liposomes at pH 7.4 and its lack of fusion activity in liposome-liposome fusion models. Cleavage of N-Ac-AA-DOPE and concomitant conversion to DOPE by human leukocyte elastase was detected by thin layer chromatography. Proteinase K, a protease with similar substrate specificity, could also cleave N-Ac-AA-DOPE, as monitored by HPLC. Several liposomal compositions containing N-Ac-AA-DOPE were tested for their ability to fuse with acceptor liposomes or with erythrocyte ghosts using the N-NBD-PE/N-Rho-PE resonance energy transfer assay. Liposomes containing N-Ac-AA-DOPE, the cationic lipid dioleoyl trimethyl ammonium-propane (DOTAP), and DOPE (1:1:3 mol ratio) appeared to fuse with acceptor liposomes (phosphatidylserine (PS)/DOPE (1:4 mol ratio)) after co-incubation with proteinase K but not in the absence of the protease. Control liposomes substituting dioleoyl phosphatidylcholine (DOPC) for DOPE did not display lipid mixing with acceptor liposomes in the absence or presence of proteinase K. Experiments are underway to monitor the fusion of DOTAP/N-Ac-AA-DOPE/DOPE liposomes with erythrocyte ghosts. These observations suggest fusogenic lipids conjugated to enzyme substrates may serve as triggerable fusion systems that may be used as specific gene and drug delivery vectors.

W-Pos303

THE MECHANISM OF THE LAMELLAR/INVERTED HEXAGONAL PHASE TRANSITION AND ITS RELATIONSHIP TO MEMBRANE FUSION: EVIDENCE FROM TIME-RESOLVED CRYOELECTRON MICROSCOPY, NMR AND DSC. ((D. P. Siegel[1] and R. M. Epand[2])) [1]Procter & Gamble Co., P.O. Box 538707, Cincinnati OH 45253, [2]Dept. of Biochemistry, McMaster Univ., 1200 Main St. West, Hamilton ON L8N 3Z5, Canada.

Recent theoretical work (D. Siegel, MS in preparation) suggests that this transition proceeds via formation of so-called "stalk" and TMC (hemifusion) intermediates [1]. TMC intermediates are thought to play a critical role: they either rupture to form fusion pores that mediate transitions to the Q_{II} phase [2-3] or assemble into a novel kind of array that elongates into bundles of H_{II} phase tubes. The relative rates of these two pathways determine the prevalence of Q_{II} vs. H_{II} phase for a given lipid composition. The TMC intermediate is also thought to be a critical intermediate in membrane fusion [1]. We attempted to verify this transition mechanism by imaging the predicted arrays of TMCs. We triggered the L_α/H_{II} phase transition in dispersions of DiPOPE LUVs at temperatures near the transition temperature T_H, and compared the dynamic morphology imaged via time-resolved cryo-TEM with data from time-resolved phosphorous ^{31}P NMR, as well as DSC. We observed large numbers of transient intermediates compatible with TMC structure forming within seconds. These were present in unordered aggregates and in what appear to be ordered arrays, at $T < T_H$, as predicted by the theory. The NMR data on acidified LUV dispersions show that these intermediates are transient: acidification at T below T_H broadens the transition (DSC), but does not induce isotropic intermediates with lifetimes longer than ca. 1-5 min (NMR). These results support the stalk/TMC fusion model, and suggest that the curious hysteresis in Q_{II} phase evolution in phospholipids is due to composition-dependent differences in TMC stability. [1] Biophys. J. 65:2124 (1993); [2] Chem. Phys. Lip. 42:279 (1986) [3] Biochem. 29:5975(1990).

W-Pos304

EVOLUTION OF LIPIDIC STRUCTURES DURING MODEL MEMBRANE FUSION AND THE RELATION OF THIS PROCESS TO CELL MEMBRANE FUSION. ((JinKeun Lee and Barry R Lentz)) Department of Biochemistry & Biophysics, University of North Carolina, Chapel Hill, NC 27599-7260.

Poly(ethylene glycol)(PEG)-mediated phosphatidylcholine vesicle fusion is a simple model (no protein, no solvent, no ionic complexes) for more complicated biomembrane fusion processes. PEG is a highly hydrated polymer that can bring vesicle membranes to near molecular contact, but is unable to induce vesicle fusion without manipulations that reduce packing density and encourage molecular motions in the backbone regions of both contacting membrane leaflets. Once this condition is achieved, the sequence of events involved in vesicle fusion is shown here to be: 1] outer leaflet mixing accompanied by 2] transient pore formation, both on a time-scale of <10 seconds; followed by 3] a 1-3 minute delay; leading to 4] inner leaflet mixing on a time-scale of ca. 100 seconds; and 5] contents mixing on a time-scale of 200-300 seconds, depending on the size of trapped aqueous markers. Inner leaflet mixing, which has never before been shown to be distinct from outer leaflet mixing, begins simultaneously with, but is completed before, contents mixing. This sequence of events for pure lipid bilayer fusion shows remarkable homology to what is known about the sequence of protein-mediated cell membrane fusion events, suggesting a commonality between these two processes. Supported by USPHS grant GM32707.

W-Pos305

LATROTOXIN-LIKE BRAIN PROTEIN AND ITS FUSOGENIC ACTIVITY. ((Ya. Terletskaya, I. Trikash, M.Malysheva, L.Kolchinskaya, T.Kastrykina, and N. Glyvuk)) Dept. of Neurochemistry, Bogomolets Institute of Physiology, 252024, Kiev, Ukraine. (Spon. by Y. Sokolov)

The fusion of synaptic vesicles with a presynaptic membrane is known to be one of the main steps in the mechanism of neurotransmission secretion. A number of intracellular proteins were shown to participate in this process and some of them possess a fusogenic activity. A cytoplasmic protein interacting with polyclonal antibodies against alpha-latrotoxin has been isolated from bovine brain earlier. This protein (alpha-latrotoxin-like, or L-protein) was suggested to be the alpha-latrotoxin intracellular analog. It was shown that L-protein is a sufficiently good as cAMP-dependent protein kinase substrate. The fusogenic activity of the protein was determined from the extend of mixing of negatively charged liposomes in the presence of native phosphorylated protein preparations. It was shown that this protein promoted fusion of negatively charged liposomes and the rate of fusion in the presence of native preparation increased under the acidification of the incubation media. the phosphorylation of the L protein dramatically decreased its fusogenic activity at pH 7.5 but increased it at pH 6.0. We suggest that this protein might play certain role in the process of secretion. Possible regulatory role of the phosphorylation in its functioning is discussed.

W-Pos306

GROWTH OF FUSION PORES CONNECTING MEMBRANES OF DIFFERENT TENSIONS. ((Yu. A. Chizmadzhev[1], D. A. Kumenko[1], L. Chernomordik[2], J. Zimmerberg[2], F.S. Cohen[3])) [1]Frumkin Institute of Electrochemistry, RAS, Moscow, Leninsky pr-t 31, 117071, Russia; [2]LTPB, NICHD, NIH, Bethesda, MD, 20892; [3]Department of Molecular Biophysics and Physiology, Rush Medical College, 1653 W. Congress Parkway, Chicago, IL 60612.

The tensions of two fusing membranes will in general be different. Tension will affect the dynamics of pore growth and will control the rate of lipid movement from one membrane to another. The role of tension in these processes is generally ignored. For example, lipid flux as a result of fusion is invariably described as a diffusive process, whereas lipid should flow when tension is present. We have calculated the time course of pore growth and lipid flux when a gradient of tension exists between fusing membranes. Lipid movement was described by Navier-Stokes using as a boundary condition a balance of forces at the edge of a toroidal pore. The predicted rate of lipid movement is significantly faster than predicted by diffusion. Fusion pores were calculated to grow under a driving force given by the gradient of energy where the boundary condition is again given by a balance of forces. The theoretically predicted lipid fluxes and pore growth are compared to experiment.

W-Pos307

ALCOHOLS PROMOTE HEMIFUSION OF LIPOSOMES TO PLANAR LIPID BILAYERS. ((A.N. Chanturiya, J. Zimmerberg and L.V. Chernomordik)) LCMB, NIH, Bethesda, MD 20892

We have studied hemifusion of lipid vesicles to planar lipid membranes, which is supposed to be an intermediate to complete fusion. Fusion was assayed by fluorescence microscopy of liposomes containing a fluorescent lipid (rhodamine phosphatidylethanolamine - RhPE) in the membrane and, in some experiments, a water-soluble fluorescent dye (calcein) in the inner aqueous volume. Hemifusion probability increases dramatically in the presence of different alcohols added between contacting membranes. Addition of 1.5-2% methanol to the compartment of the chamber containing liposomes (cis) resulted in a 5-50 times increase in the number of RhPE flashes characteristic for hemifusion, for all tested liposome preparations. Trans- side addition of alcohol did not affect rate of hemifusion. The promotion of hemifusion by alcohols was observed even in the absence of divalent ions in the buffer (containing 1 mM EDTA). Of two isoforms of propandiol, 1,2 propandiol, which incorporates into membranes, induced approximately 9 times more RhPE flashes then the 1,3 isomer. We suggest that alcohols facilitate membrane merger by facilitating formation of hydrophobic defects in the membrane and by reducing the energy barrier for formation of a hypothetical stalk intermediate, a local and transient connection between two contacting monolayers of membrane.

W-Pos308

ISOFORM-SPECIFIC INTRACELLULAR VESICLE FORMATION BY Ca²⁺/PHOSPHOLIPID BINDING PROTEIN, ANNEXIN XI-A, IN SF9 CELLS. ((T.Sudo, N.Mamiya, M.Goto, Y.Watanabe and H.Hidaka)) Department of Pharmacology, Nagoya University School of Medicine, Nagoya 466, Japan.

Annexins are a group of structurally related proteins that bind phospholipids in a Ca^{2+}-dependent manner and have the ability to self-aggregate and to promote vesicle aggregation and membrane fusion. Two isoforms of annexin XI, termed XI-A and XI-B, were previously identified. Annexin XI isoforms differ in amino acid sequence only in the alternative splicing region of the N-terminal regulatory domain. But, little is known about differences in their biological function. In the present study, we report the different subcellular distributions of recombinant annexin XI isoforms and the intracellular vesicle formation by annexin XI-A in Sf9 cells. Annexin XI isoforms were expressed in Sf9 cells using a baculovirus expression system. Most of annexin XI-A distributed in the cytoplasm of Sf9 cells in the presence of EGTA. In the presence of Ca^{2+}, it translocated to plasm membrane. On the other hand, annexin XI-B tightly binded to the plasm membrane in the presence of both Ca^{2+} and EGTA. In addition, annexin XI-A but not XI-B caused formation of spherical 'annexin XI-associated vesicles' in the cytoplasm of Sf9 cells. Calcyclin, the putative light chain of annexin XI, was able to bind both annexin XI isoforms in a Ca^{2+}-dependent manner, although previous study deduced that the calcyclin-binding site was located in the splicing region of annexin XI-A. These findings suggest that this splicing region of annexin XI has distinct biological significance in terms of membrane binding activity.

W-Pos309

BINDING AND FUSION OF N-ACYL PHOSPHATIDYLETHANOLAMINE CONTAINING LIPOSOMES TO BIOLOGICAL MEMBRANES ((T. Shangguan, C. C. Pak, S. Ali, A. S. Janoff, and P. Meers)) The Liposome Company, Inc., Princeton, NJ 08540. (Spon. by T. Shangguan)

N-acyl phosphatidylethanolamines (NAPEs) are natural lipid components of many organisms. N-acylation of unsaturated phosphatidylethanolamines with a saturated fatty acid converts them from non-lamellar phase lipids into lamellar phase, acidic lipids which can interact with cations and potentially return to non-lamellar structures and/or expose the hydrophobic N-acyl chain. These special properties of NAPEs make them candidates for fusogens. We have tested the binding and fusion ability of liposomes containing one of the NAPEs, N-dodecanoyl-dioleoylphosphatidylethanolamine (N-C12-DOPE) and dioleoylphosphatidylcholine (DOPC). At least 50-60 mol% of N-C12-DOPE was required for binding and fusion to erythrocyte ghosts in the presence of 3 mM Ca^{2+}. Fusion was not observed when phosphatidylglycerol or phosphatidylserine was substituted for the N-acyl lipid, indicating specificity for the properties of this lipid. Binding and fusion of N-C12-DOPE/DOPC (70:30) liposomes to erythrocyte ghosts were both divalent cation- and pH-dependent, whereas binding and apparent fusion with nucleated U-937 cells occurred in a partially Ca^{2+}-independent manner. Delivery of encapsulated dextrans to erythrocyte ghosts was achieved with 1.25 mM Ca^{2+}/Mg^{2+}. These data suggest that NAPE-containing liposomes may be used potentially as delivery vehicles for therapeutic agents.

W-Pos310

"SERUM INHIBITION" OF CATIONIC LIPOSOME MEDIATED TRANSFECTION IS RELATED TO THE SIZE OF THE LIPOSOME-DNA COMPLEX. ((P.C. Ross and S.W. Hui)) Biophysics Department, Roswell Park Cancer Institute, Buffalo, NY 14263.

Delivery of plasmid DNA into cells via cationic liposomes is strongly affected by the presence of serum. In systems where cationic liposomes composed of mixtures of dioleoyl-trimethylammonium propane (DOTAP) and several helper lipids were used as vectors to carry the reporter gene β-galactosidase (pSV-βGAL), the sizes of the complexes formed upon addition of the reporter gene were found to be related to the ability of the complex to transfect cultured CHO in different media. Complexes with phosphatidylethanolamine (PE) helper lipids and sizes below 700 nm in diameter were found to be more successful than larger complexes in their ability to deliver the reporter gene, with or without the presence of serum in the media, and whether SUV's or MLV's were used. Upon the addition of the endocytosis-inhibiting compound cytochalasin B, transfection rates were found to be stable in PE containing complexes but were completely inhibited when dioleoylphosphatidylcholine (DOPC) was used as a helper lipid. Resonance energy transfer studies indicate that the rate of cell-complex fusion is higher among PE containing complexes than among PC containing complexes. The results establish a mode of delivery whereby the ability of the helper lipid to cause fusion among bilayers in certain cell culture media is of great importance in the ultimate transport of the reporter gene into the cell. The size of the complexes is the determining factor in fusion efficiency. We may overcome the serum barrier of cationic liposome mediated transfection, by simply regulating the complex size.

W-Pos311

ENDOCYTOSIS AND PHOTOACTIVATED FUSION OF PHOTOSENSITIVE LIPOSOMES. ((C.R. Miller, P.J. Clapp, K. McGovern and D.F. O'Brien)) Departments of Chemistry and Biochemistry, University of Arizona, Tucson, Arizona 85721.

We have previously shown that photolysis of photosensitive liposomes composed of dioleoylphosphatidylethanolamine (DOPE) and 1,2-bis[10-(2'-hexadienoyloxy)decanoyl]-sn-glycero-3-phosphatidylcholine (bis-SorbPC) decreases the temperature for the onset of rapid liposome fusion, T_f, by 15-20°C [Bennet and O'Brien, (1995) Biochemistry 34, 3102; Miller et al. (1996) Biochemistry 35, 11782]. The photolysis of appropriately designed liposomes can significantly increase the rate of fusion at 37°. Here we report studies of visible light photolysis of photosensitive liposomes in tissue culture with HeLa cells. Since positively charged liposomes were more readily endocytosed than neutral or anionic liposomes, visible light sensitive liposomes were prepared from DOPE, bis-SorbPC and the cationic dye, DilC(18)3. The pathway for liposomal uptake appears to be receptor-mediated endocytosis since agents which raise the pH of endosomes block the acidification of liposome-encapsulated HPTS. This suggests that cytoplasmic delivery of liposome contents requires liposome-endosome fusion. Circumstances that favor the photoactivated fusion of liposomes with HeLa cell endosomes will be discussed.

W-Pos312

COMPARISON OF NOVEL INNER MONOLAYER FUSION ASSAYS WITH OTHER LIPOSOMAL FUSION ASSAYS ((Paul Meers* and Tong Shangguan)) The Liposome Company, 1 Research Way, Princeton, NJ 08540-6619 (Spon. P. Meers)

We have introduced the use of inner monolayer fluorescent labeling as a novel method to measure lipid dilution resulting from membrane fusion. These assays eliminate the potential artifacts that result from exposure of the fluorescent probe on the outer monolayer of labeled vesicles and are potentially useful to accurately monitor liposome-cell fusion. They also eliminate potential problems with aqueous probe leakage during fusion. Inner monolayer fusion assays were compared with aqueous contents mixing assays and standard bilayer labeled lipid dilution assays utilizing liposomes composed of brain phosphatidylserine (PS) and phosphatidylethanolamine (PE) transesterified from egg phosphatidylcholine. The apparent lipid dilution fusion rate of bilayer-labeled PS/PE (1/3) liposomes induced by 3 mM Ca^{2+} was much faster than inner monolayer-labeled liposomes. Thus, a significant portion of the observed lipid dilution may result from probe exchange or hemifusion under these conditions. The rate and extent of fusion obtained with the inner monolayer assays were much closer than the bilayer labeled assays to those obtained from aqueous mixing assays (Tb^{3+}/dipicolinic acid and ANTS/DPX). However, there were also some significant differences between the inner monolayer assays and the aqueous mixing assays, particularly at early times. Some speculations on the reasons for these differences and their potential relevance to the mechanism of fusion will be presented, as well as results of liposome-cell fusion monitored by inner monolayer fusion assays.

W-Pos313

CATIONIC LIPOSOME MEDIATED DRUG DELIVERY (([1]Campbell, Robert B. and [1,2]Straubinger, Robert M.)) [1]Department of Biophysics @ Roswell Park Cancer Institute and [2]Department of Pharmaceutics,State University of NY @ Buffalo).

Liposomes have demonstrated the ability to increase the solubility of paclitaxel in water and to enhance the therapeutic effect of taxol (paclitaxel). Liposomes therefore may offer significant clinical benefit for treatment of a wide range of neoplastic diseases. Efforts to develop safe and more stable liposome based paclitaxel formulations, with the use of cationic lipids are now being investigated. Circular dichroism, fluorescence spectroscopy, differential interference contrast, and dynamic light scattering were used to investigate the effect of DOTAP, (a cationic lipid) on the physical stability and encapsulation efficiency of DPPC and DOPE liposomes containing paclitaxel. The results show that cationic lipids improve physical stability of paclitaxel in liposomes. Particle size was reduced compared to paclitaxel liposomes of DPPC alone, and the increased growth inhibitory properties of encapsulated paclitaxel were preserved.

Keywords: Cationic liposomes, Paclitaxel, Drug delivery, Non-bilayer structures

W-Pos314

HYDROPHOBIC MISMATCH INFLUENCE DESORPTION RATE OF ANDROSTEROL FROM MONOLAYERS CONTAINING PHOSPHATIDYL-CHOLINES WITH DIFFERENT-LENGTH ACYL CHAINS.

((J.Peter Slotte and Henna Ohvo)) Department of Biochemistry and Pharmacy, ÅBO AKADEMI UNIVERSITY, P.O. Box 66, FIN 20521 TURKU, Finland

Cholesterol is a major component of cell membranes. By interacting with phospholipids, cholesterol modulates their physical properties in the membrane bilayer structure. Hydrophobic interactions are mainly responsible for stabilization of sterol/phospholipid associations in membranes. These interactions are in turn greatly influenced by the hydrophobic length of the interacting molecules. Calorimetric studies have demonstrated that the best hydrophobic fit for cholesterol by a phosphatidylcholine (PC) molecule was obtained with diheptadecanoyl PC [McMullen, T.P.W., Lewis, R.N.A.H. & McElhaney, R.N., (1993) Biochemistry 32, 516-522]. In this study we have examined the effect of hydrophobic mismatch between androsterol and di-saturated PCs (acyl chains from C10:0 to C16:0) on androsterol desorption from monolayers to the subphase. Monolayers contained 33 mol % sterol and were kept at a constant lateral surface pressure of 20 mN/m. β-Cyclodextrin (β-CD) was used as a sterol acceptor in the subphase (0.33 mM). The rate of androsterol desorption was slowest from a di-14:0-PC mixed monolayer (strongest sterol/PC interaction), whereas it was significantly faster (weaker sterol/PC interaction) when the phosphatidylcholine contained longer (di-15:0 or di-16:0) or shorter acyl chains (di-10:0 to di-13:0). These results clearly demonstrate that the strength of sterol/phosphatidylcholine interaction in monolayers was markedly influenced by the hydrophobic length of the interacting molecules.

W-Pos315

THE INTERFACIAL INTERACTIONS OF SPHINGOMYELINS WITH SATURATED ACYL CHAINS. ((J. M. Smaby, M. Momsen, H. L. Brockman, and R. E. Brown)) The Hormel Institute, University of Minnesota, Austin, MN

Previously, we investigated the monolayer behavior of sphingomyelins (SMs) with palmitoyl (16:0), stearoyl (18:0), oleoyl (18:1), or nervonoyl (24:1) acyl chains at 24°C [Smaby, J. M., Kulkarni, V. S., Momsen, M., & Brown, R. E. (1996) Biophys. J. 70: 868-877]. Here, we address how changing temperature (10-30°C) and changing acyl chain length affect the interfacial behavior of SM as determined using a Langmuir-type film balance. SMs containing lauroyl (12:0), myristoyl (14:0), lignoceroyl (24:0), and cerotoyl (26:0) were produced by semi-synthetic methods. Both surface pressure and dipole potential were monitored as a function of lipid molecular area under an argon atmosphere and over a buffered saline subphase. In this temperature range, 12:0 SM displayed only liquid-expanded behavior. Increasing the length of the saturated acyl chain in SM (e.g., 14:0, 16:0, or 18:0) resulted in films that displayed two-dimensional phase transitions of a liquid-expanded to liquid-condensed nature at many of the temperatures in the 10 to 30°C range. SMs with 24:0 or 26:0 acyl chains also displayed two-dimensional phase transitions at 20, 24 and 30°C, but were condensed at 10 and 15°C. Interestingly, the condensed phase produced by the lower temperatures resulted in steeper isotherms but with larger average molecular areas (at surface pressures > 30 mN/m) than that produced when the SMs passed through their two-dimensional phase transitions. Insights into the nature of these different condensed phases were provided by their interfacial elastic moduli of area compressibility. [Supported by USPHS GM-45928 and the Hormel Foundation]

W-Pos316

INVERTED LIPID CONFORMATIONS

((L. Laakkonen and P.K.J. Kinnunen)) Department of Medical Chemistry, Institute of Biomedicine, University of Helsinki, POB 8, FIN-00014 Helsinki, Finland.

Specific conformations of phospholipids, with the two hydrocarbon chains pointing to opposite derections, have been proposed from experimental biological data (Kinnunen 1992, Kinnunen 1994, Rytömaa 1995). The feasibility of such conformations has been studied computationally, both with Monte Carlo and statistical mechanics methods. Results are compared to phospholipid conformations observed in known structures.

REFERENCES:
1. Kinnunen, P.K.J. 1992. Chem.Phys.Lipids 63:251-258
2. Kinnunen, P.K.J. et al., 1994. Chem.Phys.Lipids 73:181-207
3. Rytömaa, M. and P.K.J. Kinnunen. 1995. J.Biol.Chem. 270:3197-3202

W-Pos317

Direct Force Measurements of Molecular Interactions Between Glycolipid Pairs

((Z.-W. Yu, D. Leckband*, S. Ding, and Y. Guo)), University of Illinois at Urbana-Champaign, 61801 and SUNY at Buffalo, Buffalo, NY 14260.

Glycolipids are the primary ligands in selectin-mediated cell adhesion, but recent reports suggest that specific interactions between particular glycolipid pairs may also mediate cell attachment. Such interactions are believed to enhance early cell sticking probabilities prior to the recruitment of receptors into the contact zone. In this work, we used direct molecular force measurements, turbidity assays, and fluorescence microscopy to i) to establish the glycolipid mediation of intermembrane adhesion, ii) to quantify the molecular forces that control those interactions, and iii) to estimate the glycolipid densities required to support cell adhesion. Direct force measurements demonstrated that the calcium-dependent, heterotypic attractive forces between GM_3 and lactosyl ceramide exceed the van der Waals force, but are much weaker than typical receptor-ligand bonds. Homotypic interactions between lactosyl ceramide are of the order of van der Waals forces. Measured attractive forces accounted for the observed heterotypic aggregation of glycolipid-presenting vesicles, and the adsorption of glycolipid vesicles to complementary moieties in supported planar bilayers. The relevance to cell adhesion is considered on the basis of the measured glycolipid density-dependence of intermembrane adhesion.

W-Pos318

LIPID-MEDIATED MECHANISMS FOR AGGREGATION OF INTEGRAL MEMBRANE PROTEINS: Capillary condensation, wetting, and energy dissipation by driven-diffusive proteins

M. C. Sabra, T. Gil, J. H. Ipsen, and O. G. Mouritsen
Department of Chemistry, Technical University of Denmark
Building 206, DK-2800 Lyngby, Denmark

A specific class of microscopic molecular models for lipid-protein interactions in one- and two-component lipid bilayer membranes is investigated by computer-simulation calculations in order to determine which factors, controlled by the lipid phase behavior, may be responsible for aggregation and crystallization of integral membrane proteins. Particular attention is paid to the following possibilities: (i) wetting phenomena and capillary condensation among proteins which lead to effectively attractive joining forces among the proteins, (ii) aggregation phenomena controlled by the entropy gained when annular lipids are detached from aggregating proteins, and (iii) reorganization of protein aggregates when binary lipid bilayers respond to an energy flux provided by externally driven conformational changes within the proteins.

W-Pos319

MONTE CARLO SIMULATION OF MULTIPLE PORES IN A MODEL FLUID MEMBRANE.

((J. C. Shillcock and U. Seifert)) Max Planck Institute for Colloids and Interfaces, Kantstrasse 55, Teltow 14513, Germany.

Transient pores in the membranes of cells and vesicles are produced in techniques such as DNA transfection by application of an electric field. Lipid vesicles may also be made permeable by incorporating known impurities into the bilayer creating regions of packing mismatch that have a significant conductivity.

The growth of stress-induced pores in a two-dimensional model fluid membrane is investigated by Monte Carlo simulation. The membrane is described by one material parameter: an edge energy per unit length (line tension) of a pore; and an external field is included that couples to the number of minimal-sized pores. The response of the membrane divides into two regimes: at large line tension, the stress produces multiple, quasi-independent small pores that have a large collective conductivity, as found in reversible electroporation experiments; whilst at low line tensions, the pores coalesce into a single large pore that permeabilises the membrane. The results are compared with a theory that indicates the importance of collective interactions among the pores. We predict that entropy contributes significantly to the permeabilisation of fluid membranes in contrast to previous models that are effectively zero-temperature approximations.

W-Pos320

NMR RELAXATION STUDY OF LIPID MEMBRANE DYNAMICS. ((Alexander A. Nevzorov, Stephan Moltke, Theodore P. Trouard, and Michael F. Brown)) Department of Chemistry, University of Arizona, Tucson, Arizona 85721, USA.

NMR relaxation techniques allow one to study the rich dynamics of lipid membranes encompassing faster acyl chain isomerizations, slower diffusion of single lipid molecules, and collective thermal fluctuations of the bilayer. Various dynamic models including segmental diffusion, molecular diffusion, and two- and three-dimensional (3-D) director fluctuations have been tested on their ability to describe simultaneously the frequency dispersion of the ^{13}C and ^2H R_{1z} relaxation rates for 1,2-dimyristoyl-sn-glycero-3-phosphocholine (DMPC) and 1,2-dipalmitoyl-sn-glycero-3-phosphocholine (DPPC), thus enabling unification of the ^{13}C and ^2H data for lipids.[1] The ^{13}C DMPC R_{1z} values have been predicted and compared to experiment from the results of fitting the models to the ^2H data from 2.5 to 95.3 MHz, and alternatively, ^2H DPPC R_{1z} values have been theoretically calculated from the results of the fits to the ^{13}C data from 15.0 to 151 MHz. Such a unified approach constitutes a rigorous test for the models since it involves different frequency scales and types of interaction, i.e. magnetic dipolar and electric quadrupolar for ^{13}C and ^2H nuclei respectively. The corresponding correlation functions have been calculated and compared to the results of recent molecular dynamics (MD) simulations.[2] The 3-D collective and the molecular diffusion models including the faster local segmental motions describe best the data and yield correlation functions consistent with the MD simulations. However, neither model appears at present capable of fitting simultaneously the R_{1z} frequency dependence and the orientational anisotropy,[3] which emphasizes the need for continued experimental and theoretical investigations. [1] M. F. Brown and S. I. Chan, in Encyclopedia of Nuclear Magnetic Resonance, edited by D. M. Grant and R. K. Harris (Norell, Mays Landing, 1995), Vol. 1, p. 871. [2] R. M. Venable, Y. Zhang, B. J. Hardy, et al., Science 262, 223 (1993). [3] T. P. Trouard, T. M. Alam, and M. F. Brown, J. Chem. Phys. 101, 5229 (1994). Supported by grants from the NSF and NIH.

W-Pos321

MEASUREMENT OF NBD-PHOSPHOLIPID TRANSLOCATION ACROSS YEAST SECRETORY VESICLES. ((C. A. Angeletti and J. W. Nichols)) Dept. of Physiology, Emory University School of Medicine, Atlanta GA 30322

Temperature-sensitive mutations of genes in the secretion pathway of yeast, S. cerevisiae, result in the accumulation of vesicles upstream of the defect following a shift to the non-permissive temperature. We have used the protocol of Nakomoto, Rao and Slayman, J. Biol. Chem., 7940, (1994), to isolate secretory vesicles (SVs) from sec6-4 mutants that accumulate as a result of a defect in fusion with the plasma membrane. The SVs actively transport protons inward in the presence of Mg^{++}-ATP indicating that they contain plasma membrane proteins arranged topologically inside-out. We have applied two different assays to measure the rate and extent of membrane translocation of NBD (7-nitrobenz-2-oxa-1,3-diazol-4-yl)-labeled phospholipids. In the first, resonance energy transfer is used to measure NBD-phospholipid transfer from donor liposomes to SVs. Transfer from donor liposomes to the outer leaflet of the SV membrane is detected as an increase in fluorescence. Movement to the inner leaflet is detected as a second, slower phase of fluorescence increase. The rates and equilibrium distributions measured by this method were confirmed by a second method using dithionite quenching. To avoid potential problems with dithionite leakage across the membrane, initial rates of NBD quenching by dithionite were used to quantify the time dependence of NBD in the outer leaflet. These in vitro assays when combined with the facile genetics of S. cerevisiae provide a powerful approach to understanding the role of phospholipid transport to cellular physiology. (supported in part by NIH grant GM 52410)

W-Pos322

NOVEL FLEXOELECTRICITY OF LIPID BILAYERS INDUCED BY ADSORPTION OF AMPHIPHILIC IONS ((K. Sun and D. Mauzerall)) The Rockefeller University, New York, NY 10021.

The flexoelectricity of lipid bilayers converts mechanical energy to electric energy. This has been hypothesized as a biological mechanoreceptor and a driving force of active transport. We report here the first observation of dramatic sensitivity and voltage dependence to the binding of amphiphilic ions. When AQS$^-$ (anthraquinone-2-sulfonate) is present on one side of the bilayer, an applied voltage with a negative sign on the AQS$^-$ side produces a larger increase of vibrational AC current than in the AQS$^-$ free system. However, a positive voltage of ~30 mV causes a minimum amplitude of the current. If the voltage is increased further, the current amplitude is increased towards that of the AQS$^-$ free system whose minimum amplitude is at 0 mV. In the presence of TCPB$^-$ (tetrakis(p-chlorophenyl)borate), the minimum amplitude at +30 mV can be >10 fold smaller than that at -30 mV. The symmetric addition of TCPB$^-$ greatly increases the vibrational current, but has little effect on its voltage-dependence. Similar phenomena are observed with an amphiphilic cation CQ$^+$ (protonated chloroquine) but with reversed sign of voltage. The voltage for the minimum vibration is determined by charge, structure and concentration of the amphiphilic ion. The voltage-dependent behavior is explained by the relocation and orientation of the ions, which alter the surface tension and polarization of the bilayer. This finding could offer a new tool for probing of adsorption of drugs and biomolecules to lipid bilayers and be helpful for understanding of biological mechanoreception. Supported by NIH GM 25693.

W-Pos323

LATERAL PHASE HETEROGENEITY IN DIPOLYUNSATURATED AND DISATURATED PHOSPHOLIPID BILAYERS MONITORED WITH NOVEL PYRENE-LABELED PHOSPHOLIPIDS. ((C.D. Niebylski and B.J. Litman)) Section of Fluorescence Studies, LMBB, NIAAA, NIH, Rockville MD, 20892.

The mixing behavior of disaturated (di16:0) and dipolyunsaturated (di22:6n3) PCs was studied as a model for lateral packing heterogeneity of lipids in biological membranes. Phospholipid probes were synthesized (Avanti Polar Lipids) as either di16:0- or di22:6n3- phosphatidylethanolamine labeled with pyrene at the headgroup. Probes were characterized at 1 to 10 mol% in di16:0-PC, di22:6n3-PC, or a mixture of both lipids. Pyrene excimer (490nm) and monomer (380nm) emission intensities and fluorescence lifetimes were measured. Both the di16:0Pyr and di22:6Pyr E/M ratios increased in a di16:0-PC matrix as temperature decreased below the T_m of di16:0-PC (42°C). In contrast, neither probe exhibited large changes in E/M ratio when in a di22:6-PC liquid-crystalline matrix. The E/M ratio of di16:0Pyr was higher in a di22:6-PC matrix than in a di16:0-PC matrix at LC temperatures. This result suggests that di16:0-Pyr is non-homogeneously distributed when in the di22:6-PC matrix. On the other hand, the E/M ratio of di22:6Pyr in a LC di16:0-PC matrix was similar to that in a di22:6-PC matrix. Together, these results are consistent with non-homogeneous mixing behavior of di16:0-PC and di22:6-PC in lipid bilayers.

W-Pos324

FLUORESCENCE PHOTOBLEACHING RECOVERY: MONTE CARLO SIMULATIONS ((Michael J. Saxton)) Institute of Theoretical Dynamics, University of California, Davis, California 95616.

Monte Carlo simulations are carried out for fluorescence photobleaching recovery (FPR) measurements of lateral diffusion in the presence of obstacles and traps. Several topics are examined. First, the scatter in diffusion coefficients from statistical variation in the obstacle or trap configuration is evaluated. Second, Nagle [Biophys. J. 63 (1992) 366] used one-dimensional simulations to show that in a continuous-time random walk model of anomalous diffusion, the diffusion coefficient and fractional recovery are highly sensitive to the region of the recovery curve analyzed. Nagle's work is extended to other diffusion models and to two dimensions. Third, for some models of hindered diffusion, diffusion is anomalous at short times and crosses over to normal diffusion at long times. The form of FPR recovery curves is examined to see whether the crossover can be detected. (Supported by NIH grant GM38133)

W-Pos325

BINDING OF DIPYRIDAMOLE TO PHOSPHOLIPID VESICLES AND EFFECT OF THE DRUG UPON THE BILAYER: FLUORESCENCE AND ESR STUDIES. ((Patricia M. Nassar, Luis E. Almeida and Marcel Tabak)). Instituto de Química de São Carlos-USP, Cx.Postal 780, 13560-970 São Carlos-SP,Brasil.

Interaction of the coronary vasodilator dipyridamole (DIP) with vesicles of dipalmitoyl phosphatidylcholine (DPPC) and dimirystoyl phosphatidylcholine (DMPC) has been studied by fluorescence spectroscopy of the drug and ESR spectroscopy with nitroxide radicals. In fluorescence studies the association of DIP to vesicles of DPPC and DMPC, obtained by extrusion, was studied both above and below the phase transition temperature for the lipid. Association constants (K_a) of 1.10^3 M^{-1} were obtained for DMPC both at 20 °C and at 30 °C. For DPPC it seems that the association constant is somewhat greater above the phase transition being also around 1.10^3 M^{-1}. At pH 7.0 the addition of 11% DPPG to the DPPC suspension leads to a decrease of K_a to 800 M^{-1}. Fluorescence quenching with nitroxide radicals TEMPO, 5-doxyl and 12-doxyl stearates strongly support the interfacial localization of the drug closer to the 5th carbon of the alkyl chain. Stern-Volmer constants decrease by a factor of three above the phase transition for the stearate derivatives suggesting strong static quenching. The interfacial localization of the drug as well as the association constants for binding are quite similar to previous results reported both for the interaction of DIP with micelles and phospholipid monolayers (BBA 1238,57,1995;BBA 1278,12,1996). In ESR studies multilamelar phospholipid suspensions were used and probed by 5-DSA in order to monitor the drug effect upon the bilayer. The addition of 10% of DIP shifts the phase transition of DPPC to lower temperatures suggesting a fluidizing effect upon the membrane. This effect could be relevant for the biological activity of the drug associated to its interaction with the cellular membrane.

Support:CNPq, FINEP and FAPESP.

W-Pos326

SPIN LABEL ESR CHARACTERIZATION OF LIPID CHAIN DYNAMICS OF THE INTERCELLULAR AND CORNEOCYTE MEMBRANES OF STRATUM CORNEUM. ((Antonio Alonso[1], Nilce C. Meirelles[2], Marcel Tabak[3])). [1] Instituto de Fisica "Gleb Wataghin", [2] Instituto de Biologia, Universidade Estadual de Campinas, Campinas 13083-970, [3] Instituto de Quimica de São Carlos-USP, São Carlos 13560-970, SP, Brasil.

Lipid chain motions in stratum corneum (SC) membranes have been studied through ESR spectroscopy of spin labeled stearic acids at 5th, 12th and 16th carbon atom positions of the acyl chain. Lipids from SC were extracted with a series of chloroform/methanol mixtures aiming to monitor the lipid dynamics and their thermotropic behavior in the dispersion of extracted lipids as compared to intact SC and lipid-depleted SC. The segmental motion of 5-and 12-doxyl stearic acids as well as the rotational correlation time of 16-doxyl stearic acid showed that the envelope lipids are more rigid and the extracted lipids are more fluid than the lipids of intact SC in the whole temperature range (4-80 °C). Changes in activation energy for reorientational diffusion of 16-doxyl stearic acid showed several membrane phase transitions for the three samples. A preliminary evaluation of the lipid fraction contents of 5-doxyl stearic acid between the SC mebranes showed that at 26 °C more than 70% of spin probes are structured in the envelope membrane, while at 74 °C they are predominantly structured in the intercellular membranes. Our results have contributed to the understanding of alkyl chain packing, mobility and conformational order in SC lipid multilayers, giving a spin label characterization of the fluidity of SC, the main parameter involved in the mechanism that controls the permeability of different compounds through skin.

W-Pos327

INTERACTION OF IRON TETRAPHENYLPORPHYRINE SULFONATE WITH BOVINE SERUM ALBUMIN: MCD AND OPTICAL ABSORPTION STUDIES ((Tania T. Tominaga and Hidetake Imasato)). Instituto de Química de São Carlos-USP, Cx. Postal 780, 13560-970 São Carlos-SP, Brasil

The spectral and photochemical behavior of porphyrins in homogeneous solutions differs from that in organism due to interaction with membranes, macromolecules and other isolated biological structures. In the present work we study the interaction of water soluble Fe(III) derivatives of meso-tetrakis(p-sulfonato phenyl) porphyrin (FeTPPS$_4$) with bovine serum albumin (BSA) the main transport protein in blood at pH 5.0 and pH 9.0 and its dependence on pH by Electronic Absorption Spectroscopy and Magnetic Circular Dichroism (MCD). The convex constraint analysis (CCA) method proposed by Fasman et al was used to decompose the optical and MCD spectra. The presence of three different FeTPPS$_4$ species in BSA solutions at pH 5.0 as well as at pH 9.0 was demonstrated by analysis of both absorption and MCD spectra. The relative concentrations of three species depend on the BSA concentration. However, the spectral difference of these species at pH 9.0 is much lower than at pH 5.0. All three spectral components at pH 9.0 are similar to one of the components at pH 5.0. This allowed us to conclude that at the excess of FeTPPS$_4$ in solution the presence of BSA induces the formation of FeTPPS$_4$ μ-oxo compounds, which were characterized in our previous report [1]. We can conclude that at lower concentration of BSA higher local concentration of porphyrin at the surface of protein favors the dimerization. The dilution effect upon increasing of the BSA concentration leads to the formation of a bound monomer.

[1] Tominaga, T.T; Borissevitch, I.E; Yushmanov, V.E., Imasato, H.; Tabak, M.- Aggregation phenomena in the complexes of iron tetraphenylporphyrine sulfonate with bovine serum albumin. J. Inorg. Biochem. in press

RECONSTITUTION STUDIES

W-Pos328

DIRECT EVIDENCE OF OLIGONUCLEOTIDE MOVEMENT THROUGH A CHANNEL PROTEIN ((E. Leal-Pinto, B. Hanss, L.A. Bruggeman, and P.E. Klotman)) Division of Nephrology, Department of Medicine, Mt. Sinai School of Medicine, New York, NY 10029. (Sponsored by W.B. Thornhill)

A DNA binding protein from renal brush border membrane functions as a selective channel that conducts single stranded oligonucleotides (Oligos) when reconstituted in lipid bilayers. These studies were undertaken to provide direct evidence of DNA movement through the channel by utilizing ^{32}P labeled Oligos. Proteoliposomes were formed with purified protein and reconstituted in a lipid bilayer system (lipids were 1:1 PE:PS in decane). The channel was active only when oligonucleotide (5 μM, 20 mer) was present and activity was evident as clear transitions between open and closed states. When stable activity was observed for 15 minutes, 100 ng of labeled Oligo was added to the trans (ground) chamber and holding potential was clamped at +100 mV. If the membrane remained stable and did not brake, cis buffer was collected and counted by liquid scintillation or used for electrophoresis. Collection periods ranged from 15 to 45 minutes. In 5 experiments open probability was greater than 25% for the entire collection period and the amount of radiolabeled Oligo in the cis chamber (by scintillation) ranged from 1 fmole to more than 22 fmole. In the absence of channel activity, radioactivity was not detected in the cis chamber (n=4). To verify that radioactivity detected by scintillation was associated with Oligo, aliquots of cis buffer were run on sequencing gels (7M urea, 18% acrylamide) and visualized by autoradiography (n=3). In lanes containing cis samples, a band was present that co-migrated with input Oligo and with a labeled 20 mer size standard. Bands were not detected in cis samples from heat inactivated protein controls or when the channel was not active. These data provide direct evidence that oligonucleotides move across a lipid membrane when purified DNA-conducting channel protein is present.

W-Pos329

PROTON CONDUCTANCE IN VESICLES CONTAINING A SINGLE F_0 SUBUNIT OF THE F_0F_1ATPASE ((Nancy Jingyang Cao, William S. A. Brusilow and Dixon J. Woodbury)) Departments of Physiology and Biochemistry, Wayne State Univ. School of Medicine, Detroit, MI 48201.

The F_0 protein, a proton channel of the F_0F_1ATPase, was reconstituted into 200 nm unilamellar vesicles by detergent solubilization and dialysis. Vesicles were formed of 51% PE, 22% PC, 16% PS and 11% cholesterol and sized by a polycarbonate filter. The vesicles, containing 200 mM K-acetate, were added to a low buffer-strength solution that contained 15 mM KCl at pH 6.2. Vesicles were treated sequentially with valinomycin, a K^+ transporter, and CCCP, a proton transporter. Reconstitution was quantified by the pH change that followed addition of valinomycin compared to the total pH change following addition of both drugs. A valinomycin-induced pH increase was observed in the protein containing vesicles compared with the control that showed a CCCP signal only. The valinomycin signal, an indication of proton conduction, was blocked by the F_0 antagonist, DCCD. Protein concentration was manipulated so that half of the vesicles contained only one F_0. Hence, the initial rise in pH is proportional to the single channel conductance of the F_0 subunit. Control vesicles had a proton leak that was dependent on lipid composition, transmembrane potential, and pH gradient. These parameters were adjusted so that the leak was minimal. This assay allows us to compare the proton conductance of the F_0 subunit from cells that produce normal or mutant F_0F_1ATPase. Supported in part by NIH grant MH50003 to DJW.

W-Pos330

RECONSTITUTION OF TRANSMEMBRANE CD4 INTO LIPOSOMES: STUDIES ON EFFICIENCY OF ASSOCIATION. ((C. Larsen, D. Alford, M. Stevenson and C. Nicolau)) CBR Labs, Harvard Medical School, 1256 Soldiers Field Road, Boston, MA 02135.

We produced liposomes containing a reconstituted purified recombinant form of CD4 (tmCD4, composed of the extracellular, transmembrane and truncated cytoplasmic domains) by several methods and under varying buffer conditions. CD4 reconstitution methods included full detergent dialysis, detergent co-extrusion, electroinsertion, passive insertion, organic solvent co-extrusion and co-sonication. Unassociated tmCD4 was removed by column chromatography using Sepharose CL-4B. Recovery of active liposome-associated tmCD4 was determined by a gp120-dependent ELISA. Liposome diameter and population size distribution were determined by dynamic light scattering. Liposomes contained up to at least 50 tmCD4 molecules per liposome (diameter = 100 nm). Incorporation of active tmCD4 was highly dependent on the reconstitution method and the buffer conditions. Several methods resulted in significant (up to at least 50%) recovery of active rtmCD4. CD4-liposome binding to cells expressing gp120 on their surface was solely dependent on the amount of CD4 reconstituted. The results indicate that active reconstitution of a member of the immunoglobulin superfamily containing a single transmembrane spanning region is achievable by a variety of methods.

W-Pos331

AQUEOUS SOLUTE EFFECTS ON THE VESICLE-MICELLE TRANSITION OF EGG PHOSPHATIDYLCHOLINE AND OCTYLGLUCOSIDE. ((Kerri Barnes, Gregg Vanderwaerdt and Anne Walter)) Deparment of Biology, St. Olaf College, Northfield, MN 55057.

The transition from egg phosphatidylcholine (EPC) vesicles to mixed EPC-octylglucoside vesicles was examined as a function of changes in the solute composition of the aqueous medium. Octylglucoside (OG) is a nonionic detergent neither its solubility nor its interaction with the EPC bilayer is expected to be altered by ionic (NaCl) or nonionic (sucrose) aqueous solutes. However, changes in the activity of water may alter the solubility of pure OG and its partition coefficient into EPC bilayers. We measured the cmc of OG using the fluorescent probe (ANS) as a function of aqueous solute concentration. In parallel, large unilamellar vesicles were prepared in each solution and then dissolved by continuous addition of OG while monitoring the scattered light and the energy transfer between two fluorescent probes (0.7 mol% NBD-phosphatidylethanolamine and 0.7 mol% lissamine rhodamine-PE). As [NaCl] increased from 0 to 2 M, the OG cmc decreased from 21.8 to 7.2 mM. As expected with a drop in the cmc, the aqueous [OG] at the point of micelle formation from EPC vesicles, also decreased from 17 to 6 mM. The ratio of OG/EPC in the 'detergent-saturated micelles' changed slightly from 2.25 at 0 NaCl to 3.14 at 2 M NaCl. Additional transition intermediates, including a macroscopic phase separation, appeared at high salt or high sucrose concentrations. Thus, the effects of solutes appear to be on the solubility of OG, and through changes in EPC headgroup interactions within and between vesicles and/or mixed micelles.
Supported by NSF DMB-9206615.

W-Pos332

MINOR PHOSPHOLIPIDS AND THE ACTIVITY OF PULMONARY SURFACTANT. ((R.W. Walters, R.R. Jenq, and S.B. Hall)) Oregon Health Sciences University, Portland, Oregon

Pulmonary surfactant is the mixture of lipids and proteins that coats the alveolar air spaces of the lung. In so doing, surfactant films reduce interfacial tension and the tendency to collapse the alveolus. Films reach particularly low surface tensions during exhalation when the decrease in interfacial area compresses the surface film to very high densities. It has long been recognized that dipalmitoyl phosphatidylcholine (DPPC) is critical for surfactant's ability to reach low surface tensions. DPPC is the only major component of pulmonary surfactant with a melting transition below physiological temperatures. Consequently only DPPC can withstand compression to the high densities observed in the lungs without collapse from the air-water interface. Epifluorescence microscopy allows the detection and monitoring of liquid condensed domains which form during compression and are enriched in DPPC. This compound, however, constitutes only one third of the surfactant phospholipids. The studies reported here address the issue of whether the other phospholipids have any role in the function of pulmonary surfactant.

LIPID-PROTEIN INTERACTIONS

W-Pos333

Diacylglycerol Kinase, a 13 kDa Integral Membrane Protein: Structural and Mechanistic Studies. ((Charles R. Sanders, Prakash Badola, Olga Vinogradova, and Lech Czerski)) Dept. of Physiology and Biophysics, Case Western Reserve University, Cleveland, OH 44106-4970.

Microbial diacylglycerol kinase (DAGK) is a largely helical protein with three transmembrane segments and which can spontaneously insert into pre-formed lipid vesicles (Smith et. al., *J. Bacter.* 176, 5459-5465, 1994; Sanders et. al., *Biochem.* 35, 8610-8618, 1996). DAGK catalyzes the phosphorylation of a lipid (DAG) by MgATP, a reaction which is essential to bacterial proliferation under conditions of environmental stress. In this poster progress in the determination of the structure of this enzyme and in elucidation of its catalytic mechanism are reported. Systematic efforts to identify solution NMR conditions appropriate for structural determination by that route have led to the conclusion that such conditions do not exist, partly because (it is now understood) this enzyme functions as a homotrimer. Based on these observations, we are pursuing DAGK's structure through a combination of both novel and existing solid state NMR and cysteine mutant-based approaches. Preliminary data is presented. Equilibrium binding, steady state kinetic, and kinetic inhibition studies demonstrate that DAGK catalyzes *direct* MgATP to DAG phosphoryl transfer with no enzyme-phosphate intermediate being involved. Furthermore, comparison of DAGK's k_{cat}/K_m with the estimated *in vivo* diffusion-limited rate of DAGK-substrate association leads to the conclusion that DAGK is an evolutionarily-optimized biocatalyst. The rate of transbilayer DAG flip-flop appears to be at least partially rate-limiting for the DAGK reaction *in vivo*. *This work is supported by the American Heart Association (94001540), the Herman Frasch Foundation (340-HF92), and NIH (GM47485). Thanks!*

W-Pos334

PHOSPHATIDYLSERINE (PS) BINDING SITES IN KRINGLE MODULES REGULATE THE DOMAIN ORGANIZATION AND CONFORMATION OF BOVINE PROTHROMBIN. ((Mou Banerjee, Vishwanath Koppaka, Chau-Ming Zhou, and Barry R. Lentz)) Dept. of Biochemistry & Biophysics, University of North Carolina, Chapel Hill, NC 27599-7260.

PS binding acts as critical regulator of prothrombin activation during blood coagulation, first by altering the activity of the activating enzyme (Koppaka *et al.*, Biochemistry, 35, 7483, 1996) and second, by modifying the conformation of prothrombin (Lentz *et al.*, Biochemistry, 33, 5460, 1994). To locate the PS binding site(s) on prothrombin, three methods (trp fluorescence, differential scanning calorimetry [DSC], circular dichroism [CD]) were used to define the structural consequences of soluble d-icaproylphosphatidylserine(C6PS) binding both to whole prothrombin and to its proteolytically generated fragments. The intrinsic fluorescence of prothrombin and its fragments was not sensitive to C6PS. However, the thermal denaturation profile of the N-terminal half of prothrombin (F1.2) suggested a calcium-independent, PS-induced domain reorganization within this fragment. Denaturation profile of the N-terminal, membrane binding domain (F1) and the domain (F2) that links F1 to the catalytic domain did not reveal any PS-induced changes. F2 consists mainly of a cys-rich kringle module, while F1 has an N-terminal γ-carboxyglutamic acid (GLA)-rich region and a kringle module that joins to the F2 domain. Involvement of both kringle modules in PS binding was strongly supported by the series of CD spectra observed at increasing C6PS concentrations for either F1.2 or F1.2 minus the GLA domain. The results show that C6PS 1) binds specifically to linked, calcium-independent sites formed by prothrombin's two kringle domains, and 2) induces thereby a conformational reorganization in the whole molecule. Supported by USPHS grant HL45916.

W-Pos335

A FLUORESCENCE RESONANCE ENERGY TRANSFER STUDY OF PROTHROMBINASE ASSEMBLY ON PS-CONTAINING MEMBRANES ((Jianfang Wang, Qing Chen, and Barry Lentz)) Dept. of Biochemistry & Biophysics, University of North Carolina, Chapel Hill, NC 27599-7260.

Prothrombin (II) is activated to thrombin (II_a) by a platelet-membrane-assembled proteolytic complex. Meizothrombin ($MzII_a$) is a possible membrane-bound intermediate in this process. A fluorescein-labelled double mutant bovine II (F-P[S528A,G581C]) or $MzII_a$ (F-M[S528A,G581C]) was used to address how factor X_a (enzyme) and factor V_a (cofactor) interact with either II or $MzII_a$ to assemble catalytic complexes on phosphatidylserine (PS)-containing model membranes. Eight samples, II (or $MzIIa$), II ($MzIIa$)/X_a, II ($MzIIa$)/V_a, and II ($MzIIa$)/X_a/V_a, were titrated with PS-containing (25%) phosphatidylcholine vesicles having various surface densities of rhodamine (Rh)-labelled phosphatidylethanolamine. All binding isotherms for a particular type of sample were globally simulated to estimate dissociation constants and F-Rh distances for the three possible protein-protein-membrane complexes that contribute to observed energy transfer efficiencies. The results indicated that: 1) factor X_a had no significant effect on II or $MzIIa$ binding or conformational state (reflected in F-Rh distance); 2) binding of membrane-bound V_a or the membrane-bound V_a-X_a complex to II was much weaker than to $MzIIa$ (K_d ~ 1μM *versus* 0.1μM); and only the F-Rh distance for membrane-bound $MzII_a$ was significantly altered by either membrane-bound V_a or V_a-X_a complex. These results imply that one effect of factor V_a on the rate of prothrombin activation may be to channel $MzII_a$ to the catalytic complex, while a second effect may be to optimize $MzII_a$ conformation as a substrate. Supported by USPHS grant HL45916.

W-Pos336

LIPID SORTING BY BACTERIORHODOPSIN

M. M. Sperotto,[1] F. Dumas,[2] C. Lebrun,[2] J.-F. Tocanne,[2] and O. G. Mouritsen[1]

[1]Department of Chemistry, The Technical University of Denmark, DK-2800 Lyngby, Denmark, and [2]Institut de Pharmacologie et Biologie Structurale de CNRS, Toulouse, France

A combined experimental and theoretical study based on fluorescence spectroscopy and microscopic model simulation is performed on binary DLPC-DSPC lipid bilayer membranes incorporated with bacteriorhodopsin (BR). The aim of the study was to investigate the possibility that BR, via a hydrophobic matching principle related to the difference in lipid bilayer hydrophobic thickness and protein hydrophobic length, can perform molecular sorting of the lipids at the lipid-protein interface which implies a lipid specificity/selectivity that is solely controlled by physical factors. The combined results of the experiments and the calculations provide evidence for a molecular sorting principle being active due to hydrophobic matching leading to an enrichment of one of the lipid species at the lipid-protein interface. The results are discussed in the general context of membrane organization and compartmentization and in terms of nanoscale lipid-domain formation.

W-Pos337

SPECIFIC ROLES OF PALMITIC ACID AND LYSOLECITHIN ON BILAYER HYDROLYSIS BY PHOSPHOLIPASE A2. ((J.B. HENSHAW and J.D. Bell)) Dept. of Zoology, Brigham Young University, Provo, Utah 84602

The rate of hydrolysis of dipalmitoylphosphatidylcholine bilayers by phospholipase A_2 (PLA$_2$) increases suddenly by more than an order of magnitude after an initial latency period (tau) when a threshold concentration of the hydrolysis products (X_p), palmitic acid and lysolecithin, have accumulated in the bilayer. The values of tau and X_p both depend on the concentration of calcium. To assess the specific role of each product in evoking the increased activity, we measured two kinetic parameters as a function of calcium concentration at 40 °C. These parameters were (1) X_p for each product and (2) the binding of PLA$_2$ to the vesicle surface (determined by resonance energy transfer from PLA$_2$ to dansyl–phospholipid in the bilayer). In the absence of calcium, palmitic acid, but not lysolecithin, promoted the binding of PLA$_2$ to the bilayer. At 1 μM calcium, 10–15 mol% palmitic acid was able to reduce tau to zero. Lysolecithin also reduced tau, but was much less effective than palmitic acid. In contrast, at 1 mM calcium, palmitic acid alone had no effect on tau, but the value of X_p for lysolecithin was much less than at low calcium. Repetition of the experiment as a function of pH revealed that the ionized and unionized forms of palmitic acid can both reduce tau but by different mechanisms. Furthermore, the unionized form was more effective. These data led us to conclude that both fatty acid and lysolecithin promote susceptibility to PLA$_2$ by perturbing the bilayer structure which enhances calcium–dependent binding of substrate monomers to the enzyme active site. This effect is separate from the additional effect of palmitic acid to increase the initial adsorption of the enzyme to the bilayer surface through electrostatic interactions.

W-Pos338

EFFECTS OF LYSOLECITHIN AND PALMITIC ACID ON THE WATER DYNAMICS OF PHOSPHATIDYLCHOLINE BILAYERS. ((J.D. BELL and C.A. OLSEN)) Dept. of Zoology, Brigham Young University, Provo, Utah 84602

The presence of lysolecithin and palmitic acid in dipalmitoylphosphatidylcholine bilayers increases the susceptibility of the membrane to phospholipase A$_2$. We have investigated steady–state and time–resolved emission spectra of Prodan and Laurdan to study the effects of these lipids on the bilayer to better understand how they influence the susceptibility to phospholipase A$_2$. These probes are sensitive to the dynamics of water molecules in the region of the phospholipid head groups and glycerol backbone respectively. Palmitic acid reduced the interactions between the probes and water in the bilayer. Experiments in which temperature and pH were varied revealed that this effect of palmitic acid involved the protonated state of the lipid and extended beyond the effect of the fatty acid to raise the phospholipid melting temperature. Also, the protonated form of palmitic acid caused a decrease in the partition coefficient of Prodan. In contrast, lysolecithin increased the interactions between water and the fluorescent probes. As with palmitic acid, the effect occurred at all temperatures and therefore was not simply a direct reflection of the reduction in phospholipid melting temperature caused by lysolecithin. When both lysolecithin and palmitic acid were present together in the bilayer, intermediate effects representative of the combined influence of the lipids were observed. Nevertheless, the effect of lysolecithin was more dominant when monitored with Prodan than with Laurdan. These data suggest that protonated palmitic acid enhances phospholipid interactions and increases the spacing between head groups. Lysolecithin appears to reduce interactions between phospholipids with greater influence evident nearer the surface of the bilayer.

W-Pos339

COLIPASE-LIPASE BINDING IN INTERFACES REQUIRES SUBSTRATE. ((M. Dahim and H.L. Brockman)) Hormel Inst.,U. of MN, Austin, MN 55912

Colipase is a cofactor protein which forms a 1:1 complex with lipase. This facilitates lipase adsorption to phosphatidylcholine (PC)-rich interfaces, presumably as a consequence of the higher affinity of colipase for such interfaces. According to this model, the presence of colipase in an interface should be sufficient to enable lipase adsorption from the aqueous phase. To test this hypothesis, mixed monolayers of colipase and PC +/- lipase substrate (S) at the argon-buffer interface and exposed to lipase injected into the stirred aqueous subphase. Spread colipase remained associated with the lipid monolayer in a surface pressure- and lipid composition-dependent manner. For example, with PC alone colipase remained associated with the lipid monolayer at surface pressures ≤ 20 mN/m but with pure S this was increased to ~ 40 mN/m. Contrary to the existing paradigm, the presence of colipase in a lipid monolayer was not sufficient to enable the adsorption of lipase to the interface. S was also required and its ability to enhance lipase adsorption over that observed in the absence of colipase was dependent on the S and colipase mole fractions. These results support the notion that colipase concentrates S laterally at its periphery and suggests that, together with the lipase-colipase interaction, the S-rich nano-domain surrounding colipase facilitates lipase adsorption in the 'flap-opened' conformation. Supported by HL 49180 and the Hormel Foundation.

W-Pos340

QUANTITATIVE IRRAS DETERMINATION OF LIPID ACYL CHAIN AND HELICAL PEPTIDE ORIENTATION IN BINARY MONOLAYERS ((Carol R. Flach[1], Arne Gericke[1], Joseph W. Brauner[2], and Richard Mendelsohn[1])) [1]Department of Chemistry, Rutgers University, Newark, N.J. 07102 and [2]Department of Chemistry, St. Peter's College, Jersey City, N.J. 07306.

Quantitative analysis of infrared reflection-absorption spectroscopic (IRRAS) intensities acquired in situ at the air/water interface has been performed to obtain the orientation of phospholipid acyl chains and σ-helical protein components in binary, cospread monolayers. Theoretical models were first tested using behenic acid methyl ester monolayers where splitting in the methylene scissoring mode provided direct evidence of a perpendicular orthorhombic subcell structure and the existence of all-trans conformation in the acyl chains. This provides a well-defined system where the acyl chain tilt angle with respect to the surface normal is 0°. Experimental results from methyl behenate studies performed over a range of incident angles (35-50°) for both s- and p-polarized radiation were compared to simulated IRRAS intensities for methylene and carbonyl stretching vibrations. The exercise provided confidence in the mathematical formalism applied and the overall degree of polarization for the experimental design. This last parameter is important in IRRAS simulations for p-polarized radiation near the Brewster angle. The same approach was used for pure DPPC and mixed monolayers of DPPC with lung surfactant protein SP-C. Acyl chain tilt angles in DPPC were calculated to decrease from ~ 26 to 10° upon interaction with SP-C, whereas a 70° tilt was found for the helical protein. The 70° tilt allows for maximum contact between the hydrophobic portion of SP-C and the lipid acyl chains. Studies of carbonyl group orientation in DPPC and lipid:peptide interaction in a variety of monolayer systems are continuing.

W-Pos341

FOURIER TRANSFORM INFRARED SPECTROSCOPY STUDIES OF FATTY ACID BINDING PROTEIN ((Arne Gericke[1], Judith Storch[2] and Richard Mendelsohn[1])) [1]Department of Chemistry, Rutgers University, Newark, N.J. 07102; [2]Department of Nutritional Sciences, Rutgers University, New Brunswick, N.J. 08903.

We have recently demonstrated that the gel-liquid crystal phase transition of a variety of anionic phospholipids was lowered upon their interaction with the adipocyte fatty acid binding protein (AFABP), while interaction of the protein with phosphatidylcholines was less pronounced. We are currently investigating AFABP secondary structure in the presence and absence of anionic phospholipids. The FT-IR spectrum of the protein alone reveals that the solution secondary structure is primarily β-sheet, as marked by two bands at 1627 and 1682 cm^{-1}. Upon heating, a band at 1619 cm^{-1} gains intensity, while the feature at 1627 cm^{-1} is diminished. The correlated behavior of these two bands was established by 2DIR spectroscopy. The spectral changes reveal increasing protein aggregation with heating. The effect of anionic lipids on the aggregation process will be reported. In addition, the influence of the bound fatty acid on the protein structure is under investigation.
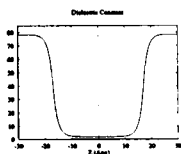
W-Pos342

PHYSICAL STATE OF NICOTINIC ACETYLCHOLINE RECEPTOR-RICH MEMBRANE AND ITS MODIFICATION BY FATTY ACIDS. ((Silvia S. Antollini and F. J. Barrantes)). Instituto de Investigaciones Bioquímicas de Bahía Blanca, 8000 Bahía Blanca, Argentina.

We have recently used the so-called generalized polarization (GP) of the fluorescent probe Laurdan (6-dodecanoyl-2-dimethylamino-naphthalene) to learn about the physical state of the lipids in the nicotinic acetylcholine receptor (AChR)-rich membrane (Antollini et al., Biophys.J. 70 (1996) 1275-1284) and cells expressing (endogenous or heterologous) AChR (Zanello et al., Biophys. J. 70 (1996) 2155-2164). Here we report the decrease in Laurdan GP and changes in anisotropy of DPH and derivatives effected by a fatty acid (18:1). Using energy transfer from the membrane protein fluorescence to Laurdan molecules, a minimal donor-acceptor distance r of 15±1 Å was calculated considering a separation of the planes containing donor and acceptor molecules of 0<H<10 Å. Higher GP values were observed under FRET conditions (290 nm excitation) indicating a lower polarity and a higher degree of order of water molecules in the immediate environment of the AChR protein in comparison to the rest of the bilayer. The wavelength dependence of Laurdan GP spectra did not change in the presence of 18:1, indicating the maintenance of a single, ordered-liquid lipid phase. A monotonic decrease in DPH, PA- and TMA-DPH anisotropy was observed as a function of temperature. Upon addition of oleic acid the fluidity increased in the hydrocarbon core of the AChR membrane to a higher extent than at more superficial levels of the bilayer.

W-Pos343

THE SAME MODEL: PARAMETERIZATION AND PRELIMINARY APPLICATION TO PEPTIDES AND HELICES ((**Alan Grossfield**, Charles R. Sanders II, Thomas B. Woolf)) Depts. Physiol. and Biophys., Johns Hopkins Univ., Baltimore, MD 21205 & Dept. Physiol. & Biophys., Case Western Reserve Univ., Cleveland, Ohio 44106.

We have parameterized a mean field representation of the membrane environment (SAME). This model allows the simulation of proteins and peptides in an environment resembling a membrane, without the computational cost of explicitly representing the lipid and water molecules. SAME treats the membrane as an infinite series of pseudo-solvents, whose properties continuously change from water-like values at the surface to hydrocaron values in the interior, and uses these properties to calculate solvation energies, on an atomic basis, using scaled particle theory. The energy terms use empirically fit weights, with different weights for each atom type. The model has been parameterized against partitioning data for single amino acids from cyclohexane ("membrane center") and octanol ("interface region") to water. We are using SAME to model the interaction of tri- and penta- peptides with the bilayer, to try to rationalize experimental results. We have also examined the energetics of helix insertion into the bilayer and helix:helix interactions in the membrane.

W-Pos344

MOLECULAR DYNAMICS SIMULATIONS OF INTESTINAL FATTY ACID BINDING PROTEIN ((**M. Tychko** and T.B. Woolf)) Depts of Physiology and Biophysics, Johns Hopkins University, School of Medicine, Baltimore, MD 21205

Fatty acid binding proteins (FABPs) are ten-stranded β-clam shell structures that selectively bind fatty acids in an internal cavity. Our investigations into the molecular basis of their discrimination could aid efforts for rational drug design and increase understanding of lipid:protein interactions. Four simulations of intestinal fatty acid binding protein (three holo and one apo form) have now been completed at the multi-nano-second level. These simulations use the CHARMm program with a water droplet solvation model. The latest results can be usefully compared with our previous simulations of human muscle and adipocyte FABP. Particular attention was paid to the interaction energies between interior amino acid residues, water, and the ligand. Dihedral transitions in the bound fatty acid similar to those detected in membrane bilayer simulations were observed. Qualitative free energy calculations, using linear response, were performed with these trajectories. The results are compared with thermodynamic data from nineteen single site alanine mutations that have been recently characterized in the Kleinfeld lab.

W-Pos345

CHOLESTEROL MODULATES ANESTHETIC SENSITIVITY IN RECONSTITUTED NICOTINIC ACETYLCHOLINE RECEPTORS ((D.E. Raines, N.S. Krishnan, K.W. Miller)) Dept. of Anesthesiology and Critical Care, Massachusetts General Hospital, Boston, MA 02114.

General anesthetics are lipophilic drugs that stabilize the nicotinic acetylcholine receptor (nAcChoR) in an inactive (desensitized) conformational state. The molecular mechanism for this action is not known, but it has been suggested that these drugs may act by disrupting critical interactions between the nAcChoR and its lipid environment. To test the hypothesis that cholesterol modulates the actions of general anesthetics, we studied the effects of two general anesthetics (isoflurane and butanol) on nAcChoRs that had been reconstituted into bilayers composed of either DOPC alone or DOPC and cholesterol (molar ratio 75:25). We used a stopped-flow fluorescence assay to determine the fraction of nAcChoRs preexisting in the desensitized state. We found that when nAcChoRs were reconstituted into bilayers containing both DOPC and cholesterol, isoflurane and butanol increased the fraction of receptors in the desensitized state with EC50s that are not significantly different from those reported for native nAcChoRs. In contrast, when nAcChoRs were reconstituted into bilayers containing DOPC alone, they were insensitive to general anesthetics. When nAcChoRs that were reconstituted into DOPC were re-reconstituted into bilayers containing both DOPC and cholesterol, anesthetic sensitivity was recovered. These results indicate that cholesterol modulates anesthetic action on nAcChoRs and supports the hypothesis that anesthetics act by perturbing lipid-protein interactions.

W-Pos346

ALZHEIMER DISEASE AMYLOID β PEPTIDE ANALOGS INTERACT WITH THE MEMBRANE BILAYER AND INHIBIT LIPID PEROXIDATION ((M.F. Walter, P.E. Mason and R.P. Mason)) Neurosciences Research Center, Allegheny University of the Health Sciences, Allegheny Campus, Pittsburgh, PA

Alzheimer disease neuropathology is characterized by neuritic plaques composed primarily of amyloid β (Aβ) peptide. The Aβ molecule has been shown to have neurotrophic activity in cultured neurons, an effect which may be related to decreased membrane susceptibility to lipid peroxidation. In this study, the membrane interactions of various Aβ analogs were probed using small-angle x-ray scattering (SAXS) approaches, and correlated with antioxidant activity. Lecithin vesicles prepared in the absence and presence of various concentrations of Aβ (25-35) were oriented by centrifugation and exposed to a focused, monochromatic x-ray source. One-dimensional electron density profiles (Å versus electrons/$Å^3$) generated from the SAXS data demonstrated that Aβ (25-35) partitions deep into the membrane hydrocarbon core, 0-12 Å from the lipid bilayer center, in a concentration-dependent manner. The membrane intrabilayer headgroup separation and unit cell periodicity were 40 Å and 54 Å, respectively. Lipid peroxidation analyses were carried out at 37°C in a multilamellar vesicle (1.0 mg/ml) system enriched with polyunsaturated fatty acids (dilinoleoyl phosphatidylcholine) under physiological-like conditions. At 10 nM, various Aβ analogs significantly inhibited lipid peroxidation (25-35 > 1-42 > 25-35 scrambled); Aβ (25-35) and Aβ (1-42) inhibited lipid peroxidation by 90% relative to control samples. These findings show that Aβ (25-35) partitions to a discrete location in the membrane and that all of the Aβ analogs inhibit lipid peroxide formation at nanomolar concentrations. The strong physico-chemical membrane interactions and potent antioxidant activity of Aβ may contribute to its neuroprotective properties.
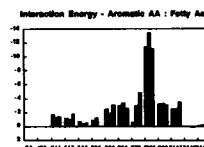
W-Pos347

Lipid dynamics as a probe of protein kinase Cα–membrane interactions. ((Cojen Ho, Simon J. Slater and Christopher D. Stubbs)) Thomas Jefferson University, Dept. of Pathology & Cell Biology, Philadelphia, PA 19107

Protein kinase C (PKC) translocates to the membrane surface as a result of interaction with Ca^{2+}. This process is enhanced by the presence of PKC activators, such as diacylglycerol and 12-O-tetradecanoylphorbol-13-acetate. This leads to a folding out of the pseudosubstrate and activation of the enzyme. In this study the intrinsic tryptophans and dansyl-labeled lipids were used to probe this protein-lipid interaction and conformational change. It was found that the emission spectra of both the tryptophan and dansyl-PE exhibit a marked blue-shift in response to the addition of Ca^{2+}, the effect being reflected in corresponding changes in the respective fluorescence lifetimes. The tryptophan shift was apparent even in the absence of membrane lipids, whereas the dansyl fluorescence emission shift was complete only when Ca^{2+}, lipid and activators were present. Cholesterol, normally found at high levels in membranes that associate with PKC, had a marked influence on the dansyl emission shift which was greatly reduced in its absence. The motional properties of the dansyl fluorophore, measured by steady state and time-resolved fluorescence anisotropy, also reflected the large change in lipid dynamics encountered on PKC-membrane interactions. Again, cholesterol was found to significantly enhance the modification of lipid rotational dynamics. It is concluded that membrane lipid composition has a significant influence on PKC-membrane interactions.

W-Pos348

ENHANCED CIRCULATION-LIFETIME OF DSPC LIPOSOMES: IMPORTANCE OF COMPLEMENT OPSONIZATION AND LIPOSOME AGGREGATION ((Patrick L. Ahl, Patricia Roberts, Rachel Stevens, Suresh Bhatia, Shaukat Ali, Paul Meers and Andrew S. Janoff)) The Liposome Company, Princeton, NJ 08540.

Certain N-(ω-carboxy)acylamidophosphatidylethanolamines (N-CAPEs), such as N-glutaryl-dipalmitoylphosphatidylethanolamine (DPPE), were found to dramatically increase the in vivo circulation lifetime of distearoylphosphatidylcholine (DSPC) large unilamellar vesicles (LUVs) in rats. Neither pure DSPC LUVs nor those with 10 mole % N-glutaryl-DPPE were found to bind significant levels of complement in vitro. Hence, the enhanced circulation lifetime induced by N-glutaryl-DPPE was not due to inhibition of complement opsonization in this case. In fact, incorporation of N-glutaryl-DPPE into a LUV formulation known to bind significant levels of complement was found to actually further increase complement binding and decrease circulation lifetime. The pure DSPC LUVs were partially aggregated below the T_m of the lipid, probably due to low hydration under these conditions. We found that certain N-CAPEs were particularly efficient inhibitors of this LUV aggregation. The apparent extent of liposomal aggregation in the presence of various N-CAPEs correlated inversely with circulation time. Therefore, these PE derivatives appeared to increase circulation lifetime by preventing the formation of excessively large liposomal aggregates. This was presumably due to the surface charge they impart and possibly their particular structural features. By contrast, incorporation of poly(ethylene glycol)-lipid into complement-fixing liposomes increased circulation lifetime by significantly decreasing complement opsonization, indicating a different operative mechanism. These results demonstrate that both levels of liposomal opsonization and aggregation must be low to attain long-circulating characteristics. Incorporation of N-CAPEs generates a new class of stable long circulating gel phase liposomes.

W-Pos349

REVERSIBLE BINDING KINETICS OF A G-PROTEIN SUBUNIT TO PHOSPHOLIPID MEMBRANES. ((Rhonda Dzakpasu[1], Richard R. Neubig[2], Ann Remmers[2], and Daniel Axelrod[1])) [1]Biophysics Research Division and Dept. of Physics, and [2]Dept. of Pharmacology, University of Michigan, Ann Arbor, MI 48109.

According to some models of signal transduction, the nonspecific adsorption of separate G-protein subunits to the cytofacial surface of the plasma membrane may affect signaling functions. To investigate such nonspecific interactions with lipids, we measure the desorption rates of the purified βγ–subunit of G-protein at supported phospholipid bilayers by Total Internal Reflection/Fluorescence Recovery after Photobleaching (TIR/FRAP). The βγ–subunit is labeled with rhodamine; the glass-supported membranes are either pure phosphatidylcholine (PC) or 3:1 mixed PC:phosphatidylserine (PS). Desorption rates are measured as functions of membrane composition, detergent (cholate) concentration, and bulk protein concentration. For the lowest cholate concentrations studied (0.1%), the desorption rate from PC/PS membranes averages about 0.05/sec; the corresponding desorption rate from pure PC is considerably faster at about 0.25/sec. On PC/PS membranes, the desorption rate increases with increasing cholate concentration; the effect is not as strong on pure PC membranes. The effect of changing G-protein concentrations in the bulk, and the differences between the kinetic behaviors of the α– and the βγ–subunits are also discussed. Supported by NSF MCB 9405928 (to D.A.) and NIH GM39561 (to R.N.).

W-Pos350

PORE FORMATION BY DIPHTHERIA TOXIN IS DEPENDENT ON PROTEIN CONCENTRATION. ((J.C. Sharpe and E. London)) Dept. of Biochemistry and Cell Biology, SUNY at Stony Brook, Stony Brook NY 11794-5215.

We have developed a method which uses Cascade Blue-labeled dextrans trapped inside large unilamellar vesicles to measure pore formation by diphtheria toxin. In order to measure the size of the pores formed by the toxin we used fluorescently-labeled dextrans with molecular weights of 3 kD, 10 kD and 70 kD, and the Cascade Blue probe 8-methoxy-pyrene-tri-sulfonate (MPT) mw 348. We measured the extent of dextran release by measuring the amount of quenching of Cascade Blue fluorescence by anti-Cascade Blue antibodies post toxin addition. Using this method we determined the effect of time, pH, protein concentration and lipid composition on diphtheria toxin pores.

Pores formed at and below pH 5.2 which is the transition pH at which the toxin becomes hydrophobic. Pore formation was rapid and leakage of the molecules was complete within minutes. The size of the dextran released from PG/PC LUVs was dependent on protein concentration. When the concentration of protein was low only the small MPT molecule was released. As toxin concentration increased we saw the release of the 3 kD dextran followed at higher toxin concentrations by the 10 kD dextran. The 70 kD dextran was not seen to be released under our experimental conditions. We also observed that lipid composition had an effect on dextran leakage. The absence of PG increased the toxin concentration needed to allow the 10 kD dextran to be released while having no affect on the release of MPT or the 3 kD dextran. The addition of cholesterol promoted the release of MPT and the 3 kD dextran while it had no effect on the release of the 10 kD dextran. We propose that diphtheria toxin pore formation is dependent on oligomerzation of the toxin in the membrane and that oligomer size is a function of protein concentration and lipid composition.

W-Pos351

STUDIES OF THE STRUCTURE OF MEMBRANE-INSERTED DIPHTHERIA TOXIN USING FLUORESCENCE QUENCHING OF TRP MUTANTS. ((Y. Wang*, S.E. Malenbaum*, C. Cui#, R.J. Collier#, and E. London*)) #Department of Microbiology and Molecular Genetics, Harvard Medical School, Boston, MA 02115; *Dept of Biochemistry and Cell Biology, S.U.N.Y. at Stony Brook, NY 11794.

Diphtheria toxin is composed of an A chain (catalytic (C) domain), and a B chain (composed of translocation (T), and receptor-binding (R) domains). The toxin enters cells by receptor-mediated endocytosis, and upon entry into the acidic lumen of an endosome, inserts into the membrane. The C domain then translocates into the cytoplasm. To better understand the translocation process toxin with Trp mutations was incorporated into model membranes, and fluorescence quenching was used to determine the depth of Trp residues and Trp exposure to lipid. The quenching of toxin in which native Trp were restricted to either the A chain or B chain showed both insert deeply into the membrane bilayer. Quenching of the fluorescence of the isolated A chain was much stronger than that for A chain in whole toxin, suggesting that in whole toxin the A chain is partially protected from contact with the lipid by the B chain. The structure of the membrane-inserted T domain is also being studied since this domain is thought to guide insertion. Using mutants with single Trp residues, it was found Trp 281 and 364 are deeply buried within the bilayer. As these residues are near the middle of hydrophobic helices TH5 and TH9, this supports a model in which these helices are partially or fully transmembraneous. Trp 206 was also significantly buried, consistent with a model in which TH1, which is somewhat amphiphilic, is associated with the bilayer surface. In contrast, Trp 375 was close to the membrane surface, consistent with its location at the terminus of a hydrophobic helix.

W-Pos352

PHOSPHOLIPID ACYL CHAIN UNSATURATION DETERMINES CHOLESTEROL EFFECTS ON RHODOPSIN PHOTOACTIVATION ((Drake C. Mitchell and Burton J. Litman NIAAA, NIH, Rockville, MD 20892))

The integral membrane protein rhodopsin was incorporated into large unilamellar vesicles consisting of a wide range of acyl chain polyunsaturation, with and without 30 mol% cholesterol. The effect of the lipid bilayer on rhodopsin function was determined by measuring the equilibrium, K_{eq}, between the active (MII) and inactive (MI) products of rhodopsin photoactivation. The fluorescent membrane probe diphenylhexatriene (DPH) was used to characterize phospholipid acyl chain packing in the rhodopsin-containing lipid bilayers. DPH anisotropy decays were analyzed with a model based on the P2-P4 formalism which yields a parameter, f_v, which characterizes acyl chain packing free volume. Both K_{eq} and f_v were measured at 10, 20, 30, and 40C. The resulting values of K_{eq} and f_v for each phospholipid were linearly related, with the slope of the correlation lines increasing in the order di 22:6 PC > 16:0, 22:6 PC > 16:0, 18:1 PC. In each phospholipid bilayer, 30 mol% cholesterol reduced both K_{eq} and f_v such that the resulting K_{eq} vs. f_v correlation line was coincident with the correlation line for the cholesterol-free bilayer. Thus, the effect of cholesterol on both acyl chain packing and the ability of rhodopsin to form MII was determined by the acyl chain composition of the host phospholipid. The magnitude of the cholesterol effect varied with acyl chain composition in the order 16:0, 18:1 PC > 16:0, 22:6 PC > di 22:6 PC. This decrease in cholesterol effect with increased acyl chain saturation is consistent with the effect of cholesterol on acyl chain packing in protein-free bilayers.

W-Pos353

SEMI-FLEXIBLE ACTIN FILAMENTS TETHERED AT LIPID MONO-LAYERS
((B. Demé, D. Hess, G. Isenberg, E. Sackmann)) TU Muenchen, Physik-Dept. E22, James-Franck-Str., D-85748 Garching, Germany

Neutron reflectivity has been shown to be a powerful technique for studying the coupling of monomeric actin to lipid monolayers mediated by the actin binding protein hisactophilin [1]. In the present study, we extend this technique to the investigation of semi-flexible actin filaments tethered at lipid monolayers. For coupling the filaments, we use two different strategies: 1) an artificial approach using the avidin-biotin system 2) a simple model for in vivo coupling using the actin and membrane binding protein talin, a major constituent of focal adhesions [2]. In addition to high resolution neutron reflectivity, we used film balance fluorescence microscopy with in-plane resolution and a newly developed scanning method [3] to observe fluorescence profiles along the z-axis.

Simulations show the feasability of determining surface excess and concentration profiles of bound actin, with reflectivity experiments currently in progress.

[1] C. Naumann et al., Biophysical Journal (1996) 811-823
[2] G. Isenberg, W.H. Goldmann, The Cytoskeleton (1995), Vol. 1, 169-204
[3] A. Behrisch et al. Biochemistry (1995) 15182-190

W-Pos354

EXPRESSION OF HUMAN HEART R-3-HYDROXYBUTYRATE DEHYDROGENASE IN *E. COLI* AND PURIFICATION BY NICKEL AFFINITY CHROMATOGRAPHY ((Dirk Chelius, Johannes Moeller, John Wise, David Green, Andrew R. Marks, Wolfgang E. Trommer, Sidney Fleischer and J. Oliver McIntyre)) Universitaet Kaiserslautern, Germany; Mt. Sinai Med. Center, New York, NY and Vanderbilt Univ., Nashville TN.

R-3-Hydroxybutyrate dehydrogenase (BDH) is a lipid-requiring mitochondrial enzyme with a specific requirement of phosphatidylcholine (PC) for function. PC serves as an allosteric activator to enhance NAD(H) binding to BDH. We previously have reported the expression of catalytically active human heart (HH) BDH in insect cells (Sf9, *Spodoptera frugiperda*) transfected with BDH-cDNA in baculovirus [Green et al., Biochem. 35, 8158-8165 (1996)]. We have now constructed a plasmid to express HH-BDH as a fusion protein with hexahistidine to permit affinity purification. A ribosomal binding site, six histidine residues and a protease cleavage site were incorporated at the N-terminus of the mature HH-BDH and the modified cDNA was then ligated into the multiple cloning site of pUC119. The hexahistidine HH-BDH fusion protein (His-BDH) has been expressed in *E. coli* to about 0.5% of total cell protein. Purification of His-BDH using Ni-NTA, a metal chelate chromatography matrix, gave about an 80-fold purification in a single step yielding a specific activity of up to 40 μmoles NAD+ reduced .min^{-1} mg^{-1}. Additional purification has been achieved using ion exchange chromatography over DEAE-Sepharose. Studies to improve yields are in progress. (Supported by NIH DK49186 to J.O.M.)

W-Pos355

VERTICAL DISPLACEMENT OF A MEMBRANAL PROTEIN REVEALED BY ARRHENIUS PLOT: A RECONSTITUTION STUDY ON ADENOSINE DEAMINASE COMPLEXING PROTEIN ((Itzhak Ben-Shooshan and Abraham H. Parola*)) Department of Chemistry, Ben-Gurion University of the Negev, Beer-Sheva, 84105, Israel.

Arrhenius plots of the activity of small subunit adenosine deaminase (ADA) free in solution and bound to its complexing protein (ADCP) are linear over the temperature range 7-37°C and exhibit similar energy of activation (Ea). On the contrary, ADA bound to ADCP reconstituted in DMPC liposomes exhibits an Arrhenius plot with two breaks at 25°C and 13°C, yielding three nearly parallel lines, at the range of 37-27°C, 25-15°C and 13-7°C, with no change in the apparent Ea. Furthermore, at each of these discontinuities a 30% increase in ADA activity is observed. These results could rise from an outward vertical displacement of ADCP-ADA complex from the lipid core, mediated by the main phase and pre-phase transitions at 23°C and 13°C, respectively. These results are supported by simulated Arrhenius plots based on a model for the dependence of active site accessibility on lipid "microviscosity", mediated by temperature.

W-Pos356

INFLUENCE OF ANNEXIN V ON THE ORGANIZATION AND DYNAMICS OF PHOSPHOLIPIDS.
L.Cézanne, O.Saurel, A.Lopez, A.Milon, P.Demange and J.F.Tocanne - Institut de Pharmacologie et de Biologie Structurale du C.N.R.S. - 118, Rte de Narbonne - 31062 - Toulouse cedex - FRANCE.

The influence of annexin V on the dynamics of lipids in model membranes was investigated using a variety of technics. Fluorescence polarization and solid state ^{2}H-NMR experiments carried out on lipid vesicles show no modification of the conformational mobility of PC and PS acyl chains and of the orientation of PC polar headgroups while monolayer experiments reveal an absence of penetration of the protein between the lipids. In contrast, FRAP experiments carried out on egg-PC/brain-PS (90/10) planar supported bilayers with NBD-PC or NBD-PS and fluorescein-labelled protein probes indicate that binding of annexin V to the lipids induce, in a dose dependent manner and in a reversible way, a marked decrease of the lateral diffusion rate of NBD-PC and a nearly complete immobilization of NBD-PS and of annexin V. Careful analysis of fluorescence recoveries show that the lateral motions of NBD-PS and of the protein decrease in a parallel way. On the ground of numerical simulations of the lateral diffusion of lipids in the presence of obstacles, these observations can be accounted for by a strong and long-lived binding of PS to annexin V and the progressive formation of a 2-D protein network at the water-lipid interface.

W-Pos357

INFLUENCES OF NON-LAMELLAR FORMING LIPIDS ON VISUAL FUNCTION. ((Yin Wang, Nicholas J. Gibson, Robin L. Thurmond, and Michael F. Brown)) Departments of Physics and Chemistry, University of Arizona, Tucson, Arizona 85721, USA

The MI-MII conformational transition of rhodopsin leads to binding of a G protein, activation of a cGMP phosphodiesterase, and the amplified visual response. We tested the hypothesis that the conformational energetics of photolyzed rhodopsin are governed by the membrane lipid composition, due to chemically non-specific material properties of the bilayer.[1,2] Flash photolysis techniques were used to study the acid-base MI-MII transition of rhodopsin in recombinant membranes, comprising binary mixtures of dioleoylphosphatidylcholine (DOPC) and dioleoylphosphatidylethanolamine (DOPE). At all pH values studied, the amount of MII produced increased with the amount of DOPE present. Thus non-lamellar forming lipids (DOPE) shift the acid-base MI-MII equilibrium to the right; whereas lipids forming the lamellar phase (DOPC) do not support native-like photochemical function of rhodopsin.[3] It was found that rhodopsin photochemical activity was correlated with an increase in the curvature stress across the bilayer. These findings indicate that the photochemical activity of rhodopsin is directly influenced by the membrane lipid composition. Average or material properties are formulated in terms of a flexible surface model, in which frustration of the curvature free energy of the bilayer is relieved by the MI-MII conformational transition of rhodopsin.[4] The free energy coupling due to the MI-MII transition may involve a protrusion of rhodopsin from the membrane,[5] as evinced by surface plasmon resonance studies. [1]A. J. Deese et al. (1981), FEBS Lett. 124, 93-99. [2]T. S. Wiedmann et al. (1988), Biochemistry 27, 6469-6474. [3]N. J. Gibson and M. F. Brown (1993), Biochemistry 32, 2438-2454. [4]M. F. Brown (1994), Chem. Phys. Lipids 73, 159-180. [5]Z. Salamon et al. (1996), Biophys. J. 71, 283-294. Work supported by NIH grants EY03754 and EY10622.

W-Pos358

INTERACTIONS OF CYTOCHROME B5 WITH BINARY LIPID MIXTURES CONTAINING PHOSPHATIDYLSERINE.
((Harold M. Goldston, Jr., A.W. Steggles*, and Peter W. Holloway)) Department of Biochemistry, Univ. of Virginia Sch. Med., Charlottesville, VA, *Northeastern Ohio Univ. Coll. Med., Rootstown, OH.

Cytochrome b$_5$ is an amphipathic integral membrane protein found in the endoplasmic reticulum. As a water-soluble amphiphile, it binds to both natural and artificial bilayer membranes through its nonpolar C-terminal domain. The present study extends previous work examining the interaction of a mutant form of b$_5$, which has a single Trp in the membrane-binding domain, with two binary mixed-lipid systems: POPE/POPS and DMPC/POPS. Through fluorescence studies, binding of b$_5$ to POPS-containing LUV's was not seen at fluid-phase temperatures but was observed upon cooling the lipid-protein mixtures to gel-phase temperatures. Calorimetry was used to examine the phase behavior in the two binary systems. The differences in the amount of b$_5$ binding in the two lipid systems were consistent with the mixing properties of the lipids as well as known charge repulsions between the negatively-charged, N-terminal domain of b$_5$ and POPS headgroups. The stabilization of gel-state lipid interactions in the presence of a relatively low protein molar ratio (L/P=500) is particularly marked in the POPE/POPS system, as evidenced by an increase in both the cooperativity and the temperature of the main phase transition. Spectroscopic techniques are utilized to further examine the molecular nature of this stabilization.

W-Pos359

MELTING OF TWO-DIMENSIONAL CRYSTALS OF THE MEMBRANE-PROTEIN BACTERIORHODOPSIN.
((I. Koltover[1], T. Salditt[1], J. Raedler[1], C. Safinya[1] and K. J. Rothschild[2])) [1]Materials,Physics Departments and Biochemistry and Molecular Biology program, UCSB; [2]Physics Department and Molecular Biophysics Laboratory, Boston University

Bacteriorhodopsin (bR), a light-driven proton pump, is an integral membrane protein and a critical component of the photosynthetic apparatus of the salt loving bacterium *Halobacterium salinarium*. In the native bacterial membrane bR self-assembles into regular hexagonal crystalline arrays in the plane of membrane. The origin of the protein-protein interactions governing this higher order self-assembly is currently unknown. However, the two-dimensional (2D) protein crystal undergoes a fully reversible melting transition as a function of temperature. We have conducted a synchrotron x-ray diffraction study of oriented multilayers of bR-containing native bacterial membrane patches, as well as of stacks of novel giant (50μm diameter) single-crystal fused bR membranes. The precise *in-situ* control of humidity and sample temperature combined with line-shape analysis allowed us to elucidate and control protein-protein interactions. The important findings are as follows. First, the ordered 2D self-assembled lattice of proteins is found to exhibit diffraction patterns characteristic of a 2D solid with power-law decay of in-plane positional correlations between the proteins. Second, the melting temperature is a function of multilayer hydration and melting can be achieved by increasing the hydration level at constant temperature. Third, at all hydration levels the melting transition is strongly first order, with the transition forced by the breakup of protein crystal into smaller domains and only a slight decrease in the protein lattice elastic constants. We discuss the models of interactions in bR multilayers consistent with our data.
Supported by NSF grant DMR-962091, the Petroleum Research Fund (No.31352-AC7) to CS and NSF grant MCB-9419059 and ARO-SBIR/AmberGen contract to KJR.

W-Pos360

UNILATERAL ADDITION OF PLA2 TO PLANAR LIPID BILAYERS GENERATES A CURRENT CARRIED BY CATALYZED FLOW OF IONIZED FATTY ACID. ((J. Walter Woodbury, Dixon J. Woodbury and Stephen N. Alix)). Departments of Physiology, University of Utah, Salt Lake City, UT 84108 and Wayne State University, Detroit, MI 48201.

Phospholipase A2 (PLA2) action produces fatty acid (FA) and lyso-phospholipid. When Ca^{2+} activated bee venom PLA2 is added to the solution bathing the cis side of a voltage clamped planar lipid bilayer, a current, Im, is generated which flows cis to trans in the external ammeter. Im has the following properties: (1) It is transient but always positive; rise ~20 s, fall ~100 s. (2) The decay time constant, τ, is decreased to 60% by a holding potential, Vcis = +60 mV. (3) Ca^{2+} addition 10 min after PLA2 shortens τ to 15% and doubles peak amplitude. (4) pH changes (5.2-8.5) have only minor effects. Passive models of ionized fatty acid (FAi) flow fail because they predict large pH effects and Im < 0 at late times. A workable model is based on catalyzed Fai transport: (1) Dissolved PLA2 binds in a form (E1) such that some of the FA produced flows through the membrane to the trans side as FAi. This is the measured current. (2) E1 changes slowly to E2 which hydrolyzes PL at the same rate but does not catalyze FAi transport, accounting for the shortening of τ in delayed Ca^{2+} addition. (3) In the transition E1→E2, a charged part of the PLA2 moves perpendicular to the membrane such that the rate constant and thus τ are altered by Vcis. One set of parameters predicts all the above effects within experimental error. Supported in part by NIH grant MH50003 to DJW.

W-Pos361

ADIPOCYTE LIPID-BINDING PROTEIN: STRUCTURAL COMPONENTS INVOLVED WITH LIGAND-BINDING SPECIFICITY AND AFFINITY. ((A. J. Reese-Wagoner, D. A. Bernlohr*, and L. J. Banaszak)) Departments of Biochemistry, University of Minnesota, Minneapolis, MN 55414. (*College of Biological Sciences; Spon. by L. J. Banaszak)

Adipocyte lipid-binding protein, ALBP, belongs to a family of 10-stranded β-barrel proteins that are involved in the intracellular transport of a range of lipids. Although the amino acid sequence identity among the intracellular lipid binding protein family members is 20%-68%, all known protein structures have the same three-dimensional fold with similar ligand-binding cavities. A pair of arginine residues and a tyrosine play a role in defining binding specificity in ALBP. However these three residues do not exclusively discriminate lipid-types as they appear in related proteins that bind different ligands. Subtle differences yet unknown must therefore contribute to specificity and affinity. Such differences should be definable using the many different types of ligand-binding proteins. To investigate the binding determinants for ALBP, a critical comparison has been made between ALBP and the cellular retinoic acid-binding protein type I (CRABP I) using their amino acid sequences and tertiary structures. Careful inspection of the two proteins suggests that a set of specific amino acids may contribute to differentiating between retinoic acid and a variety of fatty acids. Such residues effectively define the shape of the lipid binding cavity. Leaving the residues associated with head group of the lipid unchanged, we are systematically using the structural data and site directed mutagenesis to alter binding cavity residues. The primary objective is to convert the fatty acid specificity of ALBP to a high affinity retinoic acid site. An available expression system, small protein size (15 kDa), and high resolution apo- and holo- x-ray structures make ALBP an ideal candidate for mutagenesis. Supported by grants to LJB (GM13925) and DAB (NSF/MCB-9506088).

W-Pos362

BINDING OF CATIONIC SURFACTANTS TO DNA. COMPRESSIBILITY AND VOLUME EFFECTS. ((E. Kudryashov, S. Morrissey, A. Gorelov, V. Buckin, K. Dawson)) Centre for Colloid Science and Biomaterials, University College Dublin, Belfield, Dublin 4, Ireland

We have studied complex formation between different cationic surfactants and short fragments of DNA using combination of the dynamic light scattering, ultrasound velocity, and density measurements combined with surfactant selective electrode method. From the binding isotherm of the surfactant with DNA, measured by the potentiometric technique with a cationic surfactant-selective electrode, we obtained the dependence of the apparent molar volume and compressibility of DNA on the amount of surfactant bound. In addition, we obtained the volume and compressibility effects of micelle formation in solutions of surfactants alone. The compressibility of the DNA - surfactant solutions increases significantly with the binding ratio, whereas, the volume shows a negligible change. Analogous volume and compressibility changes were observed in the micelle formation of free surfactants. The results were interpreted in terms of micelle like structure of the surfactant around DNA.

W-Pos363

SYNTHESIS AND MEMBRANE-BINDING OF SEMI-SYNTHETIC PROTEIN PROBES CONTAINING N-TERMINAL FATTY-ACIDS AND HYDROPHOBIC PEPTIDES. ((Chadler T. Pool, Thomas E. Thompson.)) University of Virginia, Department of Biochemistry, Charlottesville, VA 22908

In order to produce novel protein probes for examining membrane domain structure, we have modified bovine pancreatic trypsin inhibitor (BPTI) by specifically attaching fatty-acids and hydrophobic peptides at the N-terminus. The N-terminus and Lys-15, the site of trypsin binding, are at opposite poles of BPTI. In order to protect Lys-15, Trypsin was bound to BPTI, then o-methylisourea was used to guanidinate all unprotected lysines to homoarginine. This reaction does not modify the N-terminal amine. The N-terminal amine was reacted with several saturated fatty-acid anhydrides ranging in length from 8 to 16 carbons. The BPTI/Trypsin complex was then dissociated on a sephadex G-50 column with an acetic acid buffer. The resulting product consists of BPTI with three guanidinated lysines (referred to as G-BPTI), with a fatty-acid attached to the N-terminus, and Lys-15 free for linking to any amine-reactive reagent. Following radiolabeling of the fatty-acylated proteins at Lys-15, binding of these probes to POPC LUVs was examined. Initial results indicate that the palmitoylated proteins show significant binding at high protein to lipid ratios where as the binding of the probes containing shorter chain fatty-acids display little or no binding under these conditions. Polyalanine peptides containing an N-terminal cysteine, and C-terminal leucine residues were radiolabelled, cleaved in the presence of SDS, and then immediately reacted with G-BPTI possessing a sulfhydryl-reactive-crosslinker at the N-terminus. Binding studies with these probes are in progress. All products were analyzed using electrospray or laser-desorption mass spectroscopy and purified using reverse-phase HPLC. All modifications of BPTI were verified through sequencing of endoproteinase digests. Binding studies with different protein and lipid concentrations are presently underway. (Supported by NIH Grant GM 14628)

W-Pos364

ACTIVATION OF PROTEIN KINASE C BY COEXISTING DIACYLGLYCEROL-ENRICHED AND DIACYLGLYCEROL-POOR LIPID DOMAINS ((A.K. Hinderliter, A.R.G. Dibble, R. L. Biltonen and J.J. Sando)) Department of Pharmacology, University of Virginia, Charlottesville, VA 22908.

To test the hypothesis that the activation of protein kinase C (PKC) is related to interface between coexisting diacylglycerol (DAG)-enriched and DAG-poor phases, the thermotropic phase behavior of the ternary mixtures dimyristoylphosphatidylcholine (DMPC):dimyristoylphosphatidylserine (DMPS):dioleoylglycerol (DO), DMPC:DMPS:1-palmitoyl-2-oleoylglycerol (PO) and DMPC:DMPS:dimyristoylglycerol (DM) was analyzed and compared with the ability of the lipid mixtures to support PKC activity. Differential scanning calorimetry (DSC) was used to moniter the gel-to-liquid crystalline phase transition as a function of mole fraction DO (X_{DO}), PO (X_{PO}) or DM (X_{DM}) in DMPC:DMPS (1:1) multilamellar vesicles (MLVs) and of X_{DO} in large unilamellar vesicles (LUVs). The addition of DAG in low mole fractions gave rise to the appearance of overlapping transitions comprised of a broad and sharp component. The phase boundaries of the ternary mixtures deduced from partial phase diagrams were X_{DO} =~ 0.1 and ~ 0.3 for DMPC:DMPS:DO, X_{PO} =~ 0.05 and ~ 0.4 for DMPC:DMPS:PO and X_{DM} =~ 0.025 and ~ 0.5-0.6 for DMPC:DMPS:DM. Above these mole fractions, the transitions again became very sharp. The ability of the lipid mixtures to support activity of PKC-α and PKC-η was examined below and above the gel-to-liquid crystalline phase transition. In the gel phase, PKC activity went through a maximimum as a function of increasing concentration of each DAG and was restricted to lipid compositions in which coexisting phases were observed. Maximal activity decreased with increasing saturation of the DAG. In the fluid state, maximal PKC activity was shifted to higher DO concentrations and the peak was much broader. Collectively, these data support a role for both the presence and nature of interface in activation of PKC. (Supported by NIH grants GM31184, GM37658, GM47525, DK07320 and DK07642).

W-Pos365

ELECTRON SPIN RESONANCE STUDIES ON ROTATIONAL DIFFUSION DYNAMICS OF SPIN-LABELLED FORMS OF PULMONARY SURFACTANT PROTEINS SP-B AND SP-C IN BILAYERS OF DPPC OR DPPG. ((J. Pérez-Gil[1], A. Cruz[1] and D. Marsh[2])) [1]Dept. Bioquímica y Biología Molecular I, Univ. Complutense, 28040 Madrid, SPAIN [2]Abt. Spektroskopie, Max-Planck-Institut für Biophysikalische Chemie, Göttingen, GERMANY

Pulmonary surfactant proteins SP-B and SP-C have been isolated from porcine lungs and selectively labelled with 2,2,6,6-tetramethylpiperidine-1-oxyl (TEMPO) -isothyocyanate at their N-terminal amine ends, to analyze mobility of both proteins at nanoseconds time-scale. Although the sharp ESR spectra of both labelled proteins, SL-SPB and SL-SPC, suggest their rapid and nearly isotropic rotation in chloroform/methanol solutions, clear and significant differences were found between both polypeptides suggesting that rotation of SP-C-labelled probe was somewhat more anisotropic than that of the one attached to SP-B. When these spin-labelled forms of the proteins were reconstituted in bilayers of DPPC or DPPG, they showed much more broadened and anisotropic ESR spectra, indicating extreme restrictions in the movement of the protein-attached probe when they are inserted in membranes. Mobility of both SP-B and SP-C was more restricted in bilayers of DPPG than in DPPC, suggesting that electrostatic interactions of the positively-charged residues at the surface of the proteins with negatively-charged PG headgroups influence the conformation and rotational dynamics of the proteins. SL-SPB and SL-SPC also showed clear differences in their prefered rotation axis in both lipids and at temperatures both above (50°C) and below (25°C) the gel-to-fluid transition temperature of DPPC or DPPG (41°C). Interestingly, the mobility of the protein-attached spin probes was sensitive to temperature on the time-scale of conventional ESR. Although some residual segmental mobility of the thiourea-linked probes cannot be discounted, the resilts clearly reflect differences in overall protein dynamics in phospholipid gel and fluid phases, that could be important for the biophysical properties of surfactant bilayers and monolayers.

This work has been partially funded by Fondo de Investigaciones Sanitarias (96/1290) and Universidad Complutense (PR218/94-5684) in Spain, and a NATO Collaborative Research Project (JARC-501).

W-Pos366

^{2}H NMR STUDIES OF PULMONARY SURFACTANT PROTEIN SP-B EFFECTS ON BILAYERS CONTAINING DPPG AND DPPC. ((A. S. Dico[1], J. Hancock[2], M. R. Morrow[1], J. Stewart[2], and K. M. W. Keough[2,3])) [1]Department of Physics and Physical Oceanography, [2]Department of Biochemistry, and [3] Discipline of Pediatrics, Memorial University of Newfoundland, St. John's, NF, Canada, A1B 3X9.

Pulmonary surfactant is a lipid/protein mixture which reduces the work of breathing by rapidly spreading into a monolayer at the alveolar air/water interface. ^{2}H NMR was used to examine the effect of porcine pulmonary surfactant protein SP-B on lipid phase behaviour, chain order, and dynamics in bilayers of chain-perdeuterated dipalmitoylphosphatidylglycerol (DPPG-d_{62}) or mixed bilayers containing 70 mol % dipalmitoylphosphatidylcholine (DPPC) and 30 mol % DPPG with one or the other lipid labeled. While SP-B was found to have little effect on chain order, deuteron transverse relaxation was strongly affected by the presence of the protein in both the liquid crystal and gel phases of each lipid system. Perturbation of the bilayer by SP-B was insensitive to the relative amounts of DPPC and DPPG present. There was no indication of a preferential interaction of SP-B with either lipid component. These observations may constrain possible models for SP-B/phospholipid interaction in bilayer precusors of the surfactant monolayer. (Supported by NSERC and MRC Canada.)

W-Pos367

TEMPERATURE DEPENDENT PARTITIONING OF FATTY ACIDS BETWEEN ALBUMIN AND MODEL MEMBRANES ((J.K. Ho and J.A. Hamilton)) Department of Biophysics, Boston University School of Medicine, Boston MA 02118. (Spon. by F. Caserta, Jr.)

Bovine serum albumin is widely used to deliver fatty acids to cells. Studies have been carried out over a range of temperatures (generally between 4°C and 37°C). As a model system for transfer of fatty acids from albumin to membranes, we have studied the binding of long chain fatty acids to phospholipid bilayers (small unilamellar vesicles) in the presence of fatty acid/albumin complexes. The distribution at equilibrium (partitioning) of ^{13}C carboxyl-enriched fatty acids (oleic, palmitic, stearic, arachidic) between albumin and vesicles was monitored by ^{13}C NMR spectroscopy as before (Hamilton and Cistola, Proc Natl Acad Sci USA 83, 1986) at 4°-45°C. Fatty acids partitioned more favorably to phospholipid bilayers with increasing temperature. At low temperature (4°C), the partitioning highly favored serum albumin, except for the very long chain saturated fatty acid, arachidic acid (C20:0), which binds less tightly to albumin. Cholesterol (up to 30 mol%) in phospholipid vesicles did not affect the partitioning of saturated fatty acids, but increased the partitioning of oleic acid to albumin. Studies of the "uptake" of fatty acids by cells at low temperature must consider that the thermodynamics of binding may result in decreased delivery of fatty acids to cells.

W-Pos368

UNDERSTANDING THE NATURE OF INTERACTIONS BETWEEN LIPIDS AND ENGINEERED LUNG SURFACTANT PROTEINS FOR BETTER REPLACEMENT THERAPY ((K.Y.C. Lee, M.M. Lipp, J.A. Zasadzinski and A.J. Waring)) Department of Chemical Engineering, UCSB, CA 93106-5080; Perinatal Laboratories, Harbor-UCLA, CA 90502-2064. (Spon. by K.Y.C. Lee)

A mixture of lipids and proteins, commonly known as lung surfactant (LS), lines the pulmonary air spaces of all mammalian species; a deficiency of LS at birth causes neonatal respiratory distress syndrome (RDS). Research on replacement therapy has made significant progress, and exogenous LS improved oxygenation when administered to premature infants. As LS-specific proteins are difficult to purify, synthetic, engineered proteins are therefore desirable. One LS-specific protein (SP-B), important in replacement therapy, has a net positive charge of 8 and is thought to be responsible for LS's surface activity by preventing anionic lipids from being "squeezed out" of the film during exhalation. To pinpoint the nature of the lipid/protein interaction, we used fluorescence microscopy and isotherm measurements to study the interaction between anionic lipids and 5 different proteins: (1) full length SP-B protein synthesized from its known sequence; (2) a 25-residue analog of its N-terminus (SP-B$_{1-25}$); (3) peptides with repeating KL$_4$ base units after Cochrane and Revak (Science (1991) 254, 566); (4) full length SP-B analog with charged residues replaced by serine; (5) SP-B$_{1-25}$ analog with charged residues replaced by serine. Our results show that the lipid/protein interaction is electrostatic in nature, and that synthetic proteins (1 & 2) alter the isotherm and surface morphology of the monolayer in ways similiar to those of the native protein, while KL$_4$ resembles more closely to the LS protein SP-C.
Supported by NIH 51177 (KYCL, MML, JAZ) and NIH HL 55534 (AJW).

PROTEIN FOLDING

W-Pos369

Fast Folding Dynamics in Peptides Initiated by Laser-Induced Temperature Jumps. (S.E.Vitols, C. Chapin, R. H. Callender, W.H. Woodruff and R. B. Dyer) CST-4 Bioscience and Biotechnology Group Los Alamos National Laboratory, Los Alamos NM 87545

Understanding the mechanisms of protein folding requires structural descriptions of the intermediates in the folding process on timescales ranging from picoseconds to tens of seconds. To address the fast structural dynamics, we have developed infrared techniques which allow study of folding/unfolding events from nanoseconds to milliseconds. A laser pulse creates a rapid (~10 ns) temperature jump of up to 30° C while an IR laser detects and characterizes the intermediates. Since peptides and proteins are melted or re-folded by such temperature changes, and since the amide I' IR spectra are sensitive to polypeptide structure, the fast dynamics of unfolding/folding and the specific structural changes that occur can be observed.

We have applied this approach to the folding/unfolding dynamics of a 21-residue α helical peptide (Fs peptide). The observed relaxation lifetime of the thermal melting process following the T-jump is 160 Ns at 28° C (in response to a T-jump of 18 ° C). Assuming two-state, reversible kinetics, this relaxation contains contributions from both folding and unfolding. Thus, from the relaxation time and the measured equilibrium constant for melting, the folding lifetime is ~180 Ns. We report the temperature dependence of the folding/unfolding dynamics of this peptide. In addition, an isotopic analogue of the Fs peptide has been prepared in which the carbonyls in the central alanines have been isotopically labeled with ^{13}C. Such labeling causes frequency shifts in the amide absorbances of the specific amino acids that are labeled, and thus the folding behavior of specific substructures within the peptide can be observed. We report similar measurements on this isotopically labeled Fs peptide.

W-Pos370

THE NATIVE AND THE HEAT-INDUCED DENATURED STATES OF α-CHYMOTRYPSINOGEN A: A THERMODYNAMIC AND SPECTROSCOPIC STUDY ((Tigran V. Chalikian, Jens Völker, Dan Anafi, and Kenneth J. Breslauer)) Department of Chemistry, Rutgers, The State University of New Jersey, Piscataway, NJ 08855-0939.

We use ultrasonic velocimetry, densimetry, differential scanning calorimetry, as well as UV absorbance and CD spectroscopy to study conformational transitions of α-chymotrypsinogen A as a function of both pH and temperature. Below pH 3.1, the heat-induced denatured state of the protein is molten globule (MG). The heat-induced native (N)-to-MG transition of α-chymotrypsinogen A causes increases in the protein partial specific volume, $v°$, its partial specific expansibility, $e°$, and the partial specific adiabatic compressibility, $k°_s$, equal to 0.003 cm^3g^{-1}, 1.4×10^{-4} $cm^3g^{-1}K^{-1}$, and 4.3×10^{-6} $cm^3g^{-1}bar^{-1}$, respectively, when extrapolated to 25 °C. The MG state of α-chymotrypsinogen A, which lacks the native-like tertiary structure, exhibits a significant amount of secondary structural elements and preserves a significant water-inaccessible core of loosely packed amino acid residues. At neutral and alkaline pH, the heat-induced denatured state of α-chymotrypsinogen is unfolded (U), lacking both tertiary and secondary structures. The heat-induced N-to-U transition of α-chymotrypsinogen A is accompanied by a decrease in $k°_s$ which is greater than 13×10^{-6} $cm^3g^{-1}bar^{-1}$. Our CD spectroscopic and volumetric measurements reveal that the heat-induced U state of the protein is structurally similar to the urea-unfolded state, with the majority of its atomic groups exposed to the solvent.

In the aggregate, we find that by combining volumetric, calorimetric, and optical measurements one can derive unique insights into both the hydration and intrinsic properties of the conformational states of a globular protein. The nature of these insights will be discussed in terms of the properties of the N, MG, and U states of α-chymotrypsinogen A and the transitions through which these states interconvert.

W-Pos371

ON VOLUME CHANGES ACCOMPANYING CONFORMATIONAL TRANSITIONS OF BIOPOLYMERS ((Tigran V. Chalikian and Kenneth J. Breslauer)) Department of Chemistry, Rutgers, The State University of New Jersey, Piscataway, NJ 08855-0939. (Spon. by A. R. Srinivasan)

We describe a new way of interpreting partial volume data on biopolymers. This interpretation provides, for the first time, a rationale for the longstanding "protein volume paradox" in which inexplicably small net volume changes are observed to accompany large conformational changes in proteins, in contrast to expectations of significantly negative volume changes based on small molecule data. A major feature of this interpretation that heretofore has been unappreciated is the contribution from the thermal volume which results from the thermally-induced mutual motions of solute and solvent molecules. This contribution is positive and proportional to the solvent-accessible surface area of a biopolymer. Consequently, conformational transitions of biopolymers which involve an increase in the solvent-accessible surface area will be accompanied by an increase in thermal volume. The near zero volume changes observed for the small globular proteins studied to date (~20 kDa) reflect fortuitous compensations between the negative contributions of enhanced hydration (hydrogen bonding, electrostriction) and reduced intramolecular void volume and the positive contribution of the thermal volume. Since the thermal volume contribution scales with molecular weight, we predict that complete unfolding of larger proteins should be accompanied by significant positive changes in volume. While this paper focuses on contributions from the thermal volume to rationalize the "protein volume paradox", the concepts presented are general and can be applied to explain the volumetric properties of any macromolecule in solution. More specifically, one must take into account changes in the thermal volume when interpreting volume changes associated conformational transitions in any macromolecule (nucleic acid, carbohydrate, lipid, etc.) which are accompanied by changes in the solvent accessible surface area.

W-Pos372

THE STRUCTURAL DIFFERENCES OF FIVE FORMS OF α-LACTALBUMIN AS REVEALED BY FT-IR SPECTROSCOPY: A THERMAL DENATURATION STUDY IN D2O ((H. Zhong, R. Gilmanshin and R. Callender)) Department of Physics, The City College and Graduate Center of the City University of New York, New York, N.Y. 10031

We have applied FT-IR spectroscopy in the amide I' region to studying structures of five forms of bovine α-lactalbumin (holo, acid, apo, holo cam-3ss and apo cam-3ss forms) and their temperature dependencies. Special efforts were made to obtain Ca^{2+} free protein samples. As expected, all these forms have similar conformations at high temperatures. In addition to the major cooperative transitions previously found by other methods, we found several other structural changes not previously reported. The acid state shows different behaviors at low and high temperatures which mainly associate with a diminution in helical structure content. The unfolding curve of holo cam-3ss form exhibits a structural change around 25 °C in addition to the major cooperative transition. Both apo and apo cam-3ss forms include considerable amount of β- structures. Their melting shows co-existence of two structural domains within α-lactalbumin molecules. One of them exhibits a gradual linear change with temperature while the other one includes β-sheet structure and melts cooperatively. Our study indicates that β-sheet domain can be formed without Ca^{2+} while 6-120 disulfide bridge mainly stabilizes the folded structures.

W-Pos373

CYTOCHROME *C* FOLDING INITIATED BY SUBMILLISECOND MIXING AND PROBED USING TIME-RESOLVED FLUORESCENCE ((D.S. Gottfried, S.-R. Yeh, T.K. Das, and D.L. Rousseau)) Dept. of Physiology and Biophysics, Albert Einstein College of Medicine, Bronx, NY 10461.
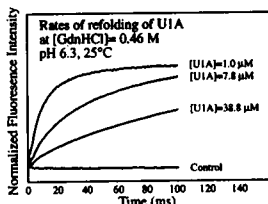
Conventional methods for monitoring the kinetic intermediates formed during folding of a protein from the denatured to the native state have been limited by the millisecond mixing times for stopped-flow devices. A new, rapid mixing apparatus based on a continuous flow technique was designed, tested, and used to study the folding of cytochrome *c* at pH 4.9. This device was evaluated and found to have a dead time of ~100 μs and a mixing efficiency of >90% prior to the mixed solution entering the observation region. Unfolded cytochrome *c* (in 4.4 M GuHCl) was diluted 6-fold with buffer to initiate folding, and the resultant stream of protein molecules was probed using time-correlated single photon counting fluorescence of the single Trp residue. A comparison of the time evolution (250 μs-10 ms) of the fluorescence intensity and lifetimes of Trp59 reveals a change in average lifetime (ascribed to changing conformations of the still unfolded protein) that has not been considered in previous studies of steady-state intensity. Furthermore, the corrected fluorescence intensity decay due to protein folding which brings the Trp within quenching range of the heme is considerably faster than formation of the native heme ligation state measured using resonance Raman spectroscopy. The data indicate a heterogeneous protein structure during the folding process including at least three conformational populations with respect to Trp fluorescence: unfolded protein with detectable fluorescence, non-native protein with quenched fluorescence, and native protein with quenched fluorescence.

W-Pos374

GLOBAL CONFORMATIONAL CHANGES IN CYTOCHROME *C* INDUCED BY INTERACTION WITH LIPIDS.
((T.J.T. Pinheiro,[f] H. Cheng,[#] G.A. Elöve,[‡] and H. Roder[§])) [f]Department of Biological Sciences, University of Warwick, Coventry CV4 7AL, UK; [§]Regeneron Pharmaceuticals, Inc., Tarrytown, NY 10591-6707, USA; [#]Fox Chase Cancer Centre, Philadelphia, PA 19111, USA.

The mechanism by which water-soluble proteins bind and insert into biological membranes is at present poorly understood. From the few cases studied, it is becoming apparent that the transition from the 'water-soluble state' to 'membrane-associated state' involves large conformational changes in the protein structure. The nature of the structural intermediates involved in this transition is of general interest to the field of protein folding.

We have shown by fluorescence, circular dichroism and absorbance spectroscopy that the interaction of cytochrome *c* with anionic lipid membranes leads to a substantial perturbation in its tertiary structure. Recently, we have used hydrogen/deuterium amide exchange methods combined with 2D NMR spectroscopy to characterise the structural changes in cytochrome *c* induced by its interaction with DOPS vesicles. Among the amide protons observed, all show comparable increase in the proton/hydrogen exchange rates relative to the native state due to interactions with the lipid. These results, combined with fluorescence-detected kinetic measurements, have lead to a plausible mechanism for the unfolding of cytochrome *c* at the membrane interface.

W-Pos375

ARE PROTEIN FOLDING INTERMEDIATES CAUSED BY TRANSIENT AGGREGATION ?

((Mia Silow and Mikael Oliveberg)) Biochemistry, Chemical Centre, BOX 124, S-221 00 Lund, Sweden. e-mail: mikael.oliveberg@biochem.lu.se

Recently some small globular proteins have been found to fold directly into their native conformations in a two-state process without populated intermediates. The findings question the role of intermediates and point at the possibility that partly structured states are misfolds trapped in non-productive pathways. We report here that the spliceosomal protein U1A, which exhibits a classical three-state folding behaviour, has an intermediate which is caused by transient aggregation of denatured protein. The aggregation behaviour is reflected in a concentration dependence of the refolding amplitudes. At low concentrations of protein, U1A folds in a two-state process directly from the denatured monomer whereas at high concentrations of protein the observed refolding takes place from an aggregate which is formed in the dead-time of the stopped-flow instrument. Is transient aggregation a general problem in time resolved folding studies or a unique feature of the polypeptide of U1A ?

Rates of refolding of U1A
at [GdnHCl]= 0.46 M
pH 6.3, 25°C
[U1A]=1.0 μM
[U1A]=7.8 μM
[U1A]=38.8 μM
Control
Normalized Fluorescence Intensity
0 20 40 60 80 100 120 140
Time (ms)

W-Pos376

MEASURING RAPID EVENTS IN TEMPERATURE INDUCED PROTEIN FOLDING((Chris Fischer, Anne Gershenson, Joseph Schauerte, Ari Gafni & Duncan Steel)) University of Michigan, Ann Arbor, MI 48109

Protein structures that form during the early events of folding or unfolding determine the pathways that follow during later stages, and in the case of folding, are critical in assuring a correct final folded state. However, their experimental detection and characterization is difficult because they are present for short periods of time (<msec) and at low concentrations. To tackle this problem, we have developed a system that exploits the fact that proteins denature both at low and elevated temperatures. By creating a rapid temperature jump across the transition temperature, it is possible, in principle, to initiate either folding or unfolding from the denatured or native state, respectively. Determination of the time scales for the changes in secondary and tertiary structure that follow the temperature jump provides important kinetic information regarding the folding/unfolding pathway. Experimental insight into the dynamics of these processes is, however, limited due to the difficulty of obtaining data on short time scales. Initiation of protein folding or unfolding using laser-based methods makes these time scales experimentally accessible. Indeed by using a Raman shifted Nd-YAG laser with a pulse width of 10 nanoseconds we achieve temperature jumps on the order of 15-20° C. The time evolution of the protein structure is followed using a UV probe beam to monitor absorption, UV excited fluorescence, and eventually CD. (Supported by ONR N00014-91-J-1938)

W-Pos377

LASER TEMPERATURE JUMP STUDIES OF THE HELIX-COIL TRANSITION OF AN ALANINE-BASED PEPTIDE (P. A. Thompson, W. A. Eaton and J. Hofrichter) Laboratory of Chemical Physics, Building 5, NIDDK, NIH, Bethesda, MD 20892-0520. (Spon. by D. R. Davies)

We have developed a laser temperature-jump instrument for investigating protein and peptide folding/unfolding. The dynamic range of the instrument is ~5 ns to >1 ms. The fundamental of a Q-switched Nd:YAG laser, Raman shifted to 1.54 μm, directly heats water by vibrational excitation. The probe source is an intracavity frequency doubled argon ion laser, which can be used for both absorption and fluorescence measurements. Uniform temperature increases of up to 30°C can be achieved. We have used this instrument to study the helix-coil transition kinetics of a synthetic, 21-residue α-helical peptide: MABA-AAAAA(AAARA)$_3$A-CONH$_2$, where MABA is the fluorescent probe 4-methylaminobenzoic acid. The carbonyl oxygen of MABA forms a hydrogen bond with the amide NH of residue 4 only in the helical conformation, producing a large increase in the fluorescence intensity. The relaxation time shows an interesting temperature dependence, with τ ~ 10 ns at both 0°C and 60°C, and a maximum at 30°C with τ ~ 20 ns. Using infrared spectroscopy to monitor the average helix content, Williams *et al.* (*Biochemistry* 35, 691, 1996) measured a relaxation time for the same peptide (without MABA) of 160 ns at 30°C. The difference in the observed relaxation times will be discussed in terms of a kinetic mechanism for the helix ⇌ coil transition.

W-Pos378

ATOMIC FORCE MICROSCOPY OF A MONOMERIC INSULIN ANALOG CRYSTAL FORM: COMPARISON WITH NATIVE STRUCTURE.
((C.M. Yip[¥], M.D. Ward[†], M.L. Brader[¥], M.R. DeFelippis[¥]))
[†]University of Minnesota Department of Chemical Engineering and Materials Science, Minneapolis, MN 55455; [¥] Eli Lilly and Company Biopharmaceutical Development, Indianapolis, IN 46285

Lys[B28]Pro[B29], a monomeric insulin analog, can be crystallized in a hexameric form in the presence of phenolic ligands where these agents serve to stabilize the Lys[B28]Pro[B29] hexamer. In situ solution tapping mode atomic force microscopy performed on crystals of Lys[B28]Pro[B29] revealed molecular scale periodicities consistent with the packing motif of the Lys[B28]Pro[B29] hexamers in the (001) crystal plane, as determined from single-crystal X-ray diffraction studies. Notably, in situ AFM revealed the presence of screw dislocations and an increased areal density of surface defects, including single hexamer "point" defects. These results suggest that the close packing of this insulin analog, which would facilitate the formation of well-defined and ordered crystals, is significantly perturbed, possibly by weak interfacial contacts between Lys[B28]Pro[B29] hexamers. Such perturbations may account for the tendency for this monomeric analog to form crystal twins. The layer-by-layer stacking motif observed in situ by AFM and the presence of these stacking and dislocation defects are of particular importance for understanding the facile hexamer-monomer dissociation of Lys[B28]Pro[B29].

W-Pos379

HYDRODYNAMIC STUDIES OF DENATURED STATES OF BPTI.

((H. Pan, G. Barany and C. Woodward)) Department of Biochemistry, University of Minnesota, St. Paul, MN 55108.

Unfolded and partially folded states of proteins are increasingly important in studies of proteins folding. They are ensembles of interconverting conformations. The NMR- and CD-detected conformations of three BPTI states, unfolded reduced BPTI ([R]$_{Abu}$), partially folded [14-38]$_{Abu}$, and unfolded [14-38]$_{Abu}$ have been characterized in our lab (Pan et al. 1995 *Biochemistry* 34:13974; Barbar et al. 1996 *Folding & Design* 1:65; refs therein). Non-random conformations sampled by [R]$_{Abu}$ and unfolded [14-38]$_{Abu}$ are different in that the former includes significant non-native structure. We recently determined the compactness of these three BPTI denatured states by pulsed-field gradient NMR. The hydrodynamic radius (R_H) of partially folded [14-38]$_{Abu}$ is 19% larger native; [R]$_{Abu}$ and unfolded [14-38]$_{Abu}$ both have values of R_H about 36% larger than native. [R]$_{Abu}$ is not as expanded as a statistical random coil of the same number of residues (58), but rather is collapsed to the extent that its average compactness is about the same as unfolded BPTI constrained by a cross link between residues 14 and 38. The hydrogen exchange rates of [R]$_{Abu}$ have also been determined.

W-Pos380

NMR Characterization of Multiple Conformations of the Partially Folded Ensemble of BPTI

((E. Barbar, G. Barany and C. Woodward)) Department of Biochemistry, University of Minnesota, St. Paul, MN 55108.

The protein [14-38]$_{Abu}$, a chemically synthesized variant of BPTI with the 14-38 disulfide bond intact and the cysteines replaced by α-amino-n-butyric acid (Abu) is an ensemble of conformations [Biochemistry, 34, (1995) 11423]. Heteronuclear NMR spectra contain two, and in a few cases three or four, exchange cross peaks for each ^{15}N-bound ^{1}H, reporting the presence of multiple conformations that interconvert on a time scale of $\geq$ milliseconds. The relative abundance of more folded *versus* disordered conformations changes throughout the molecule, indicating that various regions of the partially folded protein are disordered to different extents prior to onset of thermal denaturation [Biophysical Chemistry, (1996), in press]. In this work, we have measured the exchange rates at conditions where either local segmental fluctuations or global unfolding conditions are dominant. This system is unique in providing a measure of the populations of interconverting partially folded conformations, as well as a microscopic view of cooperative folding of a fluctuating ensemble. Furthermore, the slow chemical exchange between *partially* folded states enables us to characterize the dynamics of both conformations. For two or more conformations in slow exchange, hydrogen exchange rates, and relaxation measurements were determined. The dynamic picture that emerges is that while the central hydrophobic core of the protein is rigid, the other parts of the molecule undergo local segmental motions that are different in various segments of the protein, implying different degrees of folding. This work was supported by NIH grants GM 26242 (C.W.), GM 51628 (G.B. and C.W.), GM 17341 (EB).

W-Pos381

PRESSURE UNFOLDING OF apoMb

((Gediminas J. A. Vidugiris and Catherine A. Royer))

University of Wisconsin at Madison, School of Pharmacy, Madison, WI 53706

We investigated apoMb unfolding induced by high hydrostatic pressure. Conformational changes were monitored by intrinsic tryptophan emission fluorescence of two tryptophan residues, located in A helix of horse apoMb. Pressure induced unfolding of apoMb from the native conditions (pH 6.0) follows through an intermediate or MG state, observed at pressure >1 kBar and characterized by a fluorescence intensity maximum. Similar spectroscopic characteristics (intensity and position of fluorescence maximum) are exhibited by acid induced (pH 4.2) MG state of apoMb. The pressure profiles of emission wavelength at pH 6 were fit to a two-state transition model of native → MG and yielded a free energy change (ΔG) of 1.95 kcal/mol and a volume change (ΔV) of -67 ml/mol. Pressure under 2.5 kBar completely unfolds MG state of apoMb as evidenced by a further red shift and decrease in the total fluorescence intensity. The data fitted to a model of MG → unfolded protein transition yielded ΔG=0.7 kcal/mol and ΔV= -44 ml/mol. Addition of 0.4M of NaCl increases the stability of MG state of apoMb (pH4.2). Application of pressure to this salt-stabilized MG state results in a smaller red shift and almost no change in fluorescence intensity, indicating population of a fourth form of the protein, distinct from the native, unfolded and MG states. The transition from the salt stabilized MG to the novel intermediate state exhibited ΔG of about 1 kcal/mol and a ΔV= -34 ml/mol. Comparison of the volume changes for the native → MG transition and for the MG → unfolded transition reveals that about 60% of the total volume change of totally unfolding apoMb is associated with formation of the molten globule state. Since the volume change is a measure of the change in interaction with the solvent upon unfolding, these results indicate that the MG state exhibits hydration characteristics about halfway between those of the folded and unfolded protein.

W-Pos382

COMPARISON OF SLOW STRUCTURAL CHANGES DURING FOLDING OF ALKALINE PHOSPHATASE IN VIVO AND IN VITRO

((E. Dirnbach, D.G. Steel and A. Gafni)) Institute of Gerontology, University of Michigan, Ann Arbor, MI 48109

The late stages of the *in vitro* folding of Alkaline Phosphatase (AP) from the GuHCl denatured state are characterized by slow post-activational conformational changes. This is an annealing-like process, where the rigidity of the core increases and the overall enzymatic lability slowly decreases with time. Rigidity of the enzyme core is determined by the changing room temperature phosphorescence (RTP) lifetime of the core Tryptophan 109, and the overall enzymatic lability is measured by the rate of denaturation of refolded AP in GuHCl. Both methods have been used to study the *in vitro* folding of AP and have also recently been applied to the study of *in vivo* folding. We have induced AP synthesis in initially low-AP *E. coli* and accurately detected the synthesized *in vivo* AP population with RTP intensity. The rigidity and lability of this AP population is tracked over time to determine the extent of annealing. In comparison to *in vitro* folding, the folding of AP in the periplasm of *E. coli* has a much faster annealing process. In an attempt to better characterize this process, and resolve the annealing differences, we are examining the *in vitro* folding of AP from the denatured and reduced state. This is a more realistic folding starting point, and closer to the *in vivo* periplasmic situation. The greater initial conformational freedom of the chain may have an impact on the rate of the annealing process during folding. (Supported by NIA AG09761 and NIH 5T32GM08270-06)

W-Pos383

SUBMILLISECOND PROCESSES IN PROTEIN FOLDING STUDIED BY ULTRARAPID MIXING AND CONTINUOUS FLOW

(C.-K. Chan, W. A. Eaton and J. Hofrichter) Laboratory of Chemical Physics, Building 5, NIDDK, NIH, Bethesda, MD 20892-0520.

We are developing an ultrarapid mixing, continuous flow method to study submillisecond folding of chemically-denatured proteins. The turbulence created by pumping solutions through a small gap produces mixing and dilution of denaturant in tens of microseconds. We are using this method to study cytochrome *c* folding kinetics in the previously inaccessible time range 80 μs - 3 ms. Heme-ligand exchange chemistry introduces complexity and slowing of the folding kinetics due to trapping of misfolded structures. These were eliminated by forming the imidazole complex, making cytochrome *c* more like a protein without a prosthetic group. The distance between the lone tryptophan and the heme ($\sim$ 40 residues distant in the sequence) was monitored by heme quenching of the tryptophan fluorescence due to Forster excitation energy transfer. The fluorescence decrease is biphasic. There is an unresolved process with τ < 50 μs, corresponding to a barrier-free, partial collapse to the new equilibrium unfolded state at the lower denaturant concentration. This is followed by a slower ($\tau \geq$ 500 μs) exponential process with a rate constant that depends on denaturant concentration, and corresponds to crossing the thermodynamic barrier that separates the unfolded and folded states. Several fundamental issues concerning the dynamics of collapse and barrier crossings in protein folding are raised by these results.

W-Pos384

FLUORESCENCE QUENCHING STUDIES ON THE REFOLDING AND MEMBRANE INSERTION OF OUTER MEMBRANE PROTEIN A (OMP A) OF E. COLI.

((J. H. Kleinschmidt and L. K. Tamm)) Dept. of Mol. Physiology and Biol. Physics, Univ. of Virginia, Charlottesville, VA 22906-0011

OmpA is predicted to form an eight stranded b-barrel in the outer membrane of E. coli. Unfolded OmpA spontaneously inserts into lipid bilayers upon rapid dilution of the denaturant urea. It has recently been shown that the OmpA insertion into DOPC bilayers exhibits three kinetic phases with two membrane-bound intermediate forms (1). In the present study we sought to determine structural differences between the folding intermediates of OmpA. Kinetic refolding experiments were carried out in the presence of small unilamellar vesicles of DOPC at temperatures ranging from 2 to 40 °C. Four different brominated stearoylpalmitoylphosphatidylcholines (SPPC), with bromines in positions 4/5, 6/7, 9/10, and 11/12 were used to measure their effect on OmpA tryptophan fluorescence quenching during the time course of folding and membrane insertion. At 40°C and after 30 min or longer incubation, bilayers containing 6,7-diBrSPPC and 9,10-diBrSPPC were the most efficient quenchers of Trp-fluorescence. The next best quencher was 4,5-diBrSPPC followed by 11,12-diBrSPPC. In the first minutes of OmpA insertion differences between the different quenchers were much less expressed, with 11,12-diBrSPPC being a much more efficient quencher in the early than in the later phases of insertion. At 2 °C, 4,5- and 6,7-diBrSPPC were the most efficient quenchers even after long incubation times. A temperature jump from 2 to 37 °C converted the low-temperature into the high-temperature quenching profile, supporting the notion that the average Trp-position moves into a deeper location in the bilayer during membrane insertion of OmpA.

(1) Kleinschmidt and Tamm, 1996, Biochemistry 35, 12993-13000.

W-Pos385

PIEZOELECTRIC-COUPLED DIAMOND ANVIL CELL FOR STUDYING PRESSURE-INDUCED PROTEIN CONFORMATIONAL CHANGES.
((M. S. Hutson, J. Harrell, A. L. Klinger, M. S. Braiman.)) Biochemistry Department, University of Virginia Health Sciences Center, Charlottesville, VA 22908.

By mechanically coupling a piezoelectric pusher rod (Burleigh Instruments) to a high-pressure diamond anvil cell, we have obtained reproducible pressure changes of several thousand atm. Using this apparatus, we have reproduced the IR absorption spectral changes produced by pressure denaturation of ribonuclease A [Takeda et al, Biochemistry(1995) 34:5980-7]. In our apparatus, however, the novel use of piezoelectrics coupled to the diamond anvil cell allows the pressure to be changed reversibly by several thousand atm in under a millisecond. Such fast pressure changes are potentially a useful trigger for the study of protein folding kinetics, because many proteins denature completely and reversibly over such pressure ranges. While equilibrium studies of pressure- and temperature-induced folding reactions have generally been fit by a two-state model, additional states that are relatively unpopulated at equilibrium may be accessible by kinetic analysis.

W-Pos386

NON–COVALENT COMPLEX OF THIOREDOXIN FRAGMENTS (1-73,74-108): SECONDARY AND SUPERSECONDARY STRUCTURE BY NMR SPECTROSCOPY. ((W. Yu, V. Gibaja, E. Arevalo, MC. Petit, J-H.Li, and M.L. Tasayco)) Chemistry Department, City College of the City University of New York, New York, N.Y. 10031

The well known 108 aminoacids protein E.coli-Thioredoxin was proteolytically cleaved into the N-fragment (1-73) and C-fragment (74-108), to study their association/folding into a native-like structure. The equilibrium stoichiometric mixture of both fragments with and without isotopic labels (^{1}H, ^{15}N, ^{13}C) was studied by 2D-NMR spectroscopy using the standard DQF-COSY, TOCSY and NOESY experiments. The results of the rigorous assignment and sequencing of the complex show a native-like structure with almost the same local backbone conformation as the original protein. The secondary structure of this complex shows three alpha-helices, one 3_{10}-helix and five beta-strands. Comparison of the chemical shift values between the complex and the original protein indicates differences in the conformation of the active site and the cleavage region. Surprisingly, gradient HSQC experiments using the C-fragment with 13-enriched Proline-76 shows that this residue, located near the cleavage site, show the same cis conformation as in the original protein.

W-Pos387

SELF – ASSOCIATION VERSUS NON – SELF ASSOCIATION: FRAGMENTS OF THE PROTEIN THIOREDOXIN (1-73, 74-108) ((Jian-Hua Li, Nancy Sevieux, Maria Luisa Tasayco)) Chemistry Department, City College of the City University of New York, N.Y. 10031.

Studies were carried out to determine the ability of the complementary fragments of Thioredoxin (1-73 and 74-108) to form non-covalent complexes by oligomerization or non-self complementation. Thioredoxin was cleaved proteolytically into two fragments: the N-fragment (1-73) and the C-fragment (74-108). The isolated N- and C- fragments are essentially unfolded, while the stoichiometric mixture of the N- and C-fragments show a native-like overall structure of the intact protein, according to circular dichroism and nuclear magnetic resonance spectroscopy. Measurements were carried out using gel filtration chromatography and gel electrophoresis techniques on four samples: the N-fragment, the C-fragment, the mixture of the N- and C- fragments of Thioredoxin and the intact protein. The results of gel electrophoresis under native conditions suggest the oligomerization of the N-fragment. The results of gel filtration chromatography indicate that the hydrodynamic size is dependent on ionic strength and pH. Our results indicate a preference for non-self-association over oligomerization and additionally the preferential formation of an oligomer in the isolated N-fragment.

W-Pos388

A STOPPED-FLOW INSTRUMENT THAT CAN MONITOR BOTH FLUORESCENCE AND CIRCULAR DICHROISM SIGNALS: APPLICATION TO STUDIES WITH *Staphylococcal* NUCLEASE. ((M. R. Eftink, R. M. Ionescu, K. Gartin, and G. D. Ramsay*)) Dept. of Chemistry, University of Mississippi, University, MS, 38677, and *Aviv Associate, Lakewood, NJ 08701.

Both stopped-flow fluorescence and stopped-flow circular dichroism (CD) are valuable methods for characterizing the kinetics of the unfolding and refolding of proteins. The two methods provide complementary information, with fluorescence focusing on changes in the microenvironment of the fluorescing centers (e.g., tryptophan residues, of which there may be a small number in a protein) and with CD observing more global changes in the secondary structure of a protein. The latter method arguably provides more structural information, but CD suffers from very poor signal to noise (S/N), as compared to fluorescence. We will describe a stopped-flow instrument that enables both types of detection in order to take advantage of the favorable attributes of each. As example data we will show stopped-flow fluorescence and CD kinetic traces for the guanidine-HCl induced unfolding and refolding of nuclease. By performing a global nonlinear least squares analysis of the combined (and weighted) data sets we will show that the higher S/N of the fluorescence data can help us pull out phases in the noisier CD data. (This research was supported by NSF grant MCB 94-07167.)

W-Pos389

NON-NATIVE STRUCTURES OF *STAPHYLOCOCCAL* NUCLEASE IN TRIFLUOROETHANOL AND MOLTEN GLOBULE STATES IN MUTANTS, W140A and W140A+Y93W. ((H.Y. Hu[1] & T.Y.Tsong[1,2])). Dept Biochem, [1]Hong Kong Univ of Sci & Technol, Kowloon, Hong Kong, and [2]Univ of Minn, St. Paul, MN 55108

Trifluoroethanol (TFE) is known to disrupt tertiary structure but promote helical structure of proteins. For the wild type *staphylococcal* Nuclease (SNase), the presence of TFE in solution greatly reduces its thermal stability. At about 10-12%, ΔH_{cal} of unfolding reduces to 50%, and at 20% TFE, ΔH_{cal} reduces to a negligible amount, but the amount of the secondary structure has no significant change. However, when TFE concentration is up to 30%, the helical content of SNase reaches 1.5 times of the native state. These results indicate that SNase in TFE has structures which are non-native-like, and they have little conformational energy. Non-native-molten globule-like structures are also observed in mutants of SNase, W140A and W140A+Y93W. In aqueous solution at pH7.4, helical contents of both mutants are reduced to 1/3 that of the WT, but the sheet contents increased substantially. These non-native-like structures have no ΔH_{cal} but they bind ANS strongly. They have all the characteristics of the putative molten globular state in protein folding.
Work is in progress to measure the rate of the formation of these non-native-like-molten-globule states and determine their roles in protein folding.

W-Pos390

ENTRAPMENT OF STYRYL-7 WITHIN THE CAVITY OF HORSE SPLEEN APOFERRITIN. ((David A. Ehlert, Matthew P. Kavalauskas, and Guilherme L. Indig)) School of Pharmacy, University of Wisconsin, Madison, WI 53706.

Horse spleen ferritin is a 24-mer, spherical, iron-storage protein. Its shell (apoferritin) can accommodate approximately 4500 iron atoms inside its hollow volume. Two types of channels (3-4 Å in diameter) penetrate the protein shell at intersection points of its subunits, connecting the exterior and the interior of the protein. Although apoferritin channels are clearly involved in iron transport, the mechanisms of permeation of other species though these channels are not well understood. It is known that species with molecular cross section bigger than the diameter of the protein channels display limited permeation properties, and that other factors, such as specific interactions between protein subunits and permeating species, may play an important role in the permeation process. Another way of transferring molecules from the external bulk solution to the protein interior is brought about by the fact that apoferritin can be dissociated into its building units by exposure to acidic (pH 2) medium, and reassembled to its original 24-mer structure by further exposure of the subunits to a neutral-to-alkaline (pH 7-9) medium. As a result of this pH-induced unfolding and refolding process, relatively large molecules (cross section much bigger than the diameter of ferritin channels) present in the bulk solution may be entrapped within the interior of the protein. The entrapment of relatively large species inside ferritin is interesting under the viewpoint of drug delivery, since a variety of drugs of interest could be placed into the protein's cavity to produce a bio-compatible system. Here we report the efficiency of entrapment of a model guest molecule, styryl-7, a methachromatic photophysical probe, into the cavity of ferritin. The resulting supramolecular structure was characterized with the employment of a combination of spectroscopic methods.

W-Pos391

STUDY OF CONFORMATIONAL DYNAMICS OF HUMAN GROWTH HORMONE AND ITS RELATION TO TRANSPORT ACROSS TISSUE MEMBRANES. ((S.S.Vangala*, B.Variano*, S.Milstein* and C.A.Royer*)), *425 N. Charter St., School of Pharmacy, University of Wisconsin-Madison, Madison, WI 53705, *Emisphere Tech. Inc., 15 Skyline Dr., Hawthorne, NY 10532.

Human Growth Hormone (hGH) is used in treating hypopituitary children, bleeding ulcers, muscular dystrophy, and for its hypocholesterolemic affect. Like most protein drugs, the bio-availability of hGH through non-parenteral route of drug delivery is low. Attempts have been made to improve the drug bio-availability by use of penetration enhancers. However, most penetration enhancers have resulted in extensive tissue damage, and it is believed that the mechanism of enhanced transport is via this damage. Recently low molecular weight compounds have been tried with hGH which seem to increase the permeability of protein across the epithelial tissue without damage to the tissue by affecting the protein, not the membrane. Some of these carriers have been shown to increase the permeability of hGH more than others. It has been previously postulated that this enhancement in presence of carriers is due to stabilization of partially folded states. In addition destabilization of the native state or destabilization of aggregates in the presence of carriers would also result in increased permeability of hGH. We present here studies on the unfolding of hGH and the effect of carriers on this transition.

W-Pos392

INVESTIGATING THE HEAT SHOCK PROTEIN GROEL ((S. Neuhofen, P. Guhr, C. Coan, J.G. Wise and P.D. Vogel)) Fachbereich Chemie/Biochemie, University of Kaiserslautern, 67663 Kaiserslautern, Germany. Tel.: 49-631-205-3801, FAX: 49-631-205-3419; Email: vogel@chemie.uni-kl.de.

We employed ESR spectroscopy using spin-labeled adenine nucleotides to investigate nucleotide binding to the E. coli heat shock protein GroEL. Up to 14 moles of C8-SL-ADP or the corresponding ATP analog bound to the protein with K_D-values between 50 µM and 70 µM. Distinct conformational differences were observed upon binding of either the ATP or the ADP analogs to GroEL. A C8-spin-labeled AMPPNP-derivative in complex with GroEL resulted in ESR-spectra that were identical to those obtained with the ADP-analog, indicating that AMPPNP should be viewed as an ADP-analog for GroEL. This latter observation is especially relevant when studying the mechanism of the protein.

We also covalently modified GroEL using CrATP as a non-hydrolyzable ATP analog and CrADP as an ADP analog. Different incubation times in the presence of these nucleotide analogs resulted in differential blocking of nucleotide binding sites in the protein that was tested using ESR-titrations with the above mentioned C8-SL-ANPs. After 2 min incubation in the presence of CrATP, about seven nucleotide binding sites were no longer accessible to C8-SL-ANP. One interpretation is that one of the heptameric rings of GroEL was completely and covalently occupied by CrATP. Such treated protein exhibited 50 % of the normal ATP-hydrolysis activity and approximately 50 % of the refolding activity when assayed using previously denatured porcine lactate dehydrogenase as folding substrate.

The results of our nucleotide binding studies using C8-SL-ANPs and our studies employing covalent blocking of nucleotide binding sites with CrANPs do not support the hypothesis of intersubunit or inter-ring cooperativity as was postulated by other researchers as part of the mechanism of GroEL.

ELECTRON TRANSFER SYSTEMS

W-Pos393

THE MECHANISM OF THE REDUCTION OF DIOXYGEN TO WATER CATALYZED BY CYTOCHROME c OXIDASE. ((Artur Sucheta and Ólöf Einarsdóttir)) Department of Chemistry and Biochemistry, University of California, Santa Cruz, CA 95064.

The reaction between bovine heart cytochrome oxidase and dioxygen was investigated following photolysis of the fully reduced CO-bound enzyme. Time-resolved optical absorption difference spectra were collected by a gated multichannel analyzer in the visible and Soret regions ($\lambda = 370$-720 nm) 50 ns to 50 ms after photolysis. Singular value decomposition (SVD) analysis indicated the presence of at least seven intermediates. Multiexponential fitting gave the following apparent lifetimes: 1 µs, 10 µs, 26 µs, 32 µs, 86 µs and 1.3 ms. Based on the SVD results and a double difference map, a sequential kinetic mechanism is proposed from which the spectra and time-dependent populations of the reaction intermediates were determined. The ferrous-oxy complex with a peak at 595 nm and a trough at 612 nm versus the reduced enzyme reaches a maximum concentration at 30 µs. It decays to a mixture (1:6) of peroxy species in which cytochrome a is reduced and oxidized, respectively. Cytochrome a_3 in both species has a peak at 606 nm versus its oxidized form. The peroxy species decay to a ferryl, with a peak at 578 nm versus the oxidized enzyme, followed by electron redistribution between Cu_A and cytochrome a. The two ferryl species reach a maximum concentration ~310 µs after photolysis. The excellent agreement between the experimental and theoretical spectra of the intermediates provides unequivocal evidence for the presence of peroxy and ferryl species during the dioxygen reduction by cytochrome oxidase at room temperature.
Supported by NIH grant R29 GM45888.

W-Pos394

ALCOHOL EFFECTS ON CYTOCHROME c OXIDASE ACTIVITY AND INTRAMOLECULAR ELECTRON TRANSPORT. ((J. L. Brooks, A. Sucheta, D. W. Deamer and O. Einarsdóttir)) Department of Chemistry and Biochemistry, University of California at Santa Cruz, Santa Cruz, CA 95064.

The relationship between lipid properties and cytochrome c oxidase (CcO) function is unclear. Saturating concentrations of n-alcohols offer a convenient way to vary chain length of the lipid environment of isolated CcO. We have found that octanol, decanol and dodecanol inhibit soluble CcO and uncoupled reconstituted CcO up to 50%. At low alcohol concentrations, coupled CcO in liposomes is slightly inhibited (<10%) but is activated at higher concentrations by the uncoupling effect of the alcohols until the respiratory control ratio approaches 1. The fact that saturating alcohols only partially inhibit the enzyme suggests that the lipid environment changes the conformation of the enzyme but does not irreversibly inhibit its function by denaturation. Significantly, monocarboxylic acids in the same homologous series have little effect on the CcO. To determine how the alcohols might inhibit CcO, flash photolysis experiments were performed on fully reduced and mixed-valence CcO with bound carbon monoxide (CO) in the presence and absence of dodecanol. The alcohol had no effect on the apparent lifetimes observed after photolysis of CO from the fully reduced enzyme. Preliminary experiments on the photolysis of the mixed-valence CO-bound enzyme indicate that electron transfer between cytochrome a and Cu_A is inhibited by ~50%. Further work with other homologous series, including long chain amines, is underway. Supported by NIH grant R29 GM45888

W-Pos395

EVIDENCE FOR A BRANCHED SEQUENCE OF ELECTRON TRANSFER IN THE REDUCTION OF O_2 BY CYTOCHROME aa_3 ((S. Bose, R. W. Hendler, R. I. Shrager[a], Sunney I. Chan[b], and Paul D. Smith[c])) LCB, NHLBI,[a]LAS, DCRT, [c]BEIP, NCRR NIH, Bethesda, MD 20892, [b]LCP, CA Inst. Tech., Pasadena, CA 91125

Multichannel optical spectra obtained with a 10 µs time-resolution spectrometer were analyzed by singular value decomposition. Formation of a heme-O_2 complex was seen with a τ of ~10 µs, followed by three steps of heme reduction with τ's of 0.09, 1.0 and 30 ms. The 0.09 ms species accounted for 100% of heme a (oxidized Soret peak at 428 nm). The other two species each accounted for 50 % of heme a_3 (oxidized Soret peaks at 415 nm). The data were analyzed according to two different models; 1.) linear sequential and 2.) branched sequential. In the branched model, the transfer event with a τ of 0.09 ms was split between two separate paths, each going to a different branch. The two final electron transfers were assigned to the decays of the two branched intermediates. The traditional linear sequential model offered no clear evidence for an oxyferryl intermediate. On the other hand, the branched model produced difference spectra compatible with the presence of an oxyferryl state in one of the branches and a peroxy intermediate in the other, consistent with the findings by a combined EPR and optical spectroscopy approach in two laboratories (Clore et al. Biochem. J. 185:139-154 (1980); Blair et al. JACS 107:7389-7399 (1985)).

W-Pos396

SPECTRAL MEMORY IN CYTOCHROME OXIDASE ASCERTAINED BY pH-JUMP SPECTROSCOPY. ((H. James Harmon)) Oklahoma State University, Stillwater, OK 74078.

Spectra of reduced (succinate+PMS+ascorbate) and carboxyferrous cytochrome oxidase were measured at pH 9, 7, and 5 and before/after acidification from pH 9 to 5 in reduced light in CCCP-treated beef heart mitochondria. When a sample is reduced and CO-liganded at the same pH, the carboxyferrous minus ferrous difference spectra show a peak at 425, 427, and 430 nm at pH 9, 7, and 5, respectively, and a decrease in 446 nm absorbance at all pH values. Acidification of ferrous carboxy with 1% CO (CO/a_3 =1) results in an increase at 443 and 600 nm and a decrease at 428 and 452 nm. In the presence of 100% CO, acidification induces an absorbance increase at 443 nm and decreases at 430 and 452 nm. The carboxy minus ferrous difference spectrum obtained by subtraction of the carboxy and ferrous spectra after separate acidifications of ferrous and carboxy oxidase, however, show a peak at 425 nm, typical of oxidase at pH 9 and not at pH 5. This along with kinetics at low temperatures suggests that pH-dependent spectral changes in a_3^{2+}CO involve protonation of unliganded heme; bound CO may possibly block proton interactions.

W-Pos397

THE OXYGEN REACTION OF THE E286Q MUTANT OF CYTOCHROME C OXIDASE FROM $R.$ $SPHAEROIDES.$

((Pia Ädelroth, Margareta Svensson-Ek, David Mitchell[*], Robert B. Gennis[*], and Peter Brzezinski.), Dep. of Biochem/Biophys., Gbg Univ., Medicin.g. 9C, S-413 90 Göteborg, Sweden. [*]School of Chem. Sci., Univ. Illinois, Urbana, IL 61801, USA.)

We have studied absorbance changes associated with the reaction with dioxygen of fully reduced wildtype and E286Q (Glu →Gln) mutant cytochrome c oxidase from $R.$ $sphaeroides$, using the flow-flash technique. Proton uptake by the solubilized enzyme during dioxygen reduction was also studied, using a pH-indicator. In the crystal structure of cytochrome c oxidase from $P.$ $denitrificans$ (Iwata et al. (1995), Nature 376, 660-669), glutamate 286 (E278 in $P.d$ numbering) is the residue closest to the oxygen-binding binuclear site, that is clearly a part of the channel proposed for pumped protons. Our results show that during the reaction of the fully reduced E286Q mutant with oxygen, the peroxy intermediate is formed with approximately the same rate and extent as the wildtype enzyme. However, in the mutant the later phases are practically absent. The results further show that whereas the wildtype enzyme shows a biphasic uptake of protons from the medium during oxygen reduction, in the E286Q mutant no protons are taken up from the medium, indicating that the end-product of the reaction is the peroxy or unprotonated ferryl intermediate. In conclusion, the results suggest that the E286 residue is involved in the proton uptake needed to stabilize the peroxy intermediate and initiate the transfer of the 4th electron to the binuclear site.

W-Pos398

THE CHANNEL FOR EXOGENOUS LIGANDS TO THE ACTIVE SITE OF THE HEME-COPPER OXIDASES

((A. Puustinen, J.A. Bailey, S. Riistama[*], R.B. Dyer and W.H. Woodruff)) LANL, CST-4, Los Alamos, NM 87545 and [*] Dept. Medical Chem., University of Helsinki, Finland. (Spon. by W.H.Woodruff)

The three-dimensional structure of cytochrome c oxidase reveals a highly hydrophobic channel (Riistama et al. (1996) BBA 1275, 1-4), which could provide a dioxygen diffusion pathway to the enzyme's binuclear haem iron-copper centre, at which O_2 reduction to water occurs. Thusfar, using the site-directed mutagenesis of the quinol-oxidizing cytochrome bo_3 of $E.$ $coli$, we have been able to identify one mutated side chain (Val 287 Ile), which might slow down oxygen diffusion to the binuclear centre. This highly conserved residue in helix VI of subunit I is located closed to the two metals. Steric hindrance introduced by this mutation into the putative channel would explain the observed increase in $K_{M,app}$ without effect on V_{max}. To study this further, the time resolved IR and electronic absorption spectroscopies of CO binding were measured for wild-type and Val 287 Ile and Val 287 Ala mutant cytochrome bo_3 . The effects of mutation of the ligand channel on CO binding kinetics will be discussed.

W-Pos399

PHOSPHOLIPID VESICLES CONTAINING ONE OR TWO MOLECULES OF BOVINE HEART CYTOCHROME c OXIDASE EXHIBIT SIMILAR FUNCTIONAL ACTIVITIES. (H. Pabarue, M. Parilo, K.S. Wilson, L.A. Estey, and L.J. Prochaska) Department of Biochemistry & Molecular Biology, Wright State University, Dayton, OH 45435.

Phospholipid vesicles (40 mg/ml asolectin; 2 μM heme aa_3) containing beef heart cytochrome c oxidase (COX) were prepared by the cholate dialysis method and then fractionated by discontinuous sucrose density centrifugation in 20 mM TrisCl, pH 7.4 at 145,000 x g for 24.5 hours. Two COX-containing bands were observed; one located at the 12%/16% sucrose interface which contained about 30% of the COX loaded (light COV) and a second diffuse band located within the 16% sucrose layer which also contained about 30 % of the COX loaded (heavy COV). Light COV had from 0.40-0.60 COX molecules/per liposome, whereas heavy COV had 0.90-1.37 COX molecules/per liposome determined by heme a content, phospholipid phosphate analysis, and size measurements from gel filtration chromatography on HPLC. Neither light nor heavy COV contained any liposomes lacking COX. COX was similarly oriented in each preparation; 82% of the cytochrome c binding sites were exposed externally in light COV compared to 85% in heavy COV. Light and heavy COV exhibited similar respiratory control ratios (RCR>9.0) and also showed similar concentration dependencies for valinomycin-stimulated rates of electron transfer, suggesting that both preparations had similar endogenous permeability to protons. Proton-pumping of both preparations were measured electrometrically; light COV exhibited a proton translocated per electron transferred ratio (H+/e-) of 0.67 +/- 0.08 at two COX turnovers (1 COX turnover=4 moles of cytochrome c oxidized) and 0.48 +/- 0.07 at five COX turnovers, while heavy COV exhibited H+/e- ratios of 0.52 +/- 0.06 and 0.32 +/- 0.06 at similar turnovers. Since the intravesicular buffering capacity of COV provides the source of protons for proton-pumping, the observed H+/e- ratios for light and heavy COV were corrected for COX content per liposome; light and heavy COV at five turnovers exhibited similar proton-pumping stoichiometries of 0.48 H+/e- and 0.52 H+/e-, respectively. These results suggest that liposomes containing one or two COX molecules exhibit the same functional properties; whether the enzyme exists in a dimeric form in the heavy COV will be discussed.

W-Pos400

PHOTOINDUCED ELECTRON TRANSFER INTO REDOX-ACTIVE PROTEINS USING CARBOXYMETHYLATED CYTOCHROME C

((M. Karpefors[1], M.T. Wilson[2] and P. Brzezinski[1])) [1]Department of Biochemistry and Biophysics, Göteborg University and Chalmers University of Technology, S-413 90 Göteborg, Sweden. [2]Departments of Chemistry and Biological Chemistry, University of Essex, Wivenhoe Park, Colchester CO4 3SQ, Essex, U.K.

A new method has been developed which makes it possible to study photoinduced electron transfer (ET) from cytochrome c to a bound acceptor protein. In this study we have used cytochrome c oxidase (COX) or plastocyanin (PC) as acceptor proteins. Reduced carboxymethylated cytochrome c (CM cyt. c), with CO bound to the heme iron was mixed rapidly with oxidized PC or COX in a stopped-flow apparatus. A low ionic strength was used to facilitate complex formation. About 100 ms after mixing, CO was flashed off, which results in a drop of the apparent reduction potential of CM cyt. c from ~300 mV to ~0 mV and ET from CM cyt. c to the acceptor. This ET was not observed after addition of salt (KCl) at 200 mM. The ET rates were determined from multiwavelength exponential fits to the data and were found to be ~$1.0 \cdot 10^3$ s⁻¹ and ~$1.0 \cdot 10^4$ s⁻¹ for PC and COX, respectively. Kinetic difference spectra of the electron-transfer phases fitted well with static optical difference spectra corresponding to ET from CM cyt. c to PC or from CM cyt. c to heme a of COX. In both cases the yields of the reactions were about 70%.

W-Pos401

MECHANISM OF THE REACTION BETWEEN YEAST-ISO-1 CYTOCHROME c AND CYTOCHROME c PEROXIDASE. ((H. Mei, L. Geren, B. Durham and F. Millett)) Dept. Chem. Biochem., Univ. Arkansas, Fayetteville, AR. 72701

In stopped-flow studies at high ionic strength, equimolar yeast ferrocytochrome c was found to initially transfer an electron to the Trp-191 radical cation in cytochrome c peroxidase compound I. At 300 mM ionic strength the second-order rate constant for reduction of the radical cation is k_a = 1.8×10^8 M⁻¹s⁻¹. The value of k_a increased with decreasing ionic strength until the reaction became too fast to resolve completely in the stopped-flow spectrophotometer. At ionic strengths below 100 mM less than 25% of the reaction could be resolved, and the value of k_a is greater than 3×10^9 M⁻¹ s⁻¹. The Trp-191 radical cation is the initial site of reduction under all conditions of ionic strength. When excess ferrocytochrome c was mixed with CMPI at high ionic strength (300 mM) the kinetics were biphasic, with a fast phase due to reduction of the radical, followed by a slow phase due to reduction of the oxyferryl heme with a rate constant of 50 s⁻¹. As ionic strength decreased, the reduction of the radical became too fast to measure by stopped-flow and the rate of reduction of the oxyferryl heme increased to 600 s⁻¹ at 100 mM ionic strength. However, as the ionic strength decreased below 100 mM, k_{obs} decreased substantially and reached a value of 9 s⁻¹ at 10 mM ionic strength. This indicates that at low ionic strength the rate is limited by the rate of dissociation of ferricytochrome c from the high affinity site before a second molecule of ferrocytochrome c can bind and reduce the oxyferryl heme. A model of the reaction mechanism has been developed in which ferrocytochrome c first reduces the Trp-191 radical cation in compound I, and then a second molecule of ferrocytochrome c reduces the oxyferryl heme.

W-Pos402

RESOLUTION AND RECONSTITUTION OF $E.$ $coli$ SUCCINATE-UBIQUINONE REDUCTASE. ((X-D. Yang, L. Yu, and C. A. Yu)), Department of Biochemistry and Molecular Biology, Oklahoma State University, Stillwater, OK 74078 (Spon. by O. Spivey)

Succinate-Ubiquinone Reductase (SQR), commonly known as complex II, has been purified from numerous sources and they appear to be highly conserved in respect with the amino acid sequences, redox prosthetic groups, and subunit composition. SQR is composed of two components: succinate dehydrogenase (SDH) and the membrane-anchoring protein fraction (QPs). Resolution of SQR into SDH and QPs and reconstitution from the resolved components to form SQR have been achieved in the mitochondrial system. However, a similar study with the bacterial system was not successful until recently. $E.$ $coli$ SQR was resolved into reconstitutively active SDH and QPs by a procedure involving alkaline (pH 10) treatment of the complex in the presence of 1 M urea followed by DEAE-Sepharose CL-6B column chromatography under anaerobic conditions. When the resolved SDH and QPs were mixed together, more than 95% of the original SQR activity with full TTFA-sensitivity was obtained. In contrast to bovine heart mitochondrial cytochrome b_{560}, cytochrome b_{556} in isolated $E.$ $coli$ QPs has optical and EPR (g=3.65) spectral characteristics identical to those of cytochrome b_{556} in the intact complex and was not reactive toward carbon monoxide treatment The $E.$ $coli$ QPs does not cross-react with mitochondrial SDH and vice versa. These results indicate that the cytochrome b_{556} of $E.$ $coli$ differs from its mitochondrial counterpart and the interaction between QPs and SDH in the $E.$ $coli$ SQR is not the same as that in the mitochondrial complex. This work is

W-Pos403

EXPRESSION AND PROPERTIES OF QPS3 OF MITOCHONDRIAL
SUCCINATE-Q REDUCTASE. ((S. K. Shenoy, L. Yu, and C. A. Yu))
Department of Biochemistry and Molecular Biology, Oklahoma State
University, Stillwater, 74078-0454

The cDNA encoding QPs3 of bovine heart mitochondrial succinate-Q
reductase (SQR) has been cloned and sequenced (Gene Bank accession
number U50987). QPs3 was over-expressed in *E. coli* JM109 as a
glutathione S-transferase (GST) fusion protein using the constructed
expression vector, pGEX2T/QPs3. The yield of recombinant fusion protein
was growth conditions dependent. The maximum yield was obtained from
cells harvested 3.5 hours post-induction growth at 25 °C on SOC medium
containing 440 mM sorbitol, 2.5 mM betaine. QPs3 was released from the
fusion protein by proteolytic cleavage with thrombin. When subjected to the
high resolution SDS-PAGE analysis, the isolated QPs3 showed a single band
corresponding to the fifth band in mitochondrial SQR. Polyclonal antibodies
raised in rabbits using GST-QPs3 as the antigen, reacted to the two small
molecular weight subunits, QPs2 and QPs3, of SQR with equal intensity,
indicating that QPs2 and QPs3 have common epitopes. When hemin chloride
was added to the recombinant GST-QPs3 fusion protein, cytochrome b_{560}
was reconstituted. The reconstituted cytochrome b_{560} has absorption
characteristics similar to that of cytochrome b_{560} in isolated QPs but shows
only one EPR resonance peak with g=2.91. The optical and EPR spectral
characteristics of reconstituted cytochrome b_{560} remained unchanged upon the
removal of GST from QPs3 by thrombin cleavage, suggesting that the heme
ligands of the reconstituted cytochrome b_{560}, presumably histidines, are all
from QPs3. This work was supported by a grant from NIH (30721).

W-Pos404

DETECTION OF A MATRIX PROCESSING PEPTIDASE ACTIVITY IN
THE CYTOCHROME bc_1 COMPLEX FROM BOVINE HEART
MITOCHONDRIA ((K. P. Deng[a], D. Xia[b], A. M. Kachurin[a], H., Kim[b],
J. Deisenhofer[b], L. Yu[a], C. A. Yu[a]), [a]Oklahoma State University, Stillwater,
OK 74078-0454 and [b]Howard Hughes Medical Institute and University of
Texas, Southwestern Medical Center at Dallas, TX 75235

The cytochrome bc_1 complex (bc_1), which catalyzes the antimycin sensitive
electron transfer from ubiquinol to cytochrome c, is a segment of the
respiratory or photosynthetic electron transfer chain. The complex is present
in all aerobic organisms, from bacteria to mammalian systems. The
mitochondrial bc_1 differs from the bacterial complex by having extra subunits
without redox prosthetic groups. The function of these non-redox subunits
has been the subject of speculation. Recently plant mitochondrial bc_1 has been
shown to be bi-functional: it catalyzes the electron transfer and the protein
processing (as a peptidase). The peptidase activity was further mapped to the
two core protein subunits. A similar peptidase activity was not detected in the
mammalian bc_1 even though the core protein subunits of this complex share a
high degree of sequence identity with the mitochondrion's matrix processing
peptidase. When the purified bovine heart bc_1 was treated with low
concentrations of non-ionic detergents to partially inactivate its electron
transfer activity, the peptidase activity was observed using synthetic
polypeptides, composed of C-terminal amino acid residues of the subunit IX
and N-terminal amino acid residues of the subunit V, as a substrate. Although
the activated peptidase activity was not stimulated by the addition of divalent
cations, EDTA inhibits the peptidase activity significantly. This work was
supported by a grant from NIH (30721).

W-Pos405

THE INVOLVEMENT OF TRYPTOPHAN 56 AND TRYPTOPHAN 79 OF
SUBUNIT IV OF THE *R. SPHAEROIDES* CYTOCHROME bc_1
COMPLEX IN ITS INTERACTION WITH THE THREE-SUBUNIT CORE
COMPLEX. ((Y-R. Chen, C. A. Yu, and L. Yu)) Dept. of Biochem. and
Mol. Biol., Oklahoma State University, Stillwater, OK 74078

Previous studies established that subunit IV (S4) of the *R. sphaeroides*
cytochrome bc_1 complex involved in Q-binding and structural integrity of the
complex. S4 was recently over-expressed in *E. coli* JM109 as a glutathione
S-transferase fusion protein using the expression vector, pGEX-2T/S4. S4
was released from GST-S4 fusion protein by thrombin cleavage. Purified
recombinant S4 is functionally active as it can restore the cytochrome bc_1
complex activity to the three-subunit core complex. Chemical modification
studies have indicated that tryptophan residue(s) are essential for reconstitutive
activity of S4. There are five tryptophans contained in S4. To identify
essential tryptophan residues in S4, an approach involving site-directed
mutagenesis, expression of mutant S4 in *E. coli* followed by *in vitro*
reconstitution of recombinant mutant S4 with RSΔIV to restore cytochrome
bc_1 complex activity was employed. When all the five tryptophans, W27,
W31, W56, W58, and W79, of S4 were individually substituted with leucine,
the resulting recombinant mutant S4's have reconstitutive activities of 100,
100, 50, 100, and 72%, respectively, as compared to the reconstitutive
activity of the wild-type S4. This result indicates that W56 and W79 are
involved in interaction of S4 with the core complex. The involvement of W56
and W79 in reconstitutive activity of S4 is further evident from an recombinant
subunit IV with W56L and W79L having 33% of the reconstitutive activity of
intact S4. This work is supported by a grant from NSF (MCB9630413)

W-Pos406

A NEW NON-ROTENONE TYPE INHIBITOR OF MITOCHONDRIAL NADH-
UBIQUINONE REDUCTASE ((W. M. Anderson and D. Tan)) Ind. Univ. Sch. Med.,
N. W. Cent. Med. Ed. , 3400 Broadway, Gary, IN USA 46408

IR 125, an anionic, infrared laser dye, inhibits mitochondrial NADH oxidase,
pH 8.0 with an IC50 of 1.6 μM. Neither succinate-cytochrome c reductase
nor cytochrome oxidase activities are inhibited at any concentration tested,
localizing the inhibitory action to the NADH-ubiquinone reductase portion of
the mitochondrial electron transport chain. This compound also inhibits
NADH oxidase, pH 6.5 activity with an IC50 of 1.2 μM, but has no effect on
NADPH oxidase, pH 6.5 activity at concentration up to 100 μM. Thus IR 125
falls into the classification of a Type 2 inhibitor of NADH-ubiquinone
reductase (Anderson, WM and Trgovcich-Zacok, D. BBA, 1230, 186-193,
1995). Using artificial electron acceptors and coenzyme Q derivatives, IR
125 was shown to inhibit NADH dependent reduction of (1)
decylbenzoquinone (IC50 at pH 8.0 of 2.5 μM and at pH 6.5 of 5.5 μM);
ferricyanide (IC50 at pH 8.0 of 4 μM and at pH 6.5 of 5.8 μM). Inhibition of
NADH dependent reduction of ferricyanide by IR 125 at either pH was not
blocked by saturating concentrations of rotenone. IR 125 did not inhibit the
NADH dependent reduction of either 3-acetylpyridine adenine dinucleotide or
hexaammineruthenium (III) chloride, both of which are reported to accept
electron close to FMN. These findings, taken together, indicate that IR 125 is
a new, non-rotenone type inhibitor of mitochondrial NADH-ubiquinone
reductase activity of the Type 2 class. Based on the modified heterodimer
model of electron flow pathways in this enzyme (Anderson, WM and
Trgovcich-Zacok, D. BBA, 1230, 186-193, 1995), IR 125 is predicted to
block the pH independent reduction of iron sulfur cluster N2 by iron sulfur
cluster N3.

W-Pos407

EFFECTIVE MODELS FOR ELECTRON TRANSFER IN PROTEINS
- CONNECTION BETWEEN PATHWAY AND DETAILED HAMILTO-
NIANS. ((I. A. Balabin, J. N. Onuchic)) Department of Physics,
University of California, San Diego, La Jolla, CA 92093-0350

Understanding how the protein molecular structure controls the electron
transfer (ET) rate is critical for both achieving an insight into vital bioener-
getic reactions and designing new ET proteins. We develop and test a new
approach for computing ET tunneling matrix elements. Our goal is to pro-
vide *quantitative* results for *large* molecules with *limited* computer resources.
This connection between simple models and more detailed atomistic models
will also permit a better understanding of the basic features that control the
ET mechanism.

We introduce a series of simple Hamiltonians that incorporate effects of com-
plex molecular structure on the ET rate. Electronic orbital interactions are
categorized as classes, and only the most important of them are included.
The remaining orbitals are incorporated by means of effective (dependent on
the tunneling energy) interaction parameters. Calculations with these Hamil-
tonians are compared with "exact" extended Huckel-level results for several
biological and chemically-designed systems.

This new developed approach integrates quantum chemistry and pathway-like
methods.
* supported by the NSF-biophysics and NIH.

W-Pos408

CONTROL OF RADICAL PAIR CHEMISTRY BY A SWITCHED MAG-
NETIC FIELD.
((B. van Dijk, P. Gast and A.J. Hoff)) Dept. of Biophysics, Huygens Laboratory, Leiden
University , P.O. Box 9504, 2300 RA LEIDEN, The Netherlands
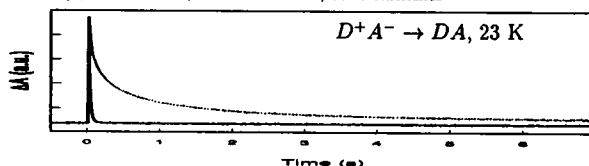
*Decay of the secondary radical pair in photosynthetic reaction centers with (dashed line)
and without (solid line) a 40 mT magnetic field switched on directly after the flash.*

Radicals produced by illumination or ionizing radiation are important in life sciences and
chemistry. Reducing the rate of radical decay by recombination can by vital for maxi-
mizing the yield of radical pair products, to study reaction pathways, and for accessing
biological damage.
We have developed a new method to reduce the probability for singlet-born radical pair
recombination, based on the population of energetically isolated radical pair spin levels by
rapidly switching on a magnetic field directly after the creation of the radical pairs. We
present an application to photo-induced radical pairs in photosynthetic reaction centers,
for which we have achieved a 40 fold increase in the low temperature (23 K) radical pair
lifetime.

W-Pos409

THE ELECTRON TRANSFER PROCESS STUDIED BY STEADY-STATE FLUORESCENCE SPECTROSCOPY. ((Marcelo K.K. Nakaema and Rosemary Sanches)) Instituto de Física de São Carlos, Universidade de São Paulo, São Carlos, SP, Brazil

The aim of this work was to obtain all possible information on the electron transfer process using only steady-state fluorescence spectroscopy. Polymeric films were made with pure tetrakis(phenyl)porphyrin (H_2TPP) and with H_2TPP plus different concentrations of duroquinone. The films were excited at 515 nm and the H_2TPP fluorescence spectra were obtained. Gaussians were fitted to the spectra and the areas of the band around 653 nm were used in the analysis. The simple Perrin model, that assumes a sphere around the donor and that the electron transfer occurs only if the acceptor is within this sphere, resulted in a critical transfer radius of 7 Å. For the model that considers an electron transfer rate $k_{ET} = Ze^{-\alpha r}$, takes into account the random distribution of acceptors and considers only transfer to first neighbors, several pairs of Z and α gave good fit to the experimental data (from $Z = 10^{15}$ s^{-1} and $\alpha = 2.4$ Å^{-1} to $Z = 10^{11}$ s^{-1} and $\alpha = 1.1$ Å^{-1}). The result was a little better if transfer to other neighbors was considered. In this case Z was in the range 10^{12}-10^{14} s^{-1} and α in the range 1.4-2.0 Å^{-1}. Due to the experimental errors (10%) the exact values of Z and α could not be obtained. (Supported by FAPESP, FINEP and CNPq)

W-Pos410

SUPEREXCHANGE vs. CONSECUTIVE ELECTRON TRANSFER THROUGH NON-DEBYE SOLVENT EFFECTS. ((Olga B. Jenkins)) Michigan State University, East Lansing, MI 48824

In a three-center ET system such as photosynthesis, the dual role of the bridging molecule (B_L) is investigated by the stochastic density matrix formalism for Non-Debye solvent fluctuations. Inclusion of the bath dynamics with more than a single dominant frequency is necessary in order to induce electronic coupling between the donor (P^*) and the acceptor (H_L) and thus create a competition between consecutive ET with formation of the intermediate (I), ($P^*B_L^-H_L$) and the superexchange (P^*H_L)->($P^+H_L^-$).In the latter ET, the direct coupling is induced by the intermolecular response of the multi-mode thermal bath to charge separation. Overdamped dynamics for the three center ET are considered to take place on multidimensional diabatic PES (one coordinate for each of the solvent modes). The superexchange coupling (D-A) zone appeared to be a projection of the overlap between the D-I and D-A zones on the D surface. Therefore, for the free- and reorganization-energies for photosynthesis accepted in literature, in the simplest two-dimensional ET, the A-D zone is a small spot on the 2D donor surface, located much higher than the saddle point for (D)-(A) surface intersection. Estimates show that an optimal solvent vibrational mode should exist to minimize the actual activation energy for the superexchange ET and thus make it preferable than the consecutive ET. A steady-state GreenUs function method allows us to estimate dynamic constants for multidimensional solvent relaxation.

W-Pos411

Thermo- and Conformational Dynamics of Photo-Induced Electron Transfer between Guanosine Mono-Phosphate and Tetra(4-N-methyl pyridyl) porphyrin Singlet Excited State.

((R. Jasuja[1], D. M. Jameson[2], T. L. Hazlett[3] and R. W. Larsen[1].))

Departments of [1]Chemistry, [2]Biophysics and Biochemistry, University of Hawaii at Manoa, Honolulu, HI 96822 .[3]Laboratory for Fluorescence Dynamics, Dept. of Physics, U.I.U.C., Urbana, Illinois, 61801.

Electron transfer (ET) rates are modulated by the relative orientation of donor and acceptor electric dipoles. We report a detailed analysis of the thermodynamics of photo-induced ET in self assembled molecular complexes of guanosine monophosphate (dGMP) and Tetra-4-N-methylpyridyl porphyrin (T4MPyP). The intra-complex electron transfer rates from the photo-excited singlet of T4MPyP to dGMP are best fit using a gaussian distribution of singlet lifetimes centered at ~690 ps (with a FWHM of ~ 1 ns). The ET rates are measured as a function of temperature, viscosity and concentration of dGMP. The association constant for the ground state complex formation between dGMP and T4MPyP decreases with increasing temperature, consistent with an exothermic process with ΔH of -13.7 kcal/mol. The width of the distribution of ET rates is modeled as distribution of relative orientations between T4MPyP and dGMP in the complex. For the intra-complex ET, $\Delta H^{\ddagger}$ and $\Delta S^{\ddagger}$ are 2.5 kcal/ mol and -50.5 cal/K mol respectively. (Authors acknowledge Arts Sc. Adv. Council grant (R.J.), NIH grant RR 03155(T.L.H.), ACS seed grant # P96-280-F452-B015(R.W.L.))

PHYSICAL CHEMISTRY OF NUCLEIC ACIDS

W-Pos412

DERIVATION OF NEAREST-NEIGHBOR PROPERTIES FROM OLIGOMERS: CONSEQUENCES OF NEAREST-NEIGHBOR ABSENCES AND TREATMENT OF ENDS. ((Donald M. Gray)) Program in Molecular and Cell Biology, University of Texas at Dallas, Box 830688, Richardson, TX 75083.

The derivation of nearest-neighbor properties from data on arrays of single-stranded or double-stranded nucleic acid polymer or oligomer sequences (with a total of N_T types of nearest neighbors, including end neighbors) is constrained. The constraints (N_C in number) each equate the number of times a given type of nucleotide or base pair occurs before another nucleotide, base pair, or end to the number of times it occurs after another nucleotide, base pair, or end (D. M. Gray & I. Tinoco, Jr., 1970, *Biopolymers 9*, 223-244; R. F. Goldstein & A. S. Benight, 1992, *Biopolymers 32*, 1679-1693). Unless specified nearest-neighbors have properties that are zero, or known, the nearest-neighbor information available is restricted to the number of linearly independent sequence combinations of nearest-neighbors, N_{IS} ($N_{IS} = N_T - N_C$). In general, there is not enough information to unambiguously assign properties to individual nearest-neighbors (other than the like neighbors A-A, or A-A/T-T, etc.). Points that are not always recognized are: (a) if k nearest-neighbors are absent from the array of sequences being analyzed, N_{IS}, but not N_C, is reduced by k, if all of the base types are still represented in the remaining sequences; (b) a minimum number of N_C properties must be known or assumed for individual nearest-neighbors in order for the properties of the remaining nearest-neighbors all to be determined; (c) equating properties of all pairs of ends to an initiation parameter may not yield a unique solution for nearest-neighbor thermodynamic properties, and (d) in some cases, values for even the like neighbors may be affected if properties of end neighbors are equated.

Supported by the Robert A. Welch Foundation (AT-503), the Texas Advanced Technology Program (No. 9741-036), and Cytoclonal Pharmaceutics, Inc.

W-Pos413

CHIRALITY, STRUCTURE AND FREE ENERGY OF DNA LIQUID CRYSTALS. H.H. Strey, R. Podgornik, D.C. Rau, L. Yu and V.A. Parsegian, National Institutes of Health, LSB/DCRT, OD/NIDDK, LCP/NIAMS, Bethesda, MD 20892-5626, J. Wang, E. Sirota, Exxon Research and Engineering, NJ

Liquid crystals of DNA are the simplest model systems for DNA packing in cell nuclei (e.g. dinoflagellates) or in phage heads. In these systems typically just one extremely long (from 10μm up to 1m) DNA molecule forms a macroscopic liquid crystal. We present a structural study on highly oriented DNA liquid crystals measuring the three dimensional structure factor $S(q_\perp, q_z)$ using small angle x-ray scattering at the synchrotron (BNL). The density of the DNA mesophases was controlled by the osmotic stress method. This method allows us to measure the equation of state and consequently changes in free energy in these systems.

At high densities DNA orders in a columnar liquid crystal with short range and long range orientational bond order (line hexatic or N+6). The line hexatic phase is the three dimensional analog to the hexatic phase in two dimensions. In contradiction with theoretical predictions this phase shows no measurable chirality. At lower DNA densities we found an intermediate region with two distinct peaks in the x-ray structure factor, a sharper one with six-fold symmetry and a broader isotropic one. Since we hold all intensive variables (p,T,μ's) fixed the measured S(q) should come from a single phase. At that point it is not yet clear whether this structure corresponds to a new phase located in between a columnar (non chiral) and cholesteric (chiral) arrangement of the DNA molecules. At even lower pressures we then found a phase transition to a cholesteric phase. with a single broad first order maximum in S(q).

In addition we measured the equation of state of DNA solutions over 5 orders of magnitude in osmotic pressure going from the hexagonal phase down to an isotropic solution of DNA. We present arguments that the equation of state can be described by contributions of the direct exponential repulsion plus a fluctuation enhanced repulsion stemming from bending fluctuations.

W-Pos414

THE EFFECTS OF BASE SUBSTITUTIONS ON THE THERMODYNAMICS OF UNFOLDING OF THE AUTOREGULATORY GENE 32 MRNA PSEUDOKNOT ENCODED BY T-EVEN PHAGES. ((C. A. Theimer, P. L. Nixon, and D. P. Giedroc)) Department of Biochemistry and Biophysics, Texas A&M University, College Station, TX 77843-2128.

In T-even bacteriophages, translational autoregulation of gene 32 protein biosynthesis requires nucleotides -71 to -38 upstream of the gene 32 initiation codon at the extreme 5' end of the mature gene 32 mRNA. A low resolution solution structural model of a 36-nucleotide RNA corresponding to T2/T6 gene 32 mRNA shows that the RNA folds into a classic H-type pseudoknot with two coaxially stacked stem connected by two loops. Loop 1 which spans the major groove of a seven base pair stem 2 consists of a single adenylate residue. To begin to define structure-stability relationships, temperature-induced unfolding models are being developed for both the T2/T6- and T4-derived gene 32 pseudoknots as monitored by UV absorption and nmr spectroscopy. The effects of base substitutions incorporated into the loops, stem-loop junction and stem-stem junction regions on the thermodynamics of unfolding are being probed to determine the origin of the secondary and tertiary structural contributions to the stability of this conformation. Preliminary studies with T2-derived RNAs suggest that both pyrimidine substitutions in loop 1 and deletion of the 3' ss tail destabilize the tertiary structure of the molecule and effectively uncouple tertiary from secondary structure unfolding over a wide range of Mg^{2+} concentration. Retroviral RNAs involved in translational frameshifting and readthrough appear to have sequences and folding topologies similar to the T-even gene 32 mRNA pseudoknot.

W-Pos415

THE SYNERGISTC EFFECT OF WATER ON DRUG BINDING TO DNA. (J.Ruggiero Neto and M.F.Colombo) Depto.Fisica-IBILCE - UNESP - São José do Rio Preto, SP, Brazil, 15.054.000

Long range deformation on DNA due to changes in torsional stress plays an important role in molecular recognition and conformational stability of the double helix. In addition, DNA deformation can modulate ligand binding. By spectrophotometric titrations of Act-D to natural DNA we have observed that changes in the water activity potentialize drug binding to DNA. The number of base pairs excluded upon binding also increased following increase in the drug affinity as water activity decreased. Both the free energy of binding and the size of the site occupied in the DNA varied linearly with the logarithm of water activity, a_w, upon addition of a neutral solute. The rate of this change, however, increased with the size of the neutral solute used to buffer a_w. Circularization of the linearized plasmid pUC18, by ligase reaction carried at several co-solvent concentrations, showed that the topoisomers generated under reduced water activity are unwound compared to the topoisomers generated in the absence of co-solvents. Analysis of these results indicated that torsional free energy change of the DNA molecule increased linearly with the decrease on water chemical potential. The observed unwinding extension also depends on the size of the solute added to buffer a_w as observed in the experiments of actD binding. This structural change on the double helix is similar to that imposed by drug intercalation, as observed by the CD spectra of the DNA. These characteristics suggest that the torsional stress imposed by the reduction of water activity on DNA was the source of the enhancement of actD binding affinity. The free energy penalty to open the DNA in the intercalation site would, then, relax more favorable at lower water activity. Also, a larger number of base pairs of DNA flanking the binding site would be deformed. Thus, water acts synergistically improving long range interaction on DNA due to ligand binding. Supported by FAPESP, CAPES and CNPq.

W-Pos416

THEORETICAL INVESTIGATIONS OF PHOSPHODIESTER HYDROLYSIS BY THIOL NUCLEOPHILES: STUDIES OF 2' THIOL NUCLEOSIDE MODELS

((J. W. Kurutz, C.L. Dantzman, and L.L. Kiessling)) University of Wisconsin, Madison, Madison, WI 53706. (Sponsored by) R.T. Raines

Experimental results indicate that attack of the 2'thiolate nucleophile on an activated phosphodiester is 10^7-fold slower than attack of an alkoxide.(1) To provide insight into the origins of these dramatic differences, quantum mechanical calculations were performed. The results from these calculations, executed at the RHF/6-31+G* level, are compared with experimental findings to ascertain differences in the phosphodiester kinetics and thermodynamics for the 2'thiol derivatives. This work represents the first quantum mechanical treatment of phosphodiester hydrolysis that includes a ribose-like ring; the effects of ring strain on these reactions are re-evaluated using this new information. Electronic structures, including bond order estimates, of the reacting species will be presented and the roles of protonation and solvation will be discussed. The calculations, in accord with experimental data, indicate that the alkoxide attack occurs through an associative mechanism. In contrast, 2'thiolate attack may proceed through a more dissociative transition state.

(1) Dantzman, C.L. and Kiessling, L.L. "Reactivity of a 2' Thio Nucleotide Analog," *J. Am. Chem. Soc.*, in press.

W-Pos417

COUPLED PROTONATION AND NUCLEIC ACID BINDING EQUILIBRIA OF POLYAMINES AND NEOMYCIN. ((D. Nag and W. H. Braunlin) Dept. of Chemistry, Univ. of Nebraska-Lincoln, Lincoln, NE 68588-0304.

Previous work from this lab has demonstrated the existence of significant pH gradients around nucleic acids. The presence of such gradients implies a coupling of protonation and binding equilibria even in the absence of specific associations. Since protonation is generally associated with large heat effects, whereas the binding of cationic ligands to nucleic acids often has only a modest intrinsic enthalpy associated with it, thermal measurements should be useful to monitor the electrostatic binding of protonatable ligands. To test such ideas, and to determine parameters for the association of biologically relevant ligands to nucleic acids, isothermal titration calorimetry measurements are being performed to monitor the association fo spermine, spermidine and neomycin with RNA and DNA substrates. The nucleic acids studied include duplex DNAs, and fragments of an RNA cleaving variant of the hairpin ribozyme. Studies are being performed using a variety of buffers and pH conditions, thereby facilitating a distinction between pK_a shifts due to nonspecific association and specific binding. An additional advantage of the method of pH variation is that higher pH measurements can be extrapolated to lower pH in order to characterize binding equilibria under conditions where the binding is tight to be monitored directly.

W-Pos418

IONIC DETERMINANTS OF HOMODUPLEX-HETERODUPLEX EQUILIBRIA OF TRIPLET REPEAT DNA. ((I. Giri, R.L. Kortum and W. H. Braunlin) Dept. of Chemistry, Univ. of Nebraska-Lincoln, Lincoln, NE 68588-0304.

Trinucleotide repeat sequences occur with some frequency in the human genome. Expansion of such sequences is associated with a number of genetic disorders, including fragile X syndrome, myotonic dystrophy, and Huntington's disease. While ten possible trinucleotide repeats are possible, only two are commonly associated with human disorders. Diseases such as myotonic dystrophy and Huntington's disease involve an unusual expansion of CAG/CTG repeats, whereas the expansion of CGG/CCG is associated with fragile X syndrome. Interestingly, these two sequences show notable propensities for homoduplex hairpin formation, which is postulated to play a role in the etiology of such diseases. Other possible self-structures, e.g. quadruplexes, might also be involved. If such self-structures are involved, then conditions must exist in the cell where they are competitive with heteroduplex DNA. We have initiated experiments to determine and to characterize factors modulating equilibria among self-structures and heteroduplex DNA. To date, we have discovered very sharp dependencies on monovalent cation concentration, suggesting a role for specific cation binding sites. For hompduplexes of -CCG- oligomers we find the order of monovalent cation stabilization to be $Li^+ > K^+ > Na^+$.

W-Pos419

STABILIZATION OF DISCOIDAL NEMATIC PHASE OF AQUEOUS LECITHIN/BILE SALT DISPERSIONS BY CHOLESTEROL: A ^2H and ^{31}P NMR STUDY. ((P.W. Westerman*‡, R. Jacquet*, P.L. Rinaldi‡, W.A. Daunch‡, and Y.Sun§)) *Northeastern Ohio Universities College of Medicine, Rootstown, Ohio 44272; ‡ Kent State University, Kent, Ohio 44242 and § University of Akron, Akron, Ohio 44325.

Previously, field induced ordering has been demonstrated[1] in several bile salt-DMPC micellar systems in the composition range 60-67% water, 30-25% DMPC, and 10-5% bile salt/DMPC. We report that small amounts of cholesterd (4 mol% total lipids) stabilize the discoidal nematic phase (N_D) and field-induced ordering is observed up to 92 wt% water, for DMPC to bile salt ratios between ~ 6/1 and 3/1. Field-induced ordering is inferred from the powder pattern line shapes and motionally- induced quadruple splittings measured in the ^2H NMR spectra, utilizing specifically ^2H-labeled DMPC and cholesterol, as well as chemical shift anisotropy measurements in the ^{31}P NMR spectra of the same systems. Higher levels of cholesterol (10 mol%) destabilize the N_D phase and produce two phase systems consisting of lamellar (L_α) and micellar aggregates.

[1]Ram, P. and J.H. Prestegard, Biochim. Biophys. Acta, **940** (1988) 289-294.

W-Pos420

A TRANSIENT POLARIZATION GRATING INSTRUMENT FOR STUDIES OF DNA BENDING AND TUMBLING DYNAMICS

((Alexei N. Naimushin, Bryant S. Fujimoto, and J. Michael Schurr)) Department of Chemistry, Box 351700, University of Washington, Seattle, WA 98195

A transient polarization grating (TPG) apparatus was constructed to measure the bending and tumbling dynamics of DNA. Two coherent excitation pulses with mutually perpendicular polarization write the grating. These pulses create a periodic polarization of the S0-S1 or T1-T2 absorbance in the sample, which then diffracts a cw probe beam. The total intensity of the combined write pulses is constant throughout the sample, which prevents periodic heating of the sample and build-up of a phase grating that would relax via thermal diffusion on the microsecond time scale. The TPG method offers significant advantages over conventional transient photodichroism or polarized triplet-triplet absorption measurements. It can in principle provide higher signal-to-noise ratio due to the angular separation and orthogonal polarization of the diffracted beam with respect to the incident probe beam. Consequently, the diffracted signal is detected against a very dark background. The instrument was initially tested on methylene blue, which under standard conditions exhibits multiple binding sites, not all of which are intercalated, so the resulting data cannot readily be interpreted. In contrast, ethidium bromide binds almost exclusively by intercalation into a single well-characterized site. The 632.8 nm probe lies to the red of its S0-S1 transition that is excited by the 532 nm write pulses, so it is absorbed exclusively by its T1-T2 transition. Interpretation of such data requires measurement of the orientation of the T1-T2 transition dipole with respect to the S0-S1 dipole and the helix-axis. Experiments to determine those angles are currently in progress.

W-Pos421

TEMPERATURE DEPENDENCE OF THE SUPERCOILING FREE ENERGY

((Jeffrey J. Delrow, Patrick J. Heath, and J. Michael Schurr)) Department of Chemistry BG-10, University of Washington, Seattle, WA 98195

Monte Carlo simulations using the measured torsional rigidity yield supercoiling free energies (ΔG_{sc}) that agree well with experiments for p30δ and certain other DNAs. For an N bp DNA with linking difference Δl, one finds $\Delta G_{sc}/RT = E_T \Delta l^2/N$, where E_T is the twist energy parameter. However, Monte Carlo simulations using constant values of the twisting and bending rigidities predict a much smaller decrease in E_T with temperature than is found experimentally from calorimetric measurements of the heat of supercoiling or from measurements of E_T over a range of temperatures. The measured torsional rigidity of an 1876 bp restriction fragment from pBR322 (or p30δ) was found to decrease substantially with increasing temperature. When such temperature dependent torsional rigidities were employed in simulations of a 4349 bp DNA, the resulting slope dE_T/dT was in good agreement with that expected from the measured heat of supercoiling. However, in the case of pBR322 DNA, neither the experimental E_T nor the experimental dE_T/dT, which are anomalously large, could be reproduced by the simulations.

W-Pos422

THE AMPLITUDE OF LOCAL ANGULAR MOTIONS OF THYMINE IN DNA IN SOLUTION

((Roy Diaz, Bryant S. Fujimoto, and J. Michael Schurr)) Department of Chemistry, Box 351700, University of Washington, Seattle, WA 98195

Previous solution NMR measurements of the rms amplitude of local angular motions of bases in duplex DNA yielded results for adenine, guanine and cytosine in the range from 9–11°. A recent uv fluorescence polarization anisotropy (FPA) study of poly(dA)·poly(dT) and $(dA)_{20}$·$(dT)_{20}$ suggested that the thymines undergo fast angular motions of very much larger amplitude. It was further suggested that similarly large amplitudes of local angular motion are observed for thymines in other sequences as well. We have obtained preliminary results of NMR R_2 measurements on ^{13}C-labelled thymines in a 16 base pair oligomer (CGAGGTTTAAACCTCG). These results are used in conjunction with FPA measurements of intercalated ethidium to determine the rms amplitude of local angular motion of the labelled thymines. The rms amplitudes we obtain are compared with previous NMR and fluorescence measurements. These rms amplitudes are much smaller than those inferred from uv FPA studies.

W-Pos423

SEQUENCE DEPENDENT FLEXIBILITY OF DUPLEX DNA

((B.H.Robinson, A.W.Reese, S.A. Alley, P.B.Hopkins)) Department of Chemistry, Box 351700, University of Washington, Seattle, WA 98195

We report on the utility of a new spin-label containing base to monitor the dynamics of duplex DNA (3). Following the protocol we recently developed (1, 2), we have examined the dynamics of the spin probe when specifically incorporated into the middle and toward the end of duplex DNA. We find that the theory of Schurr et al.(4) is very well followed and that the average dynamic persistence length is around 1250Å. We will discuss the relation of this experimentally determined persistence length to other estimates.

We have examined sequence dependence and are able to determine the relative flexibility of di- and tri-nucleotide sequences. The major conclusion is that (AT)n are the most flexible and (CG)n are the least flexible of the di-nucleotide sequences. A model of flexibility based on dinucleotide subsequences has been developed; however, it is inadequate to predict certain tri-nucleotide sequences. Specifically the sequence (ACG)n is anomalously flexible relative to the flexibility of the dinucleotide sub sequences. This range of flexibility means that the dynamic persistence length of different sequences of DNA should vary by over 50%.

1. Hustedt EJ, Kirchner JJ, Spaltenstein A, Hopkins PB, Robinson BH. 1995. *Biochemistry* 34:4369-75 and 2. Hustedt EJ, *et al*. 1993.*Biochemistry* 32(7):1774-87
3. Miller TR et al. 1995. *J. Amer. Chem. Soc.* 117:9377-8
4. Schurr JM, Fujimoto BS, Wu P, Song L. 1992. In *Topics in Fluorescence Spectroscopy*, ed. JR Lakowicz, 3:137-229.

W-Pos424

ISO-COMPETITION POINT AND DIVALENT COUNTERION BINDING.

((Anzhi Z. Li, Haiyan Huang, Kenneth A. Marx)) Dept. of Chemistry, Univ. of Mass Lowell, Lowell, MA 01854. (Spon. by A. Z. Li)

The interaction of divalent cation (Mg^{2+} and Ca^{2+}) with λ-DNA-Hind III fragments ranging from 23,130-2,027 bp was investigated by pulse gel electrophoresis, and interpreted by the Henry gel models, Manning's counterion condensation (CC) theory and the iso-competition point. The normalized mobility reduction μ/μ_0 data of DNA due to Mg^{2+} or Ca^{2+} counterion binding (0-400 μM) in tris-borate buffer were well fit by Manning's CC theory. The ionic strength effect, valence effect, and DNA size effect can be all connected and interpreted by an important parameter, we call the iso-competition point where the monovalent and multivalent cation have an equal charge neutralization fraction. For example, the normalized mobility reduction shift $\Delta(\mu/\mu_0)$ for each DNA fragment, relative to the CC prediction point, was observed and the 'shift' phenomena only occurred when the cation concentration is close to the iso-competition point. In fact, the iso-competition point presents a clear picture of the competition binding under a certain ionic environment condition. The nature of the iso-competition point/line was studied and discussed.

W-Pos425

PRESSURE DEPENDENCE OF THE HELIX-COIL EQUILIBRIUM OF DUPLEX DNA

((MC Lin & RB Macgregor*)) Faculty of Pharmacy, University of Toronto, Toronto, Ontario M5S 2S2

Through measurements of the denaturation-renaturation thermal hysteresis we have studied the kinetics of the helix-coil equilibrium of four 22-base pair homopurine-homopyrimidine duplex oligonucleotides at pressures up to 2500 bar. The fraction of GC base pairs, f(GC), was varied from 0.14 to 0.5. The experimental conditions were 20 mM NaCl, 20 mM Tris HCl, pH 7.0, each of the DNA strands were present at 4.5 μM. A two-state bimolecular mechanism adequately described the data under all experimental conditions. At 10 bar and 47 °C the rate constant for helix formation, k_1, increased by a factor of 210, and the reverse rate constant, k_{-1}, decreased by a factor of 420 as f(GC) was changed from 0.14 to 0.5. The activation energies for formation of the duplexes were negative and relatively insensitive to f(GC). Pressure causes the magnitude of k_1 to increase, and the lower the f(GC) the greater the increase. Thus, for f(GC) = 0.14, the activation volume for forward reaction, $V_1^{\ddagger}$, equals −20 mL/mol, while for f(GC) = 0.5, $V_1^{\ddagger}$ = −6.7 mL/mol. The rate constant for strand separation decreases at high pressure. The activation volume for this step, $V_{-1}^{\ddagger}$, varies from +17 mL/mol to +1.6 mL/mol for f(GC) = 0.14 and 0.5, respectively. The ΔV for *helix formation* calculated from the activation parameters changed from −23 mL/mol at f(GC) = 0.14 to −5.8 mL/mol for f(GC) = 0.5. The kinetics of other two duplex molecules, f(GC) = 0.23 and 0.32, lie between these extremes.

W-Pos426

THE FREE SOLUTION MOBILITY OF DNA. ((Nancy C.
Stellwagen*, Cecilia Gelfi⊥ and Pier Giorgio Righetti#)) *Department of
Biochemistry, University of Iowa, Iowa City IA, ⊥ITBA, CNR, Milano,
Italy, and #Department of Cell Biology, University of Calabria in
Arcavacata die Rende, Cosenza, Italy.

The free solution mobility of DNA was measured by capillary
electrophoresis in the two buffers commonly used for gel
electrophoresis, Tris-borate-EDTA (TBE) and Tris-acetate-EDTA
(TAE). The capillaries were coated with novel acrylamido polymers
which reduced the electroendosmotic mobility to zero. The free solution
mobility of DNA in TAE buffer was found to be $3.75 \pm 0.04 \times 10^{-4}$
$cm^2V^{-1}s^{-1}$ at 25°C, in good agreement with other values in the literature.
The mobility was independent of molecular weight for DNA molecules
ranging in size from ~120 bp to 48.5 kb. The free solution mobilities of
fragments smaller than 120 bp decreased with decreasing molecular
weight. Surprisingly, the free solution mobility of DNA in TBE buffer
was 20% larger than observed in TAE buffer, presumably because of the
binding of borate to the deoxyribose residues. The free solution
mobilities observed in the two buffers parallel the results obtained by
extrapolation of Ferguson plots in polyacrylamide gels to zero gel
concentration. Supported by grant GM29690 from the National Institute
of General Medical Sciences, BioMed 2, Human Genome Sequencing
Grant PL-951158, Consiglio Nazionale delle Ricerche, and Telethon
Italy (grant No. E-153).

STRUCTURE-BASED DRUG DESIGN

W-Pos427

DESIGN OF FAST ENZYMES BY OPTIMIZING INTERACTION
POTENTIAL IN ACTIVE SITE. ((Huan-Xiang Zhou)) Department of
Biochemistry, Hong Kong University of Science and Technology, Clear Water
Bay, Kowloon, Hong Kong.

The catalytic step in many enzymes has been perfected through evolution and
consequently the overall rate of the catalyzed reaction is limited by the
diffusional encounter of the substrate (S) with the active site of the enzyme
(E). Then the only practical route to rate enhancement is by accelerating the
diffusional encounter through electrostatic interactions between E and S.
Recent theoretical and simulation studies[1-3] have led to a remarkably simple
formula for predicting the effect of an interaction potential U on the
diffusional binding rate constant k. This is given by $k = k^0 <\exp(-U/k_bT)>$,
where k^0 is the rate constant in the absence of the potential and the average of
the Boltzmann factor is over the binding region. This formula is accurate if
the binding region is small and is thus expected to be useful for E-S binding.
Tests on superoxide dismutase and acetylcholinesterase show that it predicts
the binding rate constant to within a factor of 4. The interaction potential
within the active site is thus predictive of the binding rate constant. This result
is exploited to find mutants with enhanced catalytic efficiency.
1. Zhou, H.-X. (1993). Biophys. J. 64, 1711.
2. Zhou, H.-X., Szabo, A. (1996). Biophys. J. (November issue).
3. Zhou, H.-X. (1996). J. Chem. Phys. (October issue).

W-Pos428

DIFFERENCES IN BINDING OF EPOXYMORPHINAN AGONISTS AND
ANTAGONISTS TO STRUCTURAL MODELS OF THE OPIOID RECEPTOR
((Daniel Strahs, Frank Guarnieri and Harel Weinstein)) Dept. of Physiology
and Biophysics, Mount Sinai School of Medicine, New York 10029-6574

We have developed 3-D structural models of the trans-membrane region of the
cloned opioid receptors (δ, κ and μ), members of the G-protein-coupled receptor
(GPCR) superfamily, based upon homology modeling to the low resolution
rhodopsin structure and the biophysical properties of trans-membrane α-helical
domains. These models are stable to long molecular dynamics simulations in
vacuo, exceeding a total length of 2 nanoseconds. Ligands sharing a conserved
morphine-based structural core are considered to bind to these opioid receptors
through a common binding pocket located in the trans-membrane region formed
principally by helices 3, 4, 5, 6 and 7. Within this region, agonists and antagonists
share binding sites, with functional discrimination resulting from the nature of the
specific interactions with the receptor. We have used the receptor models in a
mixed mode simulation method utilizing alternating steps of stochastic dynamics
and Metropolis Monte Carlo sampling in a simulated annealing protocol with the
AMBER force field to explore the conformational states available to the receptor-
ligand complexes. The simulated complexes included morphine, nalorphine,
naloxone and oxymorphone; randomized torsional changes were applied to side
chains within 7 Å of the ligand. Common patterns of interactions observed in the
complexes sampled among the simulated ligands suggest a basis for the common
recognition of opioid ligands. In contrast, the potential interactions that may
discriminate agonists from antagonists are highlighted by the differences
consistently observed in the sampled configurations. These results present a
molecular framework integrating known QSAR determinants of ligand activity at
N_{17} and C_{14}. *Supported by NIH Grants T32DA07135, DA-00060, and DK46493.*

W-Pos429

THE INTERACTION OF DAUNOMYCIN AND ITS ANALOGUES
WITH SURFACTANTS
((Xiaogang Qu and Jonathan. B. Chaires*)) Department of Biochemistry,
The University of Mississippi Medical Center, Jackson, MS 39216-4505

The interaction of the anticancer drug daunomycin and its analogues with sodium
dodecyl sulfate (SDS) and Triton X-100 micelles was investigated using
absorbance and fluorescence spectroscopies and isothermal titration calorimetry.
The transfer of these drugs from aqueous solution to the micelle interior might be
a model for the hydrophobic transfer from solution to the DNA intercalation site.
Steady-state fluorescence and visible absorbance measurements demonstrated
that the drug molecules can partition into the micelles. Fluorescence lifetime and
anisotropy measurements showed that the lifetime and anisotropy of the drugs
increase when the drug molecules bind to the micelles. These studies suggest that
the chromophore of the drug is located in the hydrophobic interior of the
micelles. Fluorescence quenching experiments using both steady-state and
lifetime measurements showed the reduced accessibility of bound drug molecules
to an anionic quencher (I⁻), but showed that the accessibility is dependent on the
type of the surfactant. Calorimetric studies suggest that the hydrophobic
interaction between detergent micelles and drug molecules is an appropriate
model for the transfer of drug molecules from solution into the DNA
intercalation site.(Supported by N.I.H. Grant CA35635 (J.B.C.))

W-Pos430

INTERACTION OF A NEW BISINTERCALATING ANTHRACYCLINE ANTIBIOTIC-
WP631 WITH DNA ((F. Leng & J. B. Chaires)) Dept. of Biochemistry, Univ. of Mississippi
Med. Ctr., Jackson, MS 39216; ((W. Priebe)) M. D. Anderson Cancer Center, Univ. Texas,
Houston, TX 77030

UV melting, differential scanning calorimetry, absorption and fluorescence spectroscopy,
circular dichroism spectroscopy, and viscosity measurements have been used to characterize
the interaction of a new bisintercalating anthracycline antibiotic-WP631 with DNA. Relative
viscosity experiments showed that WP631 bisintercalated into DNA base pairs. A molecular
model was generated to show that two chromophores of WP631 intercalated into DNA, and
the linker between the two chromophores of WP631 fits very well in the DNA minor groove.
The method of continuous variations revealed three distinct binding stoichiometries for
WP631, corresponding to 6, 1.3 and 0.5 mole of base pairs per mole of ligand. UV melting
experiments and differential scanning calorimetry were used to measure the ultra tight
binding of WP631 to DNA. The binding constant for the interaction of WP631 with herring
sperm DNA was determined to be 2.7×10^{11} M⁻¹ at 20°C. The large, favorable binding free
energy of -15.3 kcal mol⁻¹ was found to result from a large, negative enthalpic contribution
of -30.2 kcal mol⁻¹. The DNA melting curves with different concentrations of WP631 were
fitted to McGhee's model of DNA melting in the presence of ligands, and the resulting DNA
binding parameters are in good agreement with that determined by other methods. The salt
dependence of the binding constant was examined for WP631. The slope SK =
(dlogK/dlog[Na⁺]) was found to be 1.63. By using polyelectrolyte theory to interpret the
observed salt dependence of the equilibrium constant, it can be shown that there is a
significant nonelectrostatic contribution to the binding constant. DNA UV melting studies by
using a 214 bp homogenous DNA fragment (214-mer) indicated that WP631 preferentially
binds to the GC-rich region of the DNA.

W-Pos431

UNDERSTANDING RESISTANCE MUTATIONS TO DRUG TARGETED TO THE HIV-1 PROTEASE AS STARTING POINT FOR THE DESIGN OF INHIBITORS IMMUNE TO RESISTANCE MUTATIONS.
((Fredy Sussman, M. Carmen Villaverde, **Luis Martínez**)) Protein Studies Section, Oklahoma Medical Research Foundation, Oklahoma City, OK, 73104 (Spon. by Fredy Sussman)

Many research laboratories have developed HIV-1 PR inhibitors that have served as lead compounds in the search for anti-viral drugs. Some of these compounds have been found to stop very effectively the replication of the HIV-1 virus *in vitro*. However they seem to have limited clinical benefit, due in part to the development of drug resistance, which has been shown to exist in cell cultures, and in clinical isolates from patients. Under the 'evolutionary pressure' from an anti-viral agent a drug resistant mutant is selected. The primary sequence modifications that are generated in this way are called "resistance" mutations. They maintain the level of catalytic activity, allowing the virus to replicate, but they lower the affinity of the HIV-1 PR for the anti-viral drug, reducing the drug's potential therapeutic power.
At present, the molecular mechanism that underlie resistance mutations is not known. We have developed several computer based methods for the understanding of the molecular processes involved in the reduction of inhibitor affinity towards HIV-1 PR mutants. We have applied these methods to some of the more commonly observed resistant mutations as well as to some mutations that present "resistance" like behavior. The results have enabled us to compile a list of resistance motifs as well as to design some inhibitors that are immune to the effect of the mutations. Presently, synthesis and characterization of these compounds is in progress.

W-Pos432

A SURFACE SOLID ANGLE-BASED SHAPE DESCRIPTOR FOR MOLECULAR DOCKING. ((**Donna K. Hendrix** and Irwin D. Kuntz)) Graduate Group in Biophysics and Dept. of Pharmaceutical Chemistry, University of California, San Francisco, San Francisco, CA 94143 USA. (Sponsor D.A. Agard)

We are developing a new shape descriptor for the DOCK molecular modeling program suite. Sphgen, the current shape description method for the DOCK suite, describes the pockets of a macromolecule by filling a volume with intersecting spheres. DOCK then identifies possible ligand orientations in the pocket by overlapping the atoms of proposed ligands with the sphere centers. Sphgen limits use of the DOCK program to concave binding regions, but macromolecular binding regions can be solvent-exposed rather than buried pockets. We present a more general shape descriptor (1) which represents local surface shape by determining the solid angle of exposure for points on the surface of the molecule. We then find possible ligand orientations by matching complementary shape regions on the macromolecule and proposed ligand. Orientations are evaluated using the AMBER force field based DOCK score. The surface solid angle descriptor displays the complementary characteristics of the interfaces of our test systems, trypsin/trypsin inhibitor, and dihydrofolate reductase/methotrexate. The solid angle site points can be used by DOCK to regenerate the crystal structure orientation.
(1) Connolly, M. L. J. Mol. Graphics 4: 548-558 (1986).

W-Pos433

MOLECULAR MODELING OF SINGLE-STRANDED DNA SEQUENCE SELECTIVITY IN THE BINDING OF ACTINOMYCIN D. ((R.M. Wadkins)) Cancer Therapy & Research Center, Institute for Drug Development, 14960 Omicron Dr., San Antonio, TX 78245.
    Actinomycin D (AMD) is one of the few compounds that can bind preferentially to single-stranded DNA (ssDNA) with affinities comparable to, or higher than, that for double-stranded DNA (dsDNA) of similar sequence. Our recent work has demonstrated that AMD binds with high affinity to 5'AG3' steps in ssDNA, with the sequence 5'TAGT3' possessing the highest affinity. A hemi-intercalated structure of the drug-DNA complex has been proposed, based on ¹H NMR and modeling experiments, that implies the phenoxazine chromophore of AMD is intercalated into the ssDNA at a rotation about the ssDNA pseudo-helix axis of approximately 90° to that found in AMD-dsDNA structures. In this report, we utilize molecular modeling to elucidate the details of the structure of the drug-DNA complex, and to address the hydrophobic and electronic interactions responsible for sequence selectivity. For our models, we have modified the neighboring DNA residues outside the binding region and have computed the changes in conformation and interaction energies in these complexes. Further, using ZINDO computations, we have determined the expected absorption spectrum for AMD bound to each sequence. Our models are compared to the experimental absorption and CD spectra and the thermodynamic stabilities of the AMD-ssDNA complex.

W-Pos434

THE SYNTHESIS AND CHARACTERIZATION OF BILE SALT-BASED AMINOSTEROLS AS ANALOGS OF SQUALAMINE ((S.R. Jones*, W.A. Kinney#, Y. Shu*, M. Rao#, X. Zhang#, L.M. Jones#, and B.S. Selinsky*))
*Department of Chemistry, Villanova University, Villanova, PA 19085, and #Magainin Pharmaceuticals, 5110 Campus Drive, Plymouth Meeting, PA 19462.

Squalamine is a potent antimicrobial aminosterol found in small amounts in tissues of the dogfish shark. We have synthesized a series of simple aminosterols beginning with the bile acids *deoxycholic acid, lithocholic acid,* and *chenodeoxycholic acid,* and tested them for antimicrobial activity. In our syntheses, we have varied the identity of the polyamine substituent at C-3 on various bile acids. All of the synthesized aminosterols possess antimicrobial activity, but are not as potent as squalamine. These compounds provide additional structure-activity data for the antimicrobial activity of the aminosterols, which can be compared to previously published data[1] to improve our understanding of the mechanism of the antimicrobial activity of these compounds.

[1]SR Jones, WA Kinney, X Zhang, LM Jones, and BS Selinsky (1996) *Steroids* 61: 565-571.

W-Pos435

COMPUTATIONAL STUDIES OF INHERITED MUTATIONS IN HUMAN CATHEPSIN K CAUSING PYCNODYSOSTOSIS, A LYSOSOMAL BONE DISEASE. ((E.L. Mehler, B.D. Gelb, R.J. Desnick, H. Weinstein)), Mount Sinai School of Medicine, New York, NY 10029

Inherited adverse mutations in the human cysteine proteinase, cathepsin K, cause the autosomal recessive sclerosing skeletal dysplasia, pycnodysostosis. Characteristic bone abnormalities include osteosclerosis, short stature and deformation of cranial and facial bones. Cathepsin K belongs to the papain superfamily and exhibits approximately 50% amino acid identity with papain. Seven cathepsin K mutations have been identified in pycnodysostosis patients, five in the mature portion and two in the pro-peptide. Computational approaches are being used to study the consequences of these mutations on the function of cathepsin K. Due to the high sequence identity with papain, the latter is being used as an initial structural model for the calculations. Initial modeling of the cathepsin K structure with homology methods supports the similarity to the three dimensional structure of papain. In this structural context, exploratory calculations suggest that one of the mutants, a G to R mutation in cathepsin K that corresponds to V32R in papain (papain numbering) may shift the pK's of the Cys25-His159 couple sufficiently to preclude the proton transfer required for catalysis. The effects of the G79E mutation (cathepsin K numbering) in the pro-peptide were revealed by a configurational search of a pentapeptide segment around that mutant which changed from a predominantly extended conformation in the wild type to a bent conformation in the mutated segment. This conformational difference is likely to affect the inhibitory function of the pro-peptide, or hinder the cleavage required to form the mature protein. Results from simulation studies that use such inferences in refined models of cathepsin K will aid in the development of inhibitors and/or revertant mutations that could be effective in the treatment of bone diseases with excessive bone degradation.

W-Pos436

THE RECOGNITION OF CARBOXYLATE LIGANDS AND AN INTRAMOLECULAR SURROGATE BY VANCOMYCIN: CRYSTALLOGRAPHIC AND COMPUTER SIMULATION STUDIES
((Paul H. Axelsen and Patrick J. Loll))
Department of Pharmacology, University of Pennsylvania, Philadelphia PA

Vancomycin kills bacteria by binding to polypeptide intermediates in peptidoglycan synthesis. Type A resistance to vancomycin is emerging as a serious public health threat, and is mediated by the substitution of a depsipeptide, rather than a polypeptide, intermediate. Details about molecular recognition in this system are needed to facilitate the design of therapeutic agents that specifically recognize depsipeptide ligands. The crystal structure of the vancomycin:acetate complex has been determined at 0.9 Å resolution. The heptapeptide portions of two vancomycin monomers form an antiparallel hydrogen-bonded dimer, with asymmetrically oriented disaccharide groups. An acetate molecule is bound to one monomer by an array of polar and non-polar interactions in a manner that likely represents the binding mode of natural peptide ligands. In the other monomer, an asparagine side chain serves as an intramolecular surrogate for the ligand. This crystal structure resolves a long-standing controversy about the binding mode of carboxylate-containing ligands, demonstrates the operation of a novel intramolecular flap which occupies the binding site in the absence of ligand, and suggests a possible cooperative mechanism linking ligand binding and dimerization.

W-Pos437
"MINING MINIMA": DIRECT COMPUTATION OF CONFORMA-
TIONAL FREE ENERGY ((M.S. Head, J.A. Given, M.K. Gilson))
CARB, NIST, Rockville MD 20850

We describe a novel, two-step method for directly computing the con-
formational free energy of a molecule. In the first step, a finite set
of low-energy conformations is identified, and its contribution to the
configuration integral is evaluated by a straightforward Monte Carlo
technique. The method of finding energy minima incorporates certain
features of the global underestimator method and of a genetic algo-
rithm. In the second step, the contribution to the configuration in-
tegral due to conformations not included in the initial integration is
determined by Metropolis Monte Carlo sampling. An application of
this method to cyclic urea inhibitors of HIV protease is presented.

MAGNETIC RESONANCE

W-Pos438
NUCLEOTIDE -HYDROLYSIS DEPENDENT CONFORMATIONAL CHANGES IN
P21^{HRAS} AS STUDIED USING ESR-SPECTROSCOPY((M. Haller*, U. Hoffmann*, T.
Schanding*, R. S. Goody*, P.D. Vogel*)) *Fachbereich Chemie/Biochemie, University of
Kaiserslautern, Kaiserslautern; *Abt. Physikalische Biochemie, Max Planck Institut für
Molekulare Physiologie, Dortmund, Germany. Tel.: 49-631-205-3801, FAX: 49-631-205-
3419; Email: vogel@chemie.uni-kl.de.

   We employed ESR spectroscopy and 2',3'-spin-labeled guanine nucleotides (SL-
GTP, SL-GDP and SL-GMPPNP) to study the conformational changes in p21^{Hras} that are
associated with GTP hydrolysis . At room temperature and in the presence of Mg^{2+}-ions the
nucleotide analogs in complex with p21^{Hras} exhibited ESR spectra that were very similar to the
signals of the free, not protein-bound label. Decrease of the temperature to either 5 °C or
0 °C led to signals in the ESR-spectra that are typical for protein immobilized radicals. The
2A$_{zz}$-values of SL-GTP, SL-GMPPNP and SL-GDP in complex with p21^{Hras} differed
significantly from each other at both 5 °C and 0 °C.
   In order to study hydrolysis-dependent conformational changes, we incubated SL-
GTP in complex with p21^{Hras} at 25 °C and subsequently cooled the sample to either 5 °C or 0 °C
for acquisition of the ESR spectra. The time-dependent relative change within the 2A$_{zz}$-values
was plotted versus the time the sample was incubated at 25 °C. The calculated rate for the
observed conformational change is 13.4x10^{-3} ±5x10^{-3} min^{-1}. The observed hydrolysis rate at 25
°C was determined to be 7.7x10^{-3} min^{-1} using HPLC techniques to detect products.
   The rate determined for the conformational change and the rate determined for the
hydrolysis reaction are very similar and indicate that hydrolysis and conformational changes
occur simultaneously. We were not able to detect a slow conformational change that precedes
the actual hydrolysis step as was postulated earlier by other researchers.

W-Pos439

APPLICATION OF MAS-NMR TO STUDY ANTIBIOTIC - MEMBRANE
INTERACTION IN THE LAMELLAR PHASE STATE AND PROTEINS IN
FROZEN AQUEOUS SOLUTION ((F. Volke, A. Pampel, R. Waschipky,
M. Haensler, G.Ullmann, A. Donnerstag, G. Klose, H. Pfeiffer, W. Richter,
and P. Welzel)) University of Leipzig, Linnestr. 5, D-04103 Leipzig.

Using a combination of physico-chemical techniques (MAS-NMR,
SAXS, DSC, ELMI, molecular modelling) the antibiotic moenomycin A was
found to be anchored by its hydrophobic chain into multilamellar POPC
membranes. The mobility of POPC decreases with increasing
moenomycin concentration. At high concentration, the polar sugar-group
network of moenomycin covers the membrane surface. Molecular
modelling shows that a moenomycin molecule has twice the area of a
POPC molecule.
   In another investigation a-chymotrypsin in aqueous solution and ice
was investigated with proton-MAS-NMR. Signals of mobile sidechains and
non-freezing water have been detected. The method has advantages over
transverse relaxation time studies for detection of protein associated
water.

W-Pos440

DYNAMICS OF *GRAMICIDIN A* DEDUCED FROM

HIGH-RESOLUTION MAGIC-ANGLE SPINNING NMR

((D. E. Warschawski, J. D. Gross and R. G. Griffin)) Francis Bitter Magnet
Laboratory, Massachusetts Institute of Technology, Cambridge MA 02139

   Early attempts to obtain high-resolution solid-state NMR spectra of
peptides and proteins in liquid-crystalline membranes were unsuccessful because
of problems associated with the dynamics of the molecules. All subsequent
studies have avoided them altogether by performing the experiments at very low
temperatures, where motion is frozen. Recent experiments performed in our
laboratory have given more insight on the nature of this perturbation, namely the
interference of some molecular motion with high-power ^{1}H-decoupling. We are
now able to quantitate it, to devise ways to circumvent it and, most importantly, to
extract relevant data concerning the dynamics of the observed molecules.
   Such effects are demonstrated here and studied in great detail for the case
of a membrane peptide, Gramicidin A, in an hydrated lipid bilayer. The study has
been performed over a broad temperature range, on different ^{13}C,^{15}N,^{2}H-labeled
peptides. Several dynamical models and a comparison with previously published
results will be presented. Various ways to obtain high-resolution Magic-Angle
Spinning ^{1}H, ^{13}C and ^{15}N-NMR spectra of peptides in membranes will also be
discussed.

W-Pos441

AUTOMATED PROBABILISTIC METHOD FOR ASSIGNING BACKBONE RESONANCES OF
(^{13}C, ^{15}N)− LABELED PROTEINS. ((J. A. Lukin*°, A. P. Gove[†], S. N. Talukdar[†],
and C. Ho*)) *Department of Biological Sciences and [†]Robotics Institute, Carnegie
Mellon University, Pittsburgh, PA 15213.

We have developed a computer algorithm for assigning polypeptide backbone and
^{13}Cβ resonances of any protein of known primary sequence. Input to the algorithm
consists of cross-peaks from several heteronuclear 3D-NMR experiments. These data
are analyzed statistically using Bayes' theorem to yield objective probability scoring
functions for matching chemical shifts. Such scoring is used in the initial stage of
the algorithm to combine cross-peaks to form intra-residue segments of chemical
shifts $\{N_i, H_i^N, C\alpha_i, C\beta_i, C_i'\}$ and inter-residue segments $\{C\alpha_i, C\beta_i, C_i', N_{i+1}, H_{i+1}^N\}$.
Given a tentative assignment of these segments, the second stage of the procedure
calculates probability scores based on the likelihood of matching the chemical shifts
of each segment with: (i) overlapping segments; and (ii) chemical shift distributions
of the underlying amino-acid type (and secondary structure, if known). This joint
probability is maximized by rearranging segments using an optimized simulated
annealing program. The automated assignment method is tested using CBCA(CO)NH
and HNCACB cross-peaks of two previously-assigned proteins, calmodulin and CheA.
Our algorithm is also applied to cross-peaks of the 25 kDa glutamine-binding protein
of *Escherichia coli*, observed using the following experiments: HNCA, HN(CA)CO,
HN(CA)HA, HNCACB, COCAH, HCA(CO)N, HNCO, HN(CO)CA, HN(COCA)HA, and
CBCA(CO)NH. In each case, the automated procedure yielded an assignment in
excellent agreement with that obtained by time-consuming, manual methods.
°Supported by NIH NRSA fellowship # 1F32GM17034.

W-Pos442

^{1}H, ^{13}C, ^{15}N NMR ASSIGNMENTS AND SECONDARY STRUCTURE OF THE 25 KD GLUTAMINE-BINDING PROTEIN FROM *ESCHERICHIA COLI*

((Jinghua Yu, Virgil Simplaceanu, Nico L.Tjandra[+], Patricia F. Cottam, Jonathan A. Lukin and Chien Ho)) Dept. of Biological Sciences, Carnegie Mellon University; Pittsburgh, PA 15217 [+]Laboratory of Chemical Physics, NNDDK, NIH, Bethesda, MD 20892

^{1}H, ^{13}C and ^{15}N NMR assignments of backbone and side-chain atoms have been made for liganded glutamine-binding protein (GlnBP) of *Escherichia coli*, which has 226 amino acid residues and a molecular weight of about 25 kD. Results from the 3D triple-resonance experiments, HNCO, HN(CO)CA, HN(COCA)HA, HNCA, HN(CA)HA, HN(CA)CO, and CBCA(CO)NH are the main sources used to make the sequential backbone assignments. HNCACB, COCAH, HCACO, HCACON, and HOHAHA-HMQC are used to confirm the assignments and to extend connections where resonance peaks are missing in some of the experiments mentioned above. More than 95% of polypeptide backbone resonances of GlnBP have been assigned. HCCH-TOCSY, C(CO)NH, and HOHAHA-HMQC experiments enable us to make a partial side-chain assignment. The solution secondary structure of GlnBP complexed with its substrate is obtained from the Chemical Shift Index method and sequential NOE connectivities. (Supported by a research grant from NIH).

W-Pos443

LOCATION MODELS FOR THE PROBE OXONOL V IN 1,2-DIMYRISTOYL-sn-GLYCERO-3-PHOSPHOCHOLINE (DMPC) VESICLES BY NMR SPECTROSCOPY

((*J. C. Smith and S. Chandrasekaran*)), Department of Chemistry, Georgia State University, Atlanta, GA, 30303

The location(s) assumed by the potential-sensitive molecular probe Oxonol V in small unilamellar vesicles, prepared by sonication of DMPC, has been investigated at 600 MHz using NOESY spectroscopy with the residual HOD signal suppressed by either the decoupler or by use of the probe transmitter (TNNOESY). When oxonol V is present at 8 mol percent, NOE cross peaks are observed at 50 and 150 ms mixing times between the probe phenyl protons and those of the lipid unresolved methylenes, $(CH_2)_n$, and the terminal methyl group protons. The volume ratio of these cross peaks exceeds a factor of 10, indicating a preferential localization of Oxonol V in the $(CH_2)_n$ region since this ratio exceeds that expected from the lipid proton stoichiometry. There is , however, little or no evidence for cross peaks between the Oxonol V phenyl protons and those of the DMPC head group choline $N(CH_3)_3$ protons at either 50 or 150 ms mixing times. This observation suggests that Oxonol V is virtually exclusively localized in the hydrocarbon region of the bilayer with little or no accumulation of the probe at the bilayer surface under the conditions of this experiment. The probe location favors sensitivity to transmembrane potentials to the exclusion of surface potential sensitivity.

W-Pos444

ANGLE SELECTION IN EMR OF RANDOMLY ORIENTED SAMPLES, APPLICATIONS TO TRANSFERRIN OXALATE AND LIPOXYGENASE.

((B.C. Maguire and B.J. Gaffney)) National High Magnetic Field Laboratory, Florida State University, Tallahassee, Fl 32310 (Spon. by B.J. Gaffney)

Electron Magnetic Resonance (EMR) spectra of high spin ferric iron are orientation dependent, and analysis of this dependence can lead to knowledge of structural information about the metal environment. This procedure usually requires samples which are non-randomly oriented, in the form of single crystals. However, it is also possible to select certain orientations of the principle axes of the metal complex with respect to the magnetic field direction by using selected regions of isotropic spectra. Angle selection is particularly useful when applied to multidimensional techniques such as ENDOR and ESEEM.

Transferrin oxalate, a non-heme iron (S=5/2) containing protein, has been chosen to demonstrate features of angle selection in randomly oriented paramagnetic samples with S>1/2. EMR operating frequencies in which the microwave quanta are approximately equal to 2D are the subject of this study. At these frequencies, the lowest-field maximum in the spectra corresponds to transition between Kramers doublets, and to angles intermediate between the principle axis directions. For example, calculations with D=0.26 cm^{-1} and v=14 GHz give a low field maximum corresponding to θ=55 degrees, and with D=0.51 cm^{-1} and v=30 GHz, give a low field maximum corresponding to θ=48 degrees. Similar calculations for soybean lipoxygenase, which has D between 1 and 2 cm^{-1}, will be shown for the frequency range 70-110 GHz. A range of calculations showing unique angle selections from isotropic spectra will be shown.

W-Pos445

WITHDRAWN

W-Pos446

HIGH RESOLUTION MAGNETIC RELAXATION DISPERSION.

((R. G. Bryant, S. Wagner, A. Danek)) Chemistry Department, University of Virginia, Charlottesville, VA 22901.

The magnetic field dependence of nuclear spin-lattice relaxation rates contains all the dynamical information available from NMR experiments provided that one may measure the field dependence over a sufficiently wide range. We have constructed a new spectrometer that provides nuclear spin-lattice relaxation rates over a range corresponding to proton Larmor frequencies from 0.01 to 300 MHZ. The system employs two magnetic fields in close proximity, but the two fields are isolated by a shielding system. The sample of interest is polarized and detected in the high resolution 7T field, pneumatically moved to the variable satellite field where it is permitted to relax. Unlike field switched spectrometers used previously for these experiments, this instrument provides both high sensitivity, that appropriate to a shimmed 7T magnetic field, and excellent resolution that permits study of solute resonances without difficulty. The primary data is the nuclear spin-lattice relaxation rate as a function of the Larmor frequency, which is directly proportional to spectral densities. Thus, the experiment provides a spectral density map corresponding to time scales from milliseconds to fractions of a nanosecond. Applications to protein dynamics and both cation and anion counter ion binding domain dynamics will be presented.

W-Pos447

PROTEIN NMR ASSIGNMENTS USING MEAN-FIELD SIMULATED ANNEALING.

((N. E. G. Buchler, E. R. P. Zuiderweg, H. Wang, and R. A. Goldstein)) Biophysics Research Division, University of Michigan, Ann Arbor, MI 48109-1055, USA

The use of Nuclear Magnetic Resonance spectroscopy to investigate the structure and dynamics of a protein begins with the assignment of resonances to the nuclei in the protein backbone, {HN, H_α, C_α, CO}. Using connectivity and side-chain identity data from various heteronuclear 3D NMR experiments, the solution is the sequential alignment which provides a unique and unambiguous overlap in connectivites and side-chain information. However, NMR suffers from inherent experimental limitations and these assignments must be based on noisy, ambiguous, and sometimes missing or inaccurate data. This degeneracy leads to a multitude of possible solutions. We describe a computational mean-field simulated annealing method that tackles this problem by allowing the entire assignment to evolve in a holistic manner. In contrast to previous approaches, the mean-field approach considers the assignment *probabilistically*, thus smoothing the assignment space and lessening multiple-minima problems commonly found in other energetic approaches to NMR assignments. This technique was applied to NMR data of a 172-residue peptide-binding domain of the *E. Coli* heat-shock protein, DnaK, solved by H. Wang and E. R. P. Zuiderweg. Having tested our computational method on this data, we then checked its robustness by degrading the data in a variety of ways consistent with what is encountered in NMR spectroscopy. This method is shown to be robust to significant amounts of missing, spurious, noisy, extraneous, and erroneous data.

W-Pos448

Coordination Of Cu(II) And Vo(II) To Lipophilic Bis-hydroxamate Binders As Studied by One- And Two- Dimensional Electron Spin Echo Spectroscopy

V.Kofman*‡, J.J. Shane‡, S.A. Dikanov¶, M.K. Bowman¶, J.Libman‡, A.Shanzer‡ and D. Goldfarb‡; *National High Magnetic Field Lab, Florida State University, Tallahassee, FL 32310, ‡ Weizman Institute of Science, 76100 Rehovot, Israel and ¶ Environmental Molecular Science Laboratory, Pacific Northwest Laboratories, Richland, Washington 99352.

Lipophilic carriers of metal ions are of great interest for biological applications in view of their capability to penetrate biological membranes. We applied 1D and 2D Electron Spin Echo Envelope Modulation (ESEEM) spectroscopies to examine the effects of the bis-hydroxamate ligand composition on the structure of Cu(II) and VO(II) complexes. Orientation-selective ESEEM experiments were carried out at 8-9 HGz. The spectra obtained were exceptionally well resolved and indicated that the cancellation condition is met both for VO(II) and for Cu(II). The assignment of ESEEM frequencies was achieved by the application of the two-dimensional hyperfine sublevel correlation (HYSCORE) experiment. Following the assignment, simulations of the orientation-selective spectra were performed, yielding the magnitude and orientation of the quadrupole and hyperfine tensors of the coupled nitrogens.

COMPUTER APPLICATIONS

W-Pos449

COMBINED USE OF MEAN-VARIANCE ANALYSIS AND THE VITERBI ALGORITHM TO IDEALIZE SINGLE CHANNEL AND SINGLE MYOSIN RECORDS. ((Joseph Patlak)) Department of Molecular Physiology and Biophysics, University of Vermont. Burlington, VT.

Single molecule recordings convey detailed information about the kinetic and conductance behavior of the target molecule. Accurate interpretation, however, requires that the detailed molecular behavior be correctly separated from substantial sources of noise, with the goal of reproducing the sequence of apparent states that molecule adopted during the recording. This process is called idealization. As the data's complexity increase and its quality decrease, standard methods (e.g. half-threshold crossing) for idealization become untenable.

Mean-Variance analysis (Patlak, Biophys J. 65:29;1993) is a method designed to determine average kinetic and conductance properties of such complex data without idealization. It uses a simple transform to provide graphical information about the number of observable states, their amplitudes and associated fluctuations, their interconnections, and their average dwell time distributions. However, the method cannot directly idealize unitary signals for subsequent, more detailed kinetic analysis.

The Viterbi Algorithm (Viterbi, IEEE Trans. Info. Theory, IT-13:260;1967) was designed (for decoding convolution codes) to determine, with minimal computational overhead, the most likely sequence of Markov states that a given model would have followed, given the observed data set. Although part of the background for modern methods like Hidden Markov, its requirement for *a priori* information concerning the amplitudes, noise, duration and interconnection of each Markov state make its estimations model- and parameter-dependent.

I show here that the global information about a data set generated by Mean-Variance Analysis provides the necessary input to the Viterbi Algorithm. The combined use of the two methods therefore provides the ability to "discover" and to verify the quantitative properties of the observable Markov model, permitting accurate determination of the most likely sequence of states (i.e. idealization). Both methods provide quantitative feedback regarding the likelihood that the data were derived from a given model, and of that model's ability to reproduce the global behavior seen in the original data.

W-Pos450

BAYESIAN MODELLING OF PATCH-CLAMP RECORDS ((J.A. Stark, W.J. Fitzgerald and S.B. Hladky)) Departments of Pharmacology and Engineering, University of Cambridge, CB2 1QJ, U.K.

Efficient detection of opening and closing events in recordings of small numbers of ion channels is difficult. The identification of such events is an example of the more general statistical problem of the detection of changepoints in a time series. The simplest methods for tackling this involve filtering and thresholding, but these perform badly when current levels are closely spaced, when the intervals between events are short, or when there is substantial noise. More complex methods such as hidden Markov modelling have been successfully used in the analysis of patch-clamp recordings, but these impose quite detailed assumptions about the underlying physical process and have, so far, only been implemented using the assumption that successive data points are independent events, i.e. that the data has not been filtered.

We have adopted an alternative strategy. The signal is modelled as a sequence of filtered transitions between constant levels with no further assumptions about the process underlying the transitions. The investigator must specify the spectrum of the noise, the characteristics of the data acquisition filter, and initial guesses (strictly prior distributions) of the frequency of events and their magnitudes. This information is sufficient for a Bayesian statistical analysis of the data. Locations of changepoints and currents are chosen using Markov chain Monte Carlo sampling of their posterior distribution. By fitting this type of model to the data one achieves a better trade-off between sensitivity and reliability of detection compared to thresholding methods. Examples will be displayed of estimation of closely spaced current levels and the analysis of records with flicker type events.

W-Pos451

NON-ADDITIVITY AND EFFECTS OF ELECTRIC CHARGES ON SOLVENT INDUCED FORCES (SIFs) AMONG MODEL SOLUTES IN WATER. ((V. Martorana, D. Bulone and P.L. San Biagio)). CNR-IAIF and Physics Dept., University of Palermo, Via Archirafi 36, I-90123 Palermo, Italy.

Molecular dynamics simulations are performed to test the additivity of solvent-mediated interactions among simple model solutes. Model systems are composed of several different combinations of Lennard-Jones solutes and charged particles immobilized in a bath of water molecules modeled with the TIP4P potential. Dependence upon charge sign and inter-solutes distance is studied. For a given solutes configuration the Solvent Induced Forces (SIFs) on each particle are computed and quantitatively related to configurational changes of the solvent caused by solutes. Results show sizeable non additivity and context-dependence of SIFs. The hydration pattern is found to change even at large intermolecular distances reflecting the many-body character of the potential of mean force.

W-Pos452

MONTE CARLO SIMULATION OF THE ION ATMOSPHERE DISTRIBUTION AROUND THE OPERATOR BINDING DOMAIN OF THE λ REPRESSOR PROTEIN

David C. Kombo, Matthew A. Young, G. Ravishanker & David L. Beveridge

Department of Chemistry & Molecular Biophysics Program, Wesleyan University, Middletown, CT 06457

Abstract

A Monte Carlo simulation of explicit coions and counterions around the N-terminal domain of the λ repressor protein has been carried out. The solvent was modeled as a continuum dielectric medium. The Amber 4.1 geometric and energy parameters were used to determine the configurational energy. We find that the atom distribution in the environment of Na^+ ions in the lowest-energy conformation, is in agreement with both the ones derived from the analysis of ion-binding proteins and water molecules in proteins in the Protein Data Bank. The results are also generally in good agreement with Poisson Boltzman studies on the same system. New insights, however, are revealed. The distribution of charge density appears less homogenous than previously observed. A clustering of Na^+Cl^- ions pairs noticed in some regions further emphasizes this heterogeneity.

W-Pos453

ACCELERATION OF CONVERGENCE TO THE THERMODYNAMIC EQUILIBRIUM BY INTRODUCING SHUFFLING OPERATIONS TO THE METROPOLIS ALGORITHM OF MONTE CARLO SIMULATIONS.
((H. Sun* and I.P. Sugar*)) *Baker Laboratory of Chemistry, Cornell University, Ithaca, NY 14853. *Department of Biomathematical Sciences, Mount Sinai School of Medicine, New York, NY 10029.

This paper introduces a broad class of operations, called "shuffling trials," used to design non-physical pathways. It is shown that in general the equilibrium distribution of a system can be attained when physically possible pathways are interrupted regularly by non-physical shuffling trials. Including properly chosen shuffling trials in the commonly applied Metropolis algorithm often considerably accelerates the convergence to the equilibrium distribution.

Shuffling trials are usually global changes in the system, sampling efficiently every set of the metastable configurations of the system. Shuffling trials are generated by symmetric stochastic matrices. Since ergodicity is not a required property, it is particularly easy to construct these matrices in accordance with the specificity of the system. The design, application and efficiency of the shuffling trials in Monte Carlo simulations are demonstrated on an Ising model of two-dimensional spin lattices and one-component phospholipid membranes.

W-Pos454

DEFINITION OF STATES IN THE TIME DOMAIN BASED ON REGIONS IN A MEAN-VARIANCE HISTOGRAM. ((M. Max Zviman[1], D. Restrepo[1,2], J. H. Teeter[1,2])) [1]Monell Chemical Senses Center, 3500 Market St., Philadelphia, PA 19104. [2]Department of Physiology, University of Pennsylvania. (Spon. By J. H. Teeter)

Mean-variance histograms (MVH) (Patlak. Biophys. J. 65:29-42, 1993) map recordings of currents through ion channels from the time domain to a three dimensional space (with dimensions of mean current, variance and counts) by binning the mean current and variance of a running window. The topology of the MVH reveals two types of structures: convex, relatively low variance areas which represent the conductance states of the channel, and arcs connecting to at least one conductance state area which represent the data points during the transitions from one state to another. A fit of a Gaussian-χ^2 surface to each conductance state area yields the mean current and variance for that state. The transition arcs can be analyzed by fitting a function $\sigma^2(\mu, \Phi, v)$ where μ is the mean, Φ is the acquisition filter response function and v is a function that describes the deviation from a step transition due to the gating properties of the channel. The boundaries of the various regions of the MVH can be used to investigate the data in the time domain. We have presented an algorithm to generate an idealized current trace based on the state regions (Restrepo et al., Biophys J. 70:A201, 1996). The data at and near transitions can be marked in order to perform analysis of the data in the time domain. Arcs describing transitions between each state can be classified and analyzed in the MVH or in the time domain. The algorithms are implemented as a program for the Windows operating system (Win32). We tested the algorithms using simulated data and compared the results to those obtained by using half-amplitude methods. Using simulated data with one channel with two open states and one closed state we found that estimation of open probability using our algorithm was over 90% accurate even at SNR as low as 0.8. This work is supported in part by NIH grants DC00566 and DC01838.

W-Pos455

MODELING MUTATION MATRICES USING PHYSICO-CHEMICAL PROPERTIES. ((D. M. Taverna, J. M. Koshi, and R. A. Goldstein)) Biophysics Research Division and Department of Chemistry, University of Michigan, Ann Arbor, MI 48109-1055, USA

We model site mutations as a stochastic process determined by an amino acid's physical and chemical parameters, such as size, charge or hydrophobicity. Using a linear or polynomial dependence of these parameters, a fitness function with free variables to be optimized was constructed. If we assume Boltzmann statistics and Metropolis transition probabilities, then the difference of the fitness between two amino acids governs their relative mutation rate. The matrix of calculated transition probabilities was compared to the structure-dependent mutation matrices of Koshi and Goldstein with a least squares fit in order to optimize the free variables of the fitness function. A good fit is found by minimizing both the error of the fit and the number of free variables in the function. Since the matrices of Koshi and Goldstein are structure dependent, our model can show which parameters are relevant in the evolution of specified structures. In addition, since the fitting of our model only requires previously known mutation matrices as input, the algorithm is 2 to 3 orders of magnitude faster than using the database originally used to derive the Koshi and Goldstein mutation matrices.

W-Pos456

EFFECTS OF CONNECTIVITY ON IMPULSE PROPAGATION IN A SMALL ASSEMBLY OF NEURONS IN THE CORTEX. ((C.H. Trad and H. Sabbagh)) American University of Beirut, Physics Department, Beirut-Lebanon.

A theoretical analysis has been made on the effect of connectivity on signal propagation between neurons. A model, based on the somatic shunt cable model, was constructed to describe the synaptic potentials which are induced by synaptic inputs, to understand how signal transmission could be influenced by the way of interconnection of neurons in an assembly. A neuron is represented as one or more equivalent cables connected to a somatic impedance. A more general boundary condition is applied at the ends of some cables, extending cable models in a very simple manner to the case of more than one neuron. The cables are not only emanating from the somatic surfaces but also terminating on cell bodies of other neurons. They are combined together without any disagreement with the cable model concept. The interaction between neurons could then be mediated by the spread of current in the cables between interconnected neurons. The decay constants are the same for all cables and the exponentially decaying depolarizations are below threshold.


MATHEMATICAL MODELS

W-Pos457

HIDDEN MARKOV ANALYSIS OF FILTERED, SAMPLED SINGLE CHANNEL CURRENT RECORDINGS. ((L. Venkataramanan, R. Kuc and F. J. Sigworth)) Departments of Electrical Engineering and Cellular and Molecular Physiology, Yale Univ., New Haven, CT 06510.

Vector hidden Markov models [e.g. Krishnamurthy et al, Proc. IFAC Intl. Conf. Adaptive Syst. Contr. Signal Processing, 1992] can be applied to model ion-channel kinetics in the presence of correlated background noise as seen in patch clamp recordings. These models however apply only to discrete-time processes. We present an adaptation of the HMM algorithms to characterize filtered, sampled continuous -time signals. To account for the randomness of the time of transition between two data samples, the probability density function associated with each state is modified to reflect the filtered current level and increased variance seen at times when transitions occur. The model parameters are then estimated based on the theory developed for continuous HMM representations in speech processing [Juang et al, IEEE Trans. on Information theory, vol. 32, No.2, 1986].
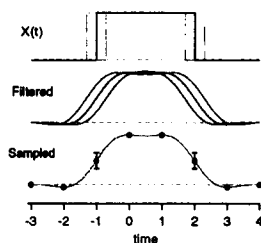
W-Pos458

A GENERALIZED MODEL UTILIZING STEADY-STATE PROBABILITIES TO STUDY INTERACTIVE CHANNEL GATING. ((K. Manivannan, S. Harju and T. N. Tassara)) Dept. of Chemistry and Physics, Southeastern Louisiana University (SLU), Hammond, LA 70402.

The gating mechanism of ion channels can be studied by single channel recordings using the patch clamp technique. In general, gating of one ion channel is independent of the other ion channels. However, in some biological preparations there is evidence for non-independent gating of ion channels suggesting interaction among channels. Although there have been several reports on the cooperative behavior of ion channels, not much progress has been made in the modelling of ion channel data. A recently formulated stochastic Markovian model describes how interaction between ion channels can be studied by considering only the steady-state probabilities of multichannels.[1] We retain the lateral interaction of the channels, but make the model more generalized by allowing interaction between closed and open channels (or, clusters of channels) as well. We investigate the steady-state properties of a system of N channels and provide a scheme to express all the probabilities in terms of two parameters. *Work supported by the Louisiana Education Quality Support Fund (1995-98)-RD-A-21 and SLU Faculty Development Grant to K.M.*
[1]Manivannan, K., E. Gudowska-Nowak, and R. T. Mathias. 1996. *Bull. of Math. Biology*, 58(1):141-174.

W-Pos459

CALCIUM DYNAMICS IN CARDIAC MYOCYTES. ((M. S. Jafri, J. J. Rice, D. T. Yue and R. L. Winslow)) Dept. of Biomedical Engineering, The Johns Hopkins Univ. School of Medicine, Baltimore, MD 21205

We construct a detailed mathematical model for Ca^{2+} regulation in the ventricular myocyte that includes novel descriptions of subcellular mechanisms based on recent experimental findings: 1) the Keizer-Levine model for the ryanodine receptor (RyR) which displays adaptation at elevated Ca^{2+} as observed by Gyorke and Fill (1993); 2) a model for the DHPR that inactivates by mode switching, as suggested by Imredy and Yue (1994); and 3) a restricted subspace into which the RyR and DHPR empty and interact via Ca^{2+}. The model is combined the Luo-Rudy (1994) Phase II ventricular cell model. The model can simulate Ca^{2+}transients during an action potential similar to those seen experimentally. The subspace $[Ca^{2+}]$ rises more rapidly and reaches a higher level than the bulk myoplasmic Ca^{2+}. Termination of SR Ca^{2+} release results from emptying of the SR and adaptation of RyR. The model is also used to explore the effects of pacing on force generation. For example, the model reproduces transitions seen in force generation due to changes in pacing that cannot be simulated by previous models. Simulation of such complex phenomena requires an interplay of both RyR adaptation and the degree of SR Ca^{2+} loading. This model shows improved behavior over existing models that lack detailed descriptions of subcellular Ca^{2+} regulatory mechanisms. (Supported by NSF BIR-9117847).

W-Pos460

THE EFFECT OF STOCHASTIC PROCESSES ON SIGNAL TRANSMISSION EFFICIENCY IN A NEURAL NETWORK. ((X. Pei, G. Lanfermann, LA. Wilkens and F. Moss)) Center for Neurodynamics, Depts. of Physics and Biology, Univ. of Missouri-St. Louis, St. Louis, MO 63121.

Noise is a random process, present in virtually all sensory nervous systems, which affects information processing. Cells often fire spontaneously in a neural network. When the signal amplitude is below a detection threshold, the presence of noise, either external or internal, can improve the coherence of the response. This process, known as *stochastic resonance*, has been recently demonstrated in mechanoreceptors and caudal photoreceptors of crayfish and similar sensory systems of other animals. By constructing a two-layer network to simulate the mechanosensory system in the crayfish tail fan and using cross-correlation analysis, we demonstrate that the signal transmission efficiency in one neuron can be regulated by the population activities in the network. For subthreshold signals, SR can improve the signal transmission. While for supra-threshold signals, adding random activities to the system only degrades the performance of the system. In conclusion, a system containing elements which process inputs in parallel can improve its performance by adjusting the internal activity level to an optimum.

W-Pos461

THE EXTRACTION OF NANOMOLAR CONCENTRATIONS OF LIGAND FROM SOLUTION. THEORETICAL CONSIDERATIONS. ((Frederic Mandel)) Baylor College of Medicine, Houston, TX 77030.

Many purification methodologies are based on the principle that the ligand of interest is retained under a particular set of conditions (eg, binding to an affinity column) and subsequently released under a second different set of conditions. It is intuitively obvious that the efficiency of such processes is a function of the affinities of the ligand for its binding site(s) under the differing binding and release conditions as well as the relative concentrations of the ligand of interest and the ligand binding site(s). For this study, we have derived the quadratic equations relating the amount of ligand that can theoretically be extracted to the four parameters discussed above. We have also written a computer program to calculate and plot the amount bound, the amount released, and the amount extracted for any given values of the four parameters. The calculations show that (1) the more different the affinities under binding and release conditions the more efficient the extraction process; (2) the efficiency of the process increases as the ligand concentration decreases; and (3) for any given pair of affinities and for a fixed ligand concentration, there is a concentration of ligand binding sites that results in optimal ligand extraction.

W-Pos462

ON THE LOW FREQUENCY DIELECTRIC PROPERTIES OF CHARGED PARTICLES
((X.-B. Wang, Y. Huang, F. F. Becker and P. R. C. Gascoyne)) Box 89, UT M. D. Anderson Cancer Center, 1515 Holcombe Blvd., Houston TX 77030

There has been a long time interest in the nature of the interaction between charged particles and applied AC electrical fields. Classical impedance measurements of particle suspensions revealed so-called α-dispersions at low frequencies ($< 1kHz$), which were accounted for by several theoretical models. The modern biophysical techniques of dielectrophoresis and electrorotation of individual particles in suspension have shown anomalous low frequency responses. Here we develop a new theoretical treatment of the problem. Based on an analysis of the electrical potential and charge distributions for the cases of charged particles under zero-applied field condition and of uncharged particles under applied field conditions, we propose to divide the suspending medium close to the surfaces of charged particles into regions of counter-ion double-layer and diffusion-ion clouds. The electrical polarizations up to these two regions will then give rise, respectively, to the dielectrophoretic and electrorotational responses and to classical suspension dielectric measurements. Theoretical responses of charged particles are calculated by using the boundary conditions for electrical potentials and charge distributions and compare favorably with experimental data for charged latex particles.

W-Pos463

AN APPROACH TO NONUNIQUENESS OF POLYEXPONENTIAL MODEL. ((Ž. Bajzer, I. Penzar and F.G. Prendergast)) Mayo Foundation, Rochester, MN 55905.

There are many areas in biophysics where the polyexponential model (PM), given by $f(t)=a_1 \exp(b_1 t)+...+a_n \exp(b_n t)$, has been the key mathematical model, e.g., fluorescence intensity and anisotropy decay, NMR spectroscopy, distribution of open and shut intervals in single channel recordings, transient chemical relaxation. The crucial problem in application of PM is that several significantly different PM functions with respect to number of compontents ($n\leq4$) and parameters are usually consistent with given experimental data. So far, many different methods have been designed to find a single "best" PM, without paying attention to possible equivalent polyexponetial models. In our approach, we first discover various PM's that are consistent with given data and their interpretation. Then, we propose more appropriate measurements (in terms of interval in t, number of points and measurement error) that would eliminate spurious models. The method we use to find equivalent PM's is based on minimizing the distance between two PM functions in an appropriate L^p space combined with the analysis of corresponding residuals. As an example, we present application of our methodology to fluorescence intensity and anisotropy decay. Supported by GM34847.

W-Pos464

SIMPLE EVOLUTIONARY MODELS. ((J. M. Koshi and R. A. Goldstein)) Biophysics Research Division and Department of Chemistry, University of Michigan, Ann Arbor, MI 48109-1055, USA

In this project we present a simple model of evolution. This model involves an order of magnitude fewer parameters than a traditional mutation matrix, and by using site classes which do not correspond to pre-defined types, also deals more effectively with the heterogeneous constraints found in proteins. Comparing the conclusions from our model of evolution and those drawn from a correlation analysis of our previously published structure-dependent mutation matrices, we verified several results regarding the importance of hydrophobicity. The additional information our model provides, such as relative population of various classes, also brought to light several new results. We further demonstrate that our model of evolution can successfully be applied to small, specific protein data sets such as those derived from the proteins of HIV-1 and HIV-2.

The reduced number of free parameters means that the evolutionary model approach does not require the large data sets necessary for deriving mutation matrices, and it also means that we are better able to treat the problem of site-heterogeneity by simultaneously optimizing separate fitness functions for various classes within a given protein. Within this model of evolution, the distribution of amino acids is based on a simple Boltzmann distribution, which is found using separate linear or quadratic fitness functions for various site classes. These fitness functions can depend on one or more amino acid indices. The kinetics in this evolutionary model is based on the Metropolis algorithm.

W-Pos465

PROTEIN EVOLUTION ON A FOLDABILITY-FITNESS LANDSCAPE.
((S. Govindarajan and R. A. Goldstein)) Department of Chemistry
and Biophysics Research Division , University of Michigan, Ann Arbor,
MI 48109-1055, USA

Evolution determines the shape and function of the biological macro-
molecules. Understanding the process of molecular evolution can pro-
vide insight into the structure and function of these macromolecules and
the properties of these molecules will in turn throw light on the process
of evolution. We model protein evolution as a random walk in a multi-
dimensional fitness landscape, the configuartion space representing all
the possible protein sequences. The fitness of any sequence corresponds
to the foldabilty of that sequence to the native state. Foldability being
a universal requirement for biological proteins, such a foldability based
fitness landscape approach will relate the features of protein structures
and evolution. Evolutionary pressure in the form of a minimum fold-
ability requirement was explicitly considered. We observe a phase tran-
sition to a slower non self-averaging dynamics in the landscape when
the evolutionary pressure is increased. At higher evolutionary pressure
sequences tend to evolve along neutral networks stretching across the
sequence space, representing particular structures.

W-Pos466

MODELING PROTEIN FOLDING AS DIFFUSION ON ENERGY LAND-
SCAPES ((T.-L. Chiu and R. A. Goldstein)) Department of Chemistry
and Biophysics Research Division , University of Michigan, Ann Arbor, MI
48109-1055, USA

The mechanism by which proteins fold into their native three-dimensional
structures remains one of the central unsolved problems of molecular biol-
ogy. Protein folding process is characterized by large *ensembles* of states,
whose components depend upon external conditions. In order to approach
such a process, recent theoretical work has developed a statistical character-
ization of the energy landscape of folded proteins. In the present study, we
consider folding as diffusion on the energy landscape and use the diffusion
equation to study the impact of the nature of the interactions on the folding
dynamics. We focus our attention on the relationship between the specific
interactions necessary for folding into the native state relative to the average
strength of the interactions that result in compaction. The energy landscape
is characterized by two different order parameters, one representing the de-
gree of compactness, the other a measure of the progress towards the folded
state. We first construct a one-dimensional reaction coordinate through the
two-dimensional order-parameter space, compute the free-energy and effec-
tive diffusion constant for motion along this reaction coordinate, and then
model the folding as diffusion along this coordinate. We find that the opti-
mal average interaction is rather large relative to the distribution of specific
interactions, meaning that under optimal conditions proteins would contract
quickly and search for their native state from among the compact states.

W-Pos467

FURTHER OBSERVATIONS ON TOTAL HEIGHT/UMBILICAL HEIGHT (H/U): THE
GOLDEN MEAN AND FIBONACCI SERIES. ((R.P. Spencer)) University of
Connecticut Health Center, Farmington, CT 06030.

As part of a study of osteoporosis in women, we also measured H/U
in order to compare the present female population with reported
classical Greek measurements. The "Golden mean" dervived from the
attempt to divide a line of unit length so that the ratio of the
longer segment (L) to the whole line was the same as that of the
shorter segment (1 - L) to the longer. Hence L = (1 - L)/L. This
solves as the quadratic (-1 +/- √5)/2, or L = 0.618.. The value
of the entire length divided by the longer segment was 1/0.618,
or 1.618. The Greek observation was that their H/U was 1.618 or
Golden mean. This number is also of interest as it is the ratio
in the Fibonacci series (number/preceding number). The Fibonacci
series has also been used to describe the growth of certain
shelled animals. The value of 1.618 also appears in Chaos theory
(Chirikov,B.V.: Chaos, Solitons and Fractals 1:79, 1991). Our
study encompassed women without a loss of height, as well as
those with a loss of 2 cm or more from osteoporotic collapse
(Clin. Nucl. Med. 14:231, 1989). Our population values of H/U
ranged from 1.57 to 1.86. "Bending over" or hyperkyphosis of
vertebral fractures would decrease H with little change in U,
lowering the value of H/U. The present population, likely older
and more obese than the ancient Greeks (and probably taller) may
have a more mobile umbilicus. More fixed sites, such as the
iliac bone height, should likely be utilized.

W-Pos468

A MATHEMATICAL MODEL OF THE CRUSTACEAN STRETCH RECEPTOR.
((B. Rydqvist and C. Swerup)). Department of Physiology and Pharmacology, Karolinska
institutet, S-171 77 Stockholm, Sweden.

Systems analysis has been applied for the investigation of the input-output relations of the
crayfish stretch receptor, a mechanoreceptor analogous to the human muscle spindle. This type
of analysis results in mathematical models consisting of a black box with input-output
properties similar to the stretch receptor. With increasing knowledge, however, it has become
possible to simulate each step in the transduction process between mechanical stimulation and
electrical response and in this way create a composite model which gives insight into the
transformation at the different stages.
In the present study a mathematical model has been developed of the transduction process in
this mechanoreceptor, taking into account the viscoelastic properties of the accessory structures
of the receptor (i.e. the receptor muscle), the biophysical properties of the mechanosensitive
channels, the passive electrical properties of the neuronal membrane (leak conductance and
capacitative properties) and voltage gated ion channels generating impulses. The parameters of
the model are derived from studies on the mechanical properties of the receptor muscle,
experiments on whole cell recordings of the sensory neuron and from single channel studies of
the mechanosensitive channels. The viscoelastic properties of the receptor muscle are modelled
by a Voigt element (spring in parallel with a dashpot) in series with a nonlinear spring. The
receptor current at different extensions of the receptor was computed using typical viscoelastic
parameters for a receptor muscle together with a transformation of tension in the muscle to
tension in the neuronal dendrites and finally taking into account the properties of the
mechanosensitive channels. The receptor potential was calculated by modelling the neuronal
membrane by a lumped leak conductance and capacitance. For the calculation of potential the
cell was treated as an idealized spherical body. Voltage gated ion channels were modeled using
Hodgkin-Huxley formalism. The model resulted in nonlinear differential equations which were
solved by an iterative, fourth order Runge-Kutta method. The performance of the model was
greatly improved by introducing an intrinsic adaptation of the mechanosensitive channels. The
model can predict a wide range of experimental data from the stretch receptor neurons
including the mechanical response of the receptor muscle, the receptor current and its voltage
dependence, the receptor potential and the impulse response.

REGULATION OF ION CHANNELS BY HETEROTRIMERIC G PROTEINS

Th-AM-SymI-1 **D. Lambright, University of Massachusetts**
Structural Determinants of G Protein Coupled Signaling
Th-AM-SymI-2 **S. Ikeda, Medical College of Georgia**
Role of G-$\beta\gamma$ Subunits in Neuronal Calcium Channel Regulation
Th-AM-SymI-3 **G. Szabo, University of Virginia**
Functional Implications of G Protein Regulated Channel Kinetics
Th-AM-SymI-4 **D. Clapham, Harvard Medical School**
G Protein Gated K^+ Channels